وزارة التعليم العالي والبحث العلمي


**BADJI MOKHTAR -ANNABA UNIVERSITY**
**UNIVERSITE BADJI MOKHTAR ANNABA**

**جامعة باجي مختار - عنابة -**

**Faculté des Sciences**

**Département de Mathématiques**


**Année : 2020**

# THÈSE

Présentée en vue de l'obtention du diplôme de

Doctorat

## Etude Mathématique et Numérique des équations d'onde dispersives

**Option**

Equations Différentielles et Applications


**Par**

BOUSBIA Farida

**DIRECTEUR DE THÈSE** : Fatma Zohra Nouri Prof U.B.M. ANNABA


**Devant le jury**

| | | | |
|---|---|---|---|
| **PRESIDENT** : | Mr. Ali Djellit | Prof | U.B.M. ANNABA |
| **EXAMINATEUR** : | Mme. Ilham Djellit | Prof | U.B.M. ANNABA |
| **EXAMINATEUR** : | Mr. Mohamed Zine Aissaoui | Prof | U. GUELMA |
| **EXAMINATEUR** : | Mr. Guesmia Amar | Prof | U. SKIKDA |
| **EXAMINATEUR** : | Mr. Taallah Frekh | M.C.A | U.B.M. ANNABA |

# Contents

# List of Figures

# Acknowledgement

First of all, my praise and thanks to my Lord Allah, the Most Gracious and Most Merciful for enabling me to complete my PhD study in time.

I would like to thank my supervisor, Prof. F.Z. Nouri, for her guidance, advices and help over the past few years. I have learned much about what it means to be an applied mathematician through working with her.

I am profoundly grateful to the whole staff of the mathematical modeling and numerical simulation research Laboratory and the PhD students for their help, advice, and friendship over the past few years. It was a great pleasure to be part of this incredible team.

I would like to thank the committee members: professors Ali Djellit, Ilham Djellit and Mohamed Zine Aissaoui, and Doctors Amar Guesmia and Frekh Taallah.

Finally, I would like to thank my family and friends for all their support over the years of my education and career goals.

# Abstract

In this thesis, we study the nonlinear dispersive wave problems analytically and numerically. Our goal to present a powerful tool can be used to find the soliton solutions of these type of equations, to establish and discuss some important mathematical aspects related to the nonlinear dispersive partial differential equations (PDEs) such as the well-posedness of the associated Cauchy problem, behavior of the solitary wave solutions, and to show the suited numerical methods used to investigate the blow-up phenomenon of the solutions.

Keywords : Nonlinear dispersive waves equations, Inverse scattering transform, Spectral methods, blow-up, Cauchy problem, Soliton and solitary wave solutions.

# Résumé

Dans cette thèse, nous étudions analytiquement et numériquement les problèmes d'ondes dispersives non linéaires. Notre but est de présenter un outil puissant qui peut être utilisé pour trouver les solutions de solitons de ce type d'équations, d'établir et de discuter certains aspects mathématiques importants liés aux équations aux dérivées partielles (EDP) dispersives non linéaires, tels que le caractère bien posé du problème de Cauchy associé, le comportement des solutions d'ondes solitaires, et de montrer les méthodes numériques appropriées utilisées pour étudier le phénomène d'explosion des solutions.

Mots-clés : Équations d'ondes dispersives non linéaires, Inverse scattering transform, Méthodes spectrales, Explosion, Problème de Cauchy, Solitons et solutions d'ondes solitaires.

# الملخص

في هذه الاطروحة، ندرس مشاكل الموجات المشتتة الغيرخطية تحليليًا وعدديًا. يمكن استخدام هدفنا لتقديم أداة قوية لإيجاد حلول السوليتون لهذا النوع من المعادلات، لإنشاء ومناقشة بعض الجوانب الرياضية المهمة المتعلقة بالمعادلات التفاضلية دات الاشتقاقات الجزئية المشتتة غير الخطية (PDEs) مثل التواجد الجيد لمعادلات كوشي المرتبطة مشكلة وسلوك حلول الموجة الانفرادية، وبيان الطرق العددية المناسبة المستخدمة في تقصي ظاهرة تفجير الحلول.

الكلمات الرئيسية: معادلات الموجات المشتتة غير الخطية، تحويل التشتت العكسي، الطرق الطيفية، التفجير، مشكلة كوشي، حلول سوليتون والموجة المنفردة.

# Introduction

The study of nonlinear evolution equations (NLEEs) is growing rapidly due to their great interest in many fields of physics as, for example plasma, fluids and optics. Many significant characteristics of NLEEs have been investigated, especially their integrability issues, Lax pairs, conservation laws and many other crucial aspects. Remarkable methods have been developed to find the exact solutions for this type equations, for instance the well known the inverse scattering method, Darboux and the Bäcklund transformation method, the Hirota bilinear and its simplified method, lie symmetry method, the generalized unified method, the sine-cosine method and Pfaffian technique and many other Powerful methods.

Wave phenomena are abundant in life and nature which are mainly include two types of waves: optical and water waves. Familiar examples are associated with the hydrodynamics context where the dispersion is a main feature of linear wave phenomena. For instance, if we consider a dewdrop falling into a lake as in Figure 1 concentric rings of ripples will immediately appear and spread out and after a little while they will disappear. The corresponding phenomenon is called dispersion and diffraction in water waves and optics, respectively. It

Figure 1: Dispersive medium

is useful now to give the difference in the notion of dispersive and dissipative PDEs for both

linear and nonlinear equations. Let us consider the following wave equation:

$$u_t + u_x = 0. \tag{1}$$

If we add a dispersion term, we get

$$u_t + u_x + u_{xxx} = 0, \tag{2}$$

equation (2) admits a solution of the form

$$u(x,t) = e^{i(kx-\omega t)}, \tag{3}$$

where $\omega$ and $k$ represent the frequency and the the wave number, respectively. If we substitute (3) in (2) we obtain the corresponding dispersion relation given by

$$\omega = k - k^3. \tag{4}$$

Hence the wave propagation velocity is written in the form

$$c = \frac{\omega}{k} = 1 - k^2, \tag{5}$$

On the other hand, adding a dissipative term we find:

$$u_t + u_x + u_{xx} = 0, \tag{6}$$

in this case we have

$$\omega = k(1 - \mathrm{i}k), \tag{7}$$

and the corresponding solution is

$$u(x,t) = e^{-k^2 t + \mathrm{i}k(x-t)}, \tag{8}$$

that indicates that the wave propagates at a unity speed and decays exponentially, which means that the wave loses its amplitude, since it losses its energy over time. This kind of wave called a dissipative wave. It is interesting to note that there are several ways to establish the dispersion of the linear wave for example: one can define the velocity as follows:

$$v_p = \frac{\omega}{|k|}\frac{k}{|k|} \quad (the\, phase\, velocity),$$

$$v_g = \nabla\omega \quad (the\, group\, velocity).$$

If $v_p \neq v_g$, the PDE is called dispersive (see Figures 2 and 3).

Although the importance of the linear wave in every day life, in 1834 an amazing phenomenon was experimentally discovered in the Union Canal in Scotland by John Scott Russell but could not be explained by the theory of linear water wave. Below Russell's quote

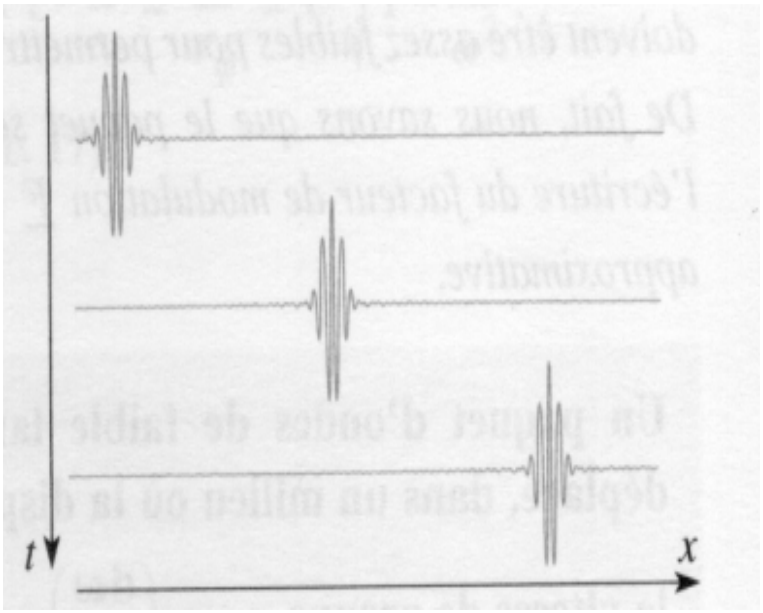


Figure 2: Non dispersive propagation

> *"I was observing the motion of a boat which was rapidly drawn along a narrow channel by a pair of horses, when the boat suddenly stopped−not so the mass of water in the channel which it had put in motion; it accumulated round the prow of the vessel in a state of violent agitation, then suddenly leaving it behind, rolled forward with great velocity, assuming the form of a large solitary elevation, a rounded, smooth and well-defined heap of water, which continued its course along the channel apparently without change of form or diminution of speed. I followed it on horseback and overtook it still rolling on at a rate of some eight or nine miles an hour* $[14km/h]$*, preserving its original figure some thirty feet* $[9m]$ *long and a foot to a foot and a half* $[300-450mm]$ *in height. Its height gradually diminished, and after a chase of one or two miles* $[2-3km]$*, I lost it in the windings of the channel. Such, in the month of August* 1834*, was my first chance interview with that singular and beautiful phenomenon which I have called the Wave of Translation"*

Nowadays, the Union Canal has attracted many tourist to get fun when they ride the famous wave, see Figure 4. This observation inspired physicists to initiate an extensive investigation of water waves. In 1895, Diederik Korteweg and Gustav de Vries recreated this problem.

They noticed that while dispersion causes a water wave to decay, nonlinear effects can cause a steepness. When self-steepening balances dispersion, a solitary wave which moves without change of shape (i.e., the "wave of translation") can be formed. The researchers Korteweg and de Vries (1895) derived the following nondimensionalized wave equation which is now called the Korteweg–de Vries (KdV) equation:

$$u_t + 6uu_x + u_{xxx} = 0. \tag{9}$$

Russell'observation was the first description of the so-called solitons as an amazing physical

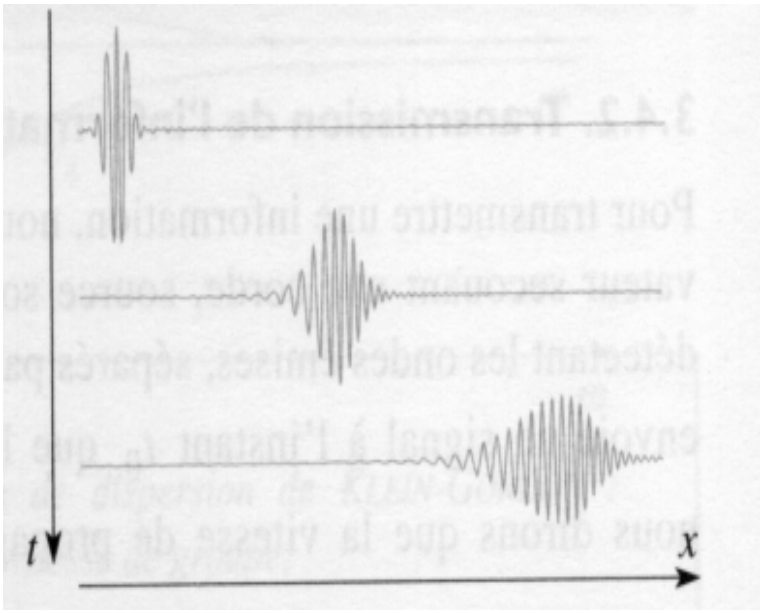


Figure 3: Dispersive propagation

phenomenon. Their original name was "translation wave", but later researchers discovered many new solitons that play an important role in many applications, physics, electronics, cosmology, biology and life sciences (see Figure 5).

No much progress in the analytical resolution of nonlinear wave and the soliton theory was made until the 1964s, when Gardner, et al. developed a very powerful tool to determine the soliton solutions of nonlinear equations. This method is based on the Lax pair corresponding to the equation and named the inverse scattering transform method. In subsequent years, several other nonlinear wave equations appeared and could be solved by the inverse scattering method such as the Benjamin-Ono equation, the Kadomtsev–Petviashvili (KP) equation, the nonlinear Schrödinger (NLS) equation, which nowdays known by integrable equations.

Even though, integrable equations have significant features, a great part of real features appear in physics and engineering areas described by nonintegrable wave equations. Thus the study of this type of equations has grown rapidly and created many exciting theories for example the wave collapse theory and the criterion of Vakhitov–Kolokolov for the linear stability of solitary waves. In addition, the investigations of the nonintegrable wave equations show that the corresponding solution dynamics can be more complex and much richer.

It is a remarkable fact that numerical analysis is a powerful resource in nonlinear waves study, allowing to illustrate significant theorems and conjectures.

## 0.1 Notation and definitions

Let us give some notations and definitions that will be used throughout this thesis.

- $\hat{u}$ or $\mathcal{F}(u)$ stand for the Fourier transformation of a function $u$.
- $D_x^\alpha$ is the derivative with respect to x of order $\alpha$.

Figure 4: Tourists riding Soliton "Translation Wave" at the place of discovery by John Scott Russell (Union Canal, Scotland)

- the gradient $\nabla u = (\partial_{x1}u, ..., \partial_{xd}u)^T$, for $u : \mathbb{R}^d \to \mathbb{R}$.
- the Laplacian $\Delta u = \partial^2_{x1}u + ... + \partial^2_{xd}u$, for $u : \mathbb{R}^d \to \mathbb{R}$
- $A \sim B$ to stand for $B \leq A \leq CB$, where $C$ is a positive constant and may vary from line to line;
- $b-$ and $b+$ the statement that $b - \epsilon$ and $b + \epsilon$ respectively.
- $\chi$ is as usual used for the characteristic functions.

**- Lebesgue spaces**

**Definition 1.** *For an open, bounded domain $\Omega$, that simply connected subset of $\mathbb{R}^d$ $(d \geq 1)$. For $1 \leq p < \infty$, $L^p(\Omega)$ space includes all Lebesgue measurable functions $u : \omega \to \mathbb{R}$, such that*

$$\|u\|_{L^p(\Omega)} := \left( \int_\Omega |u(x)|^p dx \right)^{1/p} < \infty. \tag{10}$$

**- Sobolev spaces**

- For $k \in \mathbb{N}$

  **Definition 2.** *The space $H^k(\Omega)$ consists of every functions $u \in L^2$ such that for an*

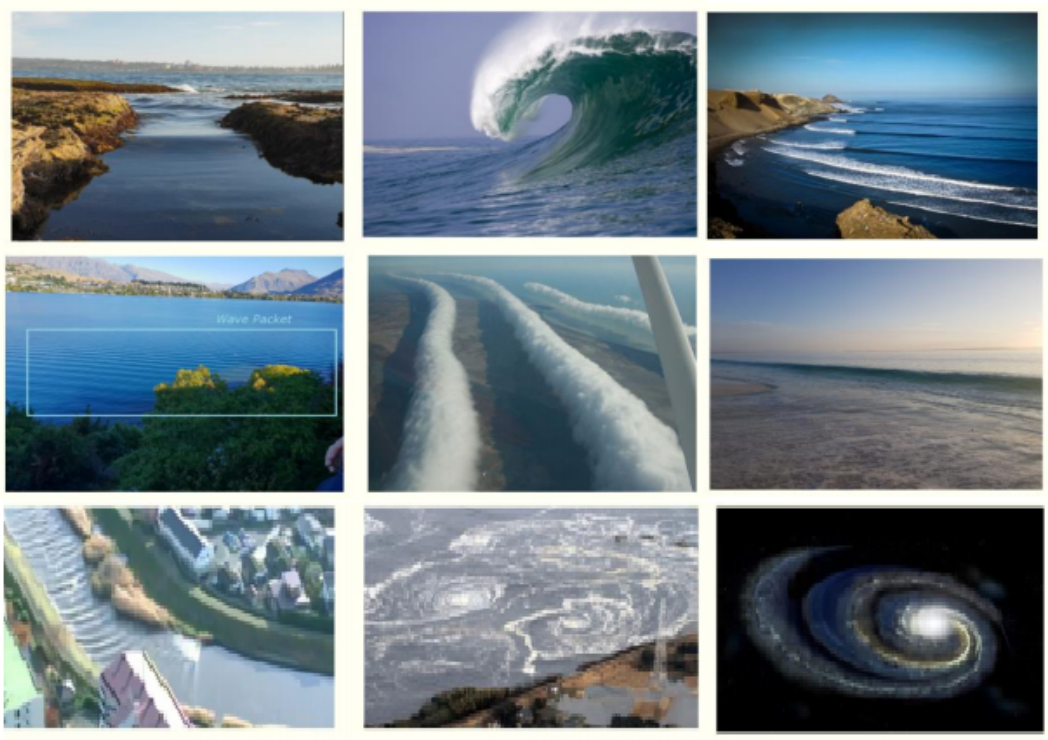


Figure 5: Solitons in nature

*integer $k$; $D^\alpha u \in L^2(\omega)$, for all $|\alpha| \leq k$. equipped with the norm*

$$\|u\|_{H^k(\Omega)} = \left( \sum_{\alpha \leq k} \int_\Omega |D^\alpha u(x)|^2 dx \right)^{1/2}. \tag{11}$$

- For $s \in \mathbb{R}$

  **Definition 3.** *For every $s \in \mathbb{R}$; the space $H^s$ is defined by*

  $$H^s(\mathbb{R}^n) = \{v \text{ is a tempered distribution}, (1 + |\eta|^2)^{s/2} \hat{v} \in L^2(\mathbb{R}^n)\}$$

  *equipped with the norm*

  $$\|u\|_{H^s(\mathbb{R}^n)} = \left( \sum_{\alpha \leq s} \int_{\mathbb{R}^n} (1 + |\eta|^2) |\hat{u}(\eta)|^s d\eta \right)^{1/2}. \tag{12}$$

**-Bourgain space**

**Definition 4.** *The Bourgain space $X^{s,b}$ is defined by*

$$\left\{ u \in : \|u\|_{X_{s,b}} = \|\langle \eta \rangle^s \langle \lambda \rangle^p \hat{u}\|_{L^2_{\tau\eta}(\mathbb{R}^2)} < \infty \right\}. \tag{13}$$

*Its restriction onto the interval time* $[0,T]$ *is denoted by* $X^T_{s,p}$*, and defined as*

$$\|u\|_{X^T_{s,b}} = inf\left\{\|v\|_{X_{s,b}} : v \in X_{s,b}, u(t) = v(t)\ for\ 0 \leq t \leq T\right\}, \tag{14}$$

*where* $< . >= (1 + |.|^2)^{1/2}$*.*

## 0.2 Outline of the thesis

The thesis is structured as follows: in the next chapter, we present some concepts related to the inverse scattering transform method and then we apply this method for one of integrable equation. Other important methods are also presented in this chapter.

The second chapter is devoted to the numerical methods that are used in the next chapter. first, we present two types of selected space discretization method, one of them is for the generation of solitary waves and the other for the evolution simulations. Time integrating methods of equations and their convergence are also discussed.

In the third chapter, we give a detailed numerical investigation of solutions to the general Benjamin-Ono equation with critical and supercritical nonlinearity in both one and two dimension. We examine the stability of solutions and present some unstable and blow-up features.

In the fourth chapter, the rotational internal dispersive wave equation is studied in detailed. We give a full description of the corresponding Cauchy problem.

We finish by a general conclusion on this work and set some perspective points.

# Chapter 1

# Analytical Methods for Nonlinear Dispersive Wave Equations

## 1.1 Introduction

Generally, nonlinear differential equations are said to be integrable systems if they can be solved analytically; which means that there is a finite number of integrations and algebraic operations where the solutions can be reduced. In fact this principled definition of integrability does not always hold for the case of PDEs. Since more than three centuries, the concept of integrable system range from notion to another. The most intresting one was introduced in the nineteenth century which is the Liouville integrability′s notion used for Hamiltonian systems. This notion is defined as follows: If a system of Hamiltonian $H$ with $n$ degrees of freedom admits $n$ independent commuting integrals of Poisson $I_1, I_2, I_3, ..., I_n$ which means that all canonical Poisson bracket vanish i.e., $\{I_k, I_j\} = 0$ for $n, j = 1..n$, then one can integrate explicitly the flow given by this Hamiltonian $H$.

$$\begin{aligned} &I_k(z(t)) = \text{const},\ 1 \leq k \leq n,\ \text{rank}(dI_1, ..., dI_n) = n,\ \{I_k, I_j\} = 0,\ 1 \leq j, \\ &k \leq n \Rightarrow \text{explicit integration.} \end{aligned} \tag{1.1}$$

In 1967 with discovering a new analytical tool to solve the KdV equation by Gardner et al, the advanced integrable systems theory was introduced. According to this method which is known as the Inverse Scattering Transform. If a system of equation admits the so-called Lax pairs representation, then this system can be of explicit solvability. However these ideas and discussion do not give a precise answer of what it means an integrable system since they lead to other complicated questions, as for example the converse of the Liouville integrability notion. Therefore, we can say that the existence unified concept of the integrable systems still an open problem.

## 1.2 Inverse scattering transform

In recent years, due to their completely integrable feature, the KdV, Intermediate Long Wave (ILW), Benjamin-Ono (BO), Non Linear Schrodinger (NLS) and Kadomtsev-Petviashvilli (KP)

equation have been widely studied. The completely integrable terminology is used for each of these equations because they can be solved by the inverse scattering method. The later was discovered by Gardner, Greene, Kruskal and Miura in 1967 [89] to solve the KdV equation for decay sufficiently rapidly initial data. The generalizations is now called by the Inverse Scattering Transform (IST), where the main idea involves associating the solution of the nonlinear equation to a linear eigenvalue one whose eigenvalues are constants of the motion for the original equation.

The IST formalism for BO equation in one dimension has been established in [2, 4] and its extensions to a larger family of potentials can also be found in [54, 114]. Let us first recall some important definitions and significant properties related to the IST context.

### 1.2.1 Soliton

**Definition 5.** *Although there is no exact definition of a soliton, we can say that a soliton is a solitary wave that asymptotically retains the velocity and shape upon nonlinear strong interaction with other localized disturbance or even with another solitary waves. Additionally a soliton exhibits the two following properties:*

- *It is localized i.e., it either approaches a constant or decays at infinity.*
- *It is made by a delicate state of equilibrium between dispersive and nonlinear consequences.*

### 1.2.2 Conservation laws

**Definition 6.** *In one dimension on both time and space, a conservation law related to a differential equation is relation may be expressed as*

$$A_t + B_x = 0, \tag{1.2}$$

*where $A$ and $B$ are dependent functions on $x$, $t$, the function $u$ and its derivatives. In (1.2), $A$ represents the conserved density while $B$ is the flux of $A$.*

For the BO equation, by $L^2$ norm the hamiltonian, we can easily find the two standard invariants of this equation $I_1$ and $I_2$, namely

$$I_1 = \frac{1}{2}\int_{\mathbb{R}} u^2 dx$$

$$I_2 = \int_{\mathbb{R}} (\frac{1}{2}|D|^1 2u|^2 - \frac{1}{6}u^3) dx.$$

In [19, 20], K.M. Case discovered the existence of an infinite conserved quantities number and calculated the first three non trivial. In fact the existence of an infinite number of invariant quantities leads to the complete integrability conjecture of BO equation.

### 1.2.3 Lax approach

**Definition 7.** *In 1968, Lax discovered a way to make the introductory inverse scattering technique for only solving KdV equation as a general method for solving other PDEs [89]. This way based on associating the nonlinear equations with a linear eigenvalue operator whose eigenvalues are constants of the original equation motion.*
*Let $L$ and $B$ two operators represent the spectral problem operator and the governing operator for the related time evolution of the corresponding eigenfunctions, respectively*

$$Lv = \lambda v. \tag{1.3}$$

$$v_t = Bv. \tag{1.4}$$

*By differentiating* (1.3) *with respect to $t$*

$$L_t v + Lv_t = \lambda_t v + \lambda v_t,$$

*from*

$$L_t v + LBv = \lambda_t v + BLv,$$

*Thus, we have that*

$$[L_t + (LB - BL)]v = \lambda_t v,$$

*then, to find the nontrivial eigenfunctions $v$ when $\lambda_t = 0$, we finally have*

$$L_t + [L, B] = 0, \quad [L, B] = LB - BL. \tag{1.5}$$

*Equation* (1.5) *is the so−called Lax's equation, so an evolution equation is said to have a Lax representation if it can be developed as the compatibility condition of two operators $L$ and $B$, known as Lax pair.*

### 1.2.4 Riemann-Hilbert problems

Riemann−Hilbert problems (RHB) have played a significant role in both IST and soliton theory. We try here to review briefly some their basic elements. Let $t \in \overline{\mathbb{C}} = \mathbb{C} + \{\infty\}$, $\Gamma$ is a closed contour in $\overline{\mathbb{C}}$. and let $\Gamma^+$ and $\Gamma^-$ be the inside an the outside of the contour $\Gamma$, respectively. Particularly, the later contour can be regarded as a real line considered as a circle in $\mathbb{C}$ moving through $\infty$.

**Definition 8.** *The Riemann−Hilbert problem of a matrix valued function $\varphi(t)$ on $\Gamma$ is the act of constructing two holomorphic matrix of functions valued $\varphi_+(t)$ and $\varphi_-(t)$ inside and outside $\Gamma$, respectively such that*

$$\varphi(t) = \varphi_+(t)\varphi_-(t) \tag{1.6}$$

*If $\Gamma$ is the real axis, then $\varphi_+(t)$ and $\varphi_-(t)$ should to be holomorphic, respectively in the upper and lower half−plane. In the case when $(\varphi_+(t), \varphi_-(t))$ is a solution of RHB, then for a invertible matrix $g$ of constant elements, we obtain that*

$$\widetilde{\varphi_+} = \varphi_+ g^{-1},$$

*and*

$$\widetilde{\varphi_-} = g\varphi_-.$$

*are also solutions of the problem. One can avoid this ambiguity by fixing* $\varphi_+$ *or* $\varphi_-$ *values at some point in their region. However this normalisation ensures the uniqueness of the solution to* (1.6) *when* $\varphi_+$ *and* $\varphi_-$ *are everywhere invertible. Looking for solutions of the RHB falls into an integral equation. By choosing a normalisation for some* $t_0 \in \mathbb{C}$, $\varphi_+(t) = I$ *and* $\varphi_-(t) = g$ *and by assuming that a solution of RHB has the following form*

$$(\varphi_+)^{-1} = h + \oint_\Gamma \frac{\Psi(\zeta)}{\zeta - t} d\zeta,$$

*in* $\Gamma^+$

$$\varphi_- = h + \oint_\Gamma \frac{\Psi(\zeta)}{\zeta - t} d\zeta,$$

*in* $\Gamma^-$ *with* $h$ *is determined as follows*

$$h = g - \oint_\Gamma \frac{\Psi(\zeta)}{\zeta - t_0} d\zeta.$$

*Now, if* $t \in \Gamma$, *one can use the Plemelj formula [3] to compute* $\varphi_+)^{-1}$ *and* $\varphi_-)$ *as follows*

$$(\varphi_+)^{-1}(t) = h + \oint_\Gamma \frac{\Psi(\zeta)}{\zeta - t} d\zeta + \pi \mathrm{i} \Psi(t),$$

*and*

$$\varphi_-(t) = h + \oint_\Gamma \frac{\Psi(\zeta)}{\zeta - t} d\zeta - \pi \mathrm{i} \Psi(t),$$

*with the assumption that principal value integrals are whenever needed. If the normalisation is canonical which means that* $h = g = 1$ *and from these expressions and* (1.6), *we finally obtain the integral equation.*

$$\frac{1}{\pi \mathrm{i}} \left( \oint_\Gamma \frac{\Psi(\zeta)}{\zeta - t} d\zeta + I \right) \Psi(t)(\varphi + I)(\varphi - I)^{-1} = 0,$$

*for* $\Psi = \Psi(t)$. *In the simplest case of the RHB, which is the scalar RHB, where* $\varphi$, $\varphi_+$ *and* $\varphi_-$ *are only ordinary functions. the solution in this simple case is given by*

$$\varphi_+ = exp\left( - \left( \frac{1}{2\pi \mathrm{i}} \int_{-\infty}^{+\infty} \frac{log\varphi(\zeta)}{\zeta - t} d\zeta \right) \right), \quad Im(t) > 0$$

$$\varphi_- = exp\left( \frac{1}{2\pi \mathrm{i}} \int_{-\infty}^{+\infty} \frac{log\varphi(\zeta)}{\zeta - t} d\zeta \right). \quad Im(t) < 0$$

*This can be verified if we take the logarithm of* (1.6) *and use the Cauchy integral formulae*

$$log\varphi = log(\varphi_-) - log(\varphi_+)^{-1}.$$

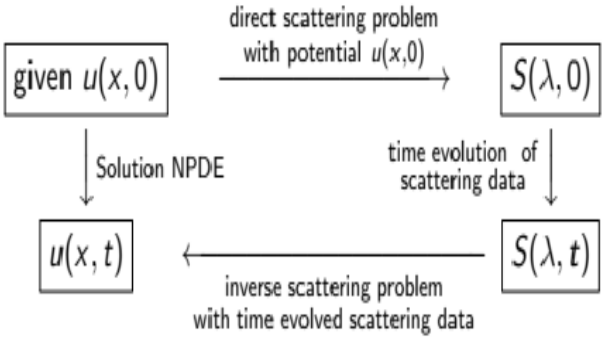


Figure 1.1: Main steps of inverse scattering transform method

Now, we are in position to present the I.S.T method. In fact, this method is not a direct tool, it can be represented by the diagram 1.1. Now, we apply the IST on BO equation that written as follows

$$u_t + (u^2 - Hu_x)_x = 0, \qquad t \in \mathbb{R}, x \in \mathbb{R}, \tag{1.7}$$

where $u(t,x)$ is a real-valued function and $H$ denotes the Hilbert transform, defined by

$$Hf(x) = \frac{1}{\pi} P.V. \int_{\mathbb{R}.} \frac{f(y)}{x-y} dy,$$

*P.V.* stands for the principal value. This equation was introduced by Benjamin [10] and later by Ono [93] and has been intensively studied both numerically and mathematically as a model in internal-wave theory.

**The Scattering Data**

More precisely, following [2, 4] the Lax pair for the BO equation is defined by

$$\mathrm{i}\omega_x^+ + k(\omega^+ - \omega^-) = -u\omega^+, \tag{1.8}$$

$$\mathrm{i}\omega_t^\pm - 2\mathrm{i}k\omega_x^\pm + \omega_{xx}^\pm - 2\mathrm{i}[u]_x^\pm \omega^\pm = -\alpha\omega^\pm, \tag{1.9}$$

where the spectral parameter here is the constant $k$, $\rho$ is an arbitrary constant, $[u]^-$ and $[u]^+$ are analytic functions in the lower and upper half complex $z-$planes, respectively. Similarly for $\omega^\pm$ which is considered as the boundary values of functions, that is $\omega^\pm = \lim_{y\to 0} \omega(x \pm \mathrm{i}y)$ and

$$[u]^\pm = \pm\frac{1}{2}u - \frac{1}{2}\mathrm{i}Hu. \tag{1.10}$$

The linear spectral problem defined by equation (1.8) represents a RHB in the complex $z-$plane. By imposing some suitable boundary conditions when $z \to \infty$, (1.8) leads to unique solutions for both $\psi^+$ and $\psi^-$. following [2], the choice as $z \to \infty$ would be either $\psi^+ \to 0$ or 1.

One may only interest in the positive eigenfunctions, thus from now on, the superscript $^+$ can be dropped. Let $N$, $\overline{N}$ and $M$, $\overline{M}$ denote the right and the left eigenfunctions, respectively. These eigenfunctions are specified by the asymptotic behavior:

$$N(x;k) \sim e^{\mathrm{i}kx} \quad \overline{N}(x;k) \sim 1 \text{ as } x \to \infty, \tag{1.11}$$

$$M(x;k) \sim 1 \quad \overline{M}(x;k) \sim e^{\mathrm{i}kx} \text{ as } x \to -\infty, \tag{1.12}$$

They also satisfy the following integral representation

$$\begin{pmatrix} N(x;k) \\ \overline{N}(x;k) \end{pmatrix} = \begin{pmatrix} e^{\mathrm{i}kx} \\ 1 \end{pmatrix} + \int_{-\infty}^{+\infty} \varphi_-(x,y;k)u(y) \begin{pmatrix} N(y;k) \\ \overline{N}(y;k) \end{pmatrix}, \tag{1.13}$$

$$\begin{pmatrix} M(x;k) \\ \overline{M}(x;k) \end{pmatrix} = \begin{pmatrix} 1 \\ e^{\mathrm{i}kx} \end{pmatrix} + \int_{-\infty}^{+\infty} \varphi_+(x,y;k)u(y) \begin{pmatrix} M(y;k) \\ \overline{M}(y;k) \end{pmatrix}, \tag{1.14}$$

that are called Fredholm integral equations, with $\varphi_-$, $\varphi^+$ represent respectively the $(-)$ and $(+)$ regions of the following holomorphic function

$$\varphi(x,y;k) = \frac{1}{2\pi} \int_0^\infty \frac{e^{\mathrm{i}(x-y)\zeta}}{\zeta - \tau} d\zeta, \tag{1.15}$$

with $\tau$ is the complex extension of $k$. This yields

$$\varphi_\mp(x,y;k) = \frac{1}{2\pi} \int_0^\infty \frac{e^{\mathrm{i}(x-y)\zeta}}{\zeta - (k \mp \mathrm{i}0)} d\zeta. \tag{1.16}$$

As mentioned in the previous part, we can use the Plemelj formulae to get

$$\varphi_+(x,y;k) - \varphi_-(x,y;k) = \mathrm{i}\theta(k) e^{\mathrm{i}(x-y)k}, \tag{1.17}$$

where $\theta(k)$ denotes the Heaviside function ($\theta(k) = 1$ if $k > 0$ or 0 if $k < 0$). Then, one can focuses on the following scattering equation

$$M(x,k) = \overline{N}(x,k) + \alpha(k) N(x,k), \tag{1.18}$$

with

$$\alpha(k) = \mathrm{i}\theta(k) \int_{-\infty}^{+\infty} u(y) M(y,k) e^{\mathrm{i}ky} dy. \tag{1.19}$$

To derive the later equation, we need to define

$$\Delta(x;k) = M(x;k) - \overline{N}(x;k). \tag{1.20}$$

then, by (1.13) and (1.14), we find that

$$\begin{aligned} \Delta(x;k) &= \textstyle\int_{-\infty}^{+\infty} \varphi_+(x,y;k)u(y)M(y,k)dy - \int_{-\infty}^{+\infty} \varphi_-(x,y;k)u(y)\overline{N}(y,k)dy \\ &= \textstyle\int_{-\infty}^{+\infty} \varphi_-(x,y;k)u(y)\Delta(y,k)dy \\ &\quad \textstyle- \int_{-\infty}^{+\infty} [\varphi_+(x,y;k) - \varphi_-(x,y;k)]u(y)M(y,k)dy. \end{aligned} \tag{1.21}$$

Thus from (1.17) ,(1.18) and (1.19)

$$\Delta(x;k) \;= \int_{-\infty}^{+\infty} \varphi_-(x,y;k)u(y)\Delta(y,k)dy + \mathrm{i}e^{\mathrm{i}kx}\int_{-\infty}^{+\infty} e^{\mathrm{i}ky}u(y)M(y;k)dy, \tag{1.22}$$

and this implies that

$$\Delta(x;k) = \alpha(k)N(x;k). \tag{1.23}$$

### 1.2.5 Inverse scattering data

The solitons of the BO equation arise as poles of the left and right eigenfunctions $M$ and $\overline{N}$. The integral equations (1.13) and (1.14) have $\psi_j(x)$ as nontrivial solutions, for some negative $k_j$.

$$\psi_j(x) = \int_{-\infty}^{\infty} \varphi(x,y;k_j)u(y)\psi_j(y)dy, \quad \text{as } k_j < 0 \tag{1.24}$$

where

$$\varphi(x,y;k_j) = \frac{1}{2\pi}\int_0^{\infty} \frac{e^{\mathrm{i}(x-y)\zeta}}{\zeta - k_j}d\zeta. \tag{1.25}$$

Since the kernels of (1.13) and (1.14) are $(+)$ and $(-)$ function in $k$ for $M$ and $\overline{N}$, respectively then

$$M(x,k) = 1 + \sum_{j+1}^{n} \frac{C_j\psi_j(x)}{k-k_j} + m_+(x,k), \tag{1.26}$$

and

$$\overline{N}(x,k) = 1 + \mathrm{i}\sum_{j+1}^{n} \frac{C_j\psi_j(x)}{k-k_j} + \overline{n}_-(x,k), \tag{1.27}$$

where the constants $C_j$ will be equal to $-\mathrm{i}$ after some normalization for $j = 1, 2, ..., n$. The next step is to make equations (1.18) and (1.19) be a RHB in $k-$plane. To do so we have to investigate an existent symmetry relation between $\overline{N}$ and $N$ and establish appropriate analytic characteristics of the eigenfunctions. By differentiating equations (1.15) with (1.16) and then integrating them by parts with respect to $k$ and $\zeta$, respectively, we write

$$\frac{\partial}{\partial k}(\varphi_\pm(x,y,k) = -\frac{1}{2\pi k} + \mathrm{i}(x-y)\varphi_\pm(x,y;k). \tag{1.28}$$

By differentiating equation (1.13) with respect to $k$, we find that

$$\begin{aligned} \tfrac{\partial}{\partial k}(N(x,k)e^{\mathrm{i}kx}) \;&= \int_{-\infty}^{\infty} \tfrac{\partial}{\partial k}(\varphi_-(x,y;k)e^{\mathrm{i}k(x-y)})u(y)N(y;k)e^{\mathrm{i}ky}dy \\ &\quad + \int_{-\infty}^{\infty}(\varphi_-(x,y;k)e^{\mathrm{i}k(x-y)}u(y)\tfrac{\partial}{\partial k}(N(x,k)e^{\mathrm{i}ky})dy. \end{aligned} \tag{1.29}$$

Therefore

$$\begin{aligned} \tfrac{\partial}{\partial k}(N(x,k)e^{\mathrm{i}kx}) \;&= e^{\mathrm{i}kx})f(k) + \int_{-\infty}^{\infty} \tfrac{\partial}{\partial k}(\varphi_-(x,y;k)e^{\mathrm{i}k(x-y)})u(y)N(y;k)e^{\mathrm{i}ky}dy \\ &\quad + \int_{-\infty}^{\infty}(\varphi_-(x,y;k)e^{\mathrm{i}k(x-y)}u(y)\tfrac{\partial}{\partial k}(N(x,k)e^{\mathrm{i}ky})dy, \end{aligned} \tag{1.30}$$

with

$$f(k) = -\frac{1}{2\pi k}\int_{-\infty}^{\infty} u(y)N(y;k)dy. \tag{1.31}$$

Now, we can obtain the symmetry relation by comparing the three equations (1.13), (1.30) and (1.31).

$$\frac{\partial}{\partial k}(N(x,k)e^{\mathrm{i}kx}) = f(k)\overline{N}(x;k)e^{\mathrm{i}kx}. \tag{1.32}$$

Thus (1.18), (1.19) and (1.33) imply that

$$M(x;k) = \overline{N} + \alpha(k)e^{\mathrm{i}kx}\int_0^k f(\lambda)e^{\mathrm{i}x\lambda}\overline{N}(x,\lambda)d\lambda. \tag{1.33}$$

For negative $k$, equation (1.13) gives

$$\begin{aligned} &\overline{N}^j(x;k) - \textstyle\int_{-\infty}^{\infty}\varphi(x,y;k)u(y)\overline{N}^j(y;k)dy \\ &= 1 + \tfrac{1}{k-k_j}[\psi_j(x) - \textstyle\int_{-\infty}^{\infty}\varphi(x,y;k)u(y)\psi_j(y)dy], \end{aligned} \tag{1.34}$$

where

$$\overline{N}^j(x;k) = \overline{N}(x;k) + \frac{\mathrm{i}\psi_j(x)}{k-k_j}. \tag{1.35}$$

By using (1.28) and letting the negative $k$ tends to $k_j$ we get

$$\begin{aligned} &\overline{N}^j(x;k_j) - \textstyle\int_{-\infty}^{\infty}\varphi(x,y;k_j)u(y)\overline{N}^j(y;k_j)dy \\ &= \delta_j + \textstyle\int_{-\infty}^{\infty}(x-y)\varphi(x,y;k_j)u(y)\psi_j(y)dy, \end{aligned} \tag{1.36}$$

where

$$\delta_j = 1 + \frac{\mathrm{i}}{2\pi k_j}\int_{-\infty}^{\infty}\psi_j(y)u(y)dy, \tag{1.37}$$

Letting $x \to 0$ in (1.15) gives

$$\varphi(x,y;k) = \frac{1}{2\mathrm{i}\pi k_j} + O(x^{-2}) \tag{1.38}$$

where

$$\mathrm{i}\frac{\partial\psi_j^+}{\partial x} + k_j(\psi_j^+ - \psi_j^-) = -u(x)\psi_j^+ \tag{1.39}$$

Moreover as $x \to \infty$, $\psi_j^{\pm} \sim 1$, then we have that

$$\begin{aligned} -\textstyle\int_{-\infty}^{\infty}u(y)\psi_j^+(y)dy \quad &= k_j[\textstyle\int_{-\infty}^{\infty}(\psi_j^+(y) - \frac{1}{y+\mathrm{i}})dy \\ &- \quad \textstyle\int_{-\infty}^{\infty}(\psi_j^-(y) - \frac{1}{y-\mathrm{i}})dy - \textstyle\int_{-\infty}^{\infty}(\frac{1}{y+\mathrm{i}} - \frac{1}{y+\mathrm{i}})dy] \end{aligned} \tag{1.40}$$

By integrating, it follows that

$$\int_{-\infty}^{\infty}(\psi_j^+(y) - \frac{1}{y+\mathrm{i}})dy = 0 = \int_{-\infty}^{\infty}(\psi_j^-(y) - \frac{1}{y-\mathrm{i}})dy \tag{1.41}$$

and

$$k_j = \frac{1}{2\pi \mathrm{i}} \int_{-\infty}^{\infty} u(y)\psi_j^+(y)dy \tag{1.42}$$

Thus $\delta_j$ vanish for $j = 1, 2, ...$ and $\overline{N}^j(x; k_j) = x\psi_j(x)$ represents a special solution. By using the Fredholm′s alternative theorem, we get

$$\lim_{k \to k_j} [N(x; k) + \frac{\mathrm{i}\psi_j(x)}{(k - k_j)}] = [x + \gamma_j(t)]\psi_j(x). \tag{1.43}$$

The following integral equation is equivalent to RHB

$$\begin{aligned} &N(x, t; k) - \tfrac{1}{2\pi} \textstyle\int_0^{\infty} \omega(x, t; k, \lambda)\alpha(\lambda, t)N(x, t; k)d\lambda + \sum_{j=1}^{n} \psi_j(x, t)\omega(x, t; k, k_j) \\ &\quad = v(x, t, k) \end{aligned} \tag{1.44}$$

with

$$[x + \gamma_j]\psi_j(x, t) - \frac{1}{2\pi \mathrm{i}} \int_0^{\infty} \frac{\delta(\lambda, t)N(x, t, \lambda}{\lambda - k_j} d\lambda + \mathrm{i} \sum_{\substack{l=1 \\ l \neq j}}^{n} \frac{\psi_l(x, t)}{(k_j - k_l)} = 1 \tag{1.45}$$

where

$$v_t(x, t; k) = \int_0^k [f(\lambda, t)e^{\mathrm{i}x(k-\lambda} + g(\lambda)e^{\mathrm{i}\lambda x}]dy, \tag{1.46}$$

and

$$g(\lambda) = \frac{1}{\lambda ln\lambda}, \tag{1.47}$$

as well as

$$\omega(x, t, k, \lambda) = e^{\mathrm{i}(k-\lambda)x} \int_{-\infty}^{x} v(\delta, k)e^{-\mathrm{i}(k-\lambda)s}ds, \quad \lambda > 0. \tag{1.48}$$

$$\begin{aligned} &\omega(x, t, k, \lambda) = e^{\mathrm{i}(k-\lambda)x} \textstyle\int_{\delta}^{x} v(\delta, k)e^{-\mathrm{i}(k-k_j)s}ds + e^{-\mathrm{i}(k-k_j)(x-\delta)} \\ &\textstyle\int_0^k (\frac{f(\lambda,t)e^{-\mathrm{i}\delta(k-\lambda)}}{k_j-\lambda} + \frac{g(\lambda)}{k_j})d\lambda \end{aligned} \tag{1.49}$$

Equation (1.44)−(1.49) can be integrated by substituting (1.26)−(1.27) into (1.18)−(1.19) and then deal with (−) part, so that

$$N(x, t; k) - \frac{1}{2\mathrm{i}\pi} \int_0^{\infty} \frac{\alpha(\lambda, t)N(x, t, \lambda)}{\lambda - (k - \mathrm{i}0)} d\lambda + \mathrm{i} \sum_{j=1}^{n} \frac{\psi_j(x, t)}{k - k_j} = 1. \tag{1.50}$$

By using the following formula

$$\frac{e^{\mathrm{i}x(\lambda-k)}}{\lambda - (k - i0)} = \mathrm{i} \int_{-\infty}^{x} e^{\mathrm{i}s(\lambda-k)}ds, \tag{1.51}$$

and letting $k = 0$ in (1.50) with equation (1.33), equation (1.44), we find that.

$$\frac{e^{\mathrm{i}x(\lambda-k)}}{\lambda-k} = \mathrm{i}\int_{\delta}^{x} e^{\mathrm{i}s(\lambda-k)}ds + \frac{e^{\mathrm{i}\delta(\lambda-k)}}{\lambda-k}. \tag{1.52}$$

It follows from (1.13) that

$$\overline{N} \sim 1 - \frac{u^{+}}{k}, \text{ as } k \to \infty. \tag{1.53}$$

Thus from (1.53) and by using the asymptotics of (1.50) when $k$ tends to $\infty$, we find that

$$u^{+}(x,t) = \frac{1}{2\mathrm{i}\pi}\int_{0}^{\infty} \alpha(k;t)N(x,t;k)dk + \mathrm{i}\sum_{j=1}^{n}\psi_j(x,t). \tag{1.54}$$

Eventually, if we assume that $u$ is real, then the potential will be given by

$$u(x,t) = u^{+}(x,t) + \overline{u^{+}(x,t)} \tag{1.55}$$

Therefore, the potential $u(x,t)$ is defined by equations (1.44)−(1.49) and (1.54)−(1.55) in terms of $\alpha(k,t)$, $f(k,t)$, $\gamma_j$ and $k_j$. The time evolution of these scattering data is shown below.

### 1.2.6 The Time Dependence

From equation (1.9) and $M(x,t;k)$, the time dependence of the scattering data can be determined as follows

$$\mathrm{i}M_t - 2\mathrm{i}M_x + M_{xx} - 2\mathrm{i}[u]_x^{+}M + \alpha M = 0. \tag{1.56}$$

Since $|u|$ tends to zero as $|x|$ tends to infinity, then

$$\mathrm{i}M_t - 2\mathrm{i}M_x + M_{xx} \sim 0, \tag{1.57}$$

as $|x|$ tends infinity. Substituting (1.18) in equation (1.57) with the use of (1.11), gives

$$\alpha_t(k;t) = \mathrm{i}k^2\alpha(k;t). \tag{1.58}$$

Thus

$$\alpha(k;t) = \alpha(k;0)e^{\mathrm{i}k^2t}. \tag{1.59}$$

Substituting eqution (1.33) in (1.57), yields

$$f_t(k;t) = -\mathrm{i}k^2 f(k,t), \tag{1.60}$$

then

$$f(k;t) = f(k;0)e^{-\mathrm{i}k^2t}, \tag{1.61}$$

eventually, from (1.43), we find that $\gamma_{j,t}(t) = 2k_j$ and $\gamma_j(t) = 2k_jt + \mathrm{i}\gamma_{j,0}$ for $j = 0, 1, ..., n$.

## 1.3 Others methods

It is impotrant to point out that there is no available technique for all types of PDEs. As shown previously IST is used to compute single soliton solutions, however there are various others well-known methods that have also been used to derive this type of solutions. Among others, we can cite: tanh-coth method, the sine-cosine method and Hirota's bilinear method. Here, one presents the main features of these three later methods, which are proved to be effective and useful techniques for many number of nonlinear evolution equations.

### 1.3.1 The tanh-coth technique

By wave variable $\varphi = x - ct$, some $PDE$,

$$P(u, u_t, u_x, u_{xx}, u_{xxx}, ...) = 0, \tag{1.62}$$

can be converted to an ODE

$$R(u, u', u'', u''', ...) = 0, \tag{1.63}$$

then rather than integrate equation (1.62), one deals with equation (1.63) as long as every term includes derivatives with making the constants of integration to be zeros. The standard tanh-coth technique was introduced by Malfliet [82] and based on introducing tanh as a new variable and representing all derivatives by this new variable as in the following example

**Example 9.** *When we set $T = tanh(\varphi)$, $\varphi = x - ct$, this gives*

$$\begin{aligned} T &= tanh(\varphi), \\ T' &= 1 - T^2, \\ T'' &= -2T + 2T^3, \\ T''' &= -2 + 8T^2 - 6T^4, \\ T^4 &= 16T - 40T^3 + 24T^6, \end{aligned} \tag{1.64}$$

more precisely, regarding a new independent variable

$$X = tanh(k\varphi), \quad \varphi = x - ct, \tag{1.65}$$

with the wave number $k$, due to this step, all derivatives will also change as follows

$$\begin{aligned} \tfrac{d}{d\varphi} &= k(1 - X^2)\tfrac{d}{dX}, \\ \tfrac{d^2}{d\varphi^2} &= -2k^2X(1 - X^2)\tfrac{d}{dX} + k^2(1 - X^2)^2\tfrac{d^2}{dX^2}, \\ \tfrac{d^3}{d\varphi^3} &= 2k^3(1 - X^2)(3X^2 - 1)\tfrac{d}{dX} - 6k^3X(1 - X^2)^2\tfrac{d^2}{dX^2} + k^3(1 - X^2)^3\tfrac{d^3}{dX^3}, \\ \tfrac{d^4}{d\varphi^4} &= -8k^4X(1 - X^2)(3X^2 - 2)\tfrac{d}{dX} + 4k^4(1 - X^2)^2(9X^2 - 2)\tfrac{d^2}{dX^2} \\ &\quad -12k^4X(1 - X^2)^3\tfrac{d^3}{dX^3} + k^4(1 - X^2)\tfrac{d^4}{dX^4}, \end{aligned} \tag{1.66}$$

As was shown in [112] that the solution in the tanh-coth method can be expressed by the finite expansion

$$u(k\varphi) = S(X) = \sum_{j=0}^{N} a_j X^j + \sum_{j=1}^{N} b_j X^{-j}, \tag{1.67}$$

$N$ can be either a positive integer or noninteger and should be determined. if $b_j = 0,\ 1 \leq k \leq N$, then Expansion (1.67) turn to the standard tanh technique. In order to accomplish the balance method, we can observe from (1.66) and (1.67) that the highest order for $u$ and its derivatives are

$$\begin{aligned} u &\to N \\ u^n &\to nN \\ u' &\to N+1 \end{aligned} \tag{1.68}$$

$$u'' \to N+2 \tag{1.69}$$

$$u^s \to N+s$$

we need to balance the linear and the nonlinear highest order terms to determine the parameter $N$.

### 1.3.2 The sine-cosine technique

The same procedure is followed for equation (1.63) as in the previous method. In this technique, the following forms of solutions are useful and written in the form

$$u(x,t) = \lambda cos^{\alpha}(k\varphi), \quad |\varphi| \leq \frac{\pi}{2k}, \tag{1.70}$$

and

$$u(x,t) = \lambda sin^{\alpha}(k\varphi), \quad |\varphi| \leq \frac{\pi}{k}, \tag{1.71}$$

where $\lambda$, $k$ and $\alpha$ are parameters that will be determined. From (1.70) and (1.71), one gets

$$\begin{aligned} (u^n)'(k\varphi) &= -n\alpha k\lambda^n cos^{n\alpha-1}(k\varphi)sin(k\varphi) \\ (u^n)''(k\varphi) &= -n^2\alpha^2k^2\lambda^n cos^{n\alpha}(k\varphi) + nk^2\lambda^n\alpha(n\alpha-1)cos^{n\alpha-2}(k\varphi), \end{aligned} \tag{1.72}$$

and

$$\begin{aligned} (u^n)'(k\varphi) &= n\alpha k\lambda^n sin^{n\alpha-1}(k\varphi)cos(k\varphi) \\ (u^n)''(k\varphi) &= -n^2\alpha^2k^2\lambda^n sin^{n\alpha}(k\varphi) + nk^2\lambda^n\alpha(n\alpha-1)sin^{n\alpha-2}(k\varphi). \end{aligned} \tag{1.73}$$

We obtain a trigonometric equation by substituting (1.72) or (1.73) in (1.63) and the parameters can then be determined by applying first the balance method on each pair powers of cosine or sine. the next step is to collect all the same exponent coefficients in cosine or sine,

where these coefficients should be vanish. after these two steps, one gets a system of algebraic equations with the unknowns parameters $\alpha$, $\lambda$ and $k$ that should be determined. Then the solutions will follow immediately. As we notice that these two methods ( the tanh$-$coth and the sine$-$cosine technique ) require less computational work than some well$-$known methods as truncated Painlev′e expansion, IST and Hirota′s bilinear method.

### 1.3.3 Hirota's bilinear technique

This method was introduced by Hirota in [44], where his bilinear operators was defined by

$$D_t^n D_x^m(E,F) = \left(\frac{\partial}{\partial t} - \frac{\partial}{\partial t'}\right)^n \left(\frac{\partial}{\partial x} - \frac{\partial}{\partial x'}\right)^m E(x,t)F(x',t')|x'=x, t'=t. \tag{1.74}$$

In what follows, the main steps of this technque is shown. One begins by presenting some differentials of the bilinear $D-$operators

$$\begin{aligned}
&D_x(E,F) = E_xF - EF_x,\\
&D_x^2(E,F) = E_{2x}F - 2E_xF_x + EF_{2x},\\
&D_xD_t(E,F) = D_x(E_tF - EF_t) = E_{xt}F - E_tF_x - E_xF_t + EF_{xt},\\
&D_xD_t(E,E) = 2(EE_{xt} - E_xE_t),\\
&D_x^4(E,F) = E_{4x}F - 4E_{3x}F_x + 6E_{2x}F_{2x} - 4E_xF_{3x} + EF_{4x},\\
&D^n(E,E) = 0, \text{ if } n \text{ is odd.}
\end{aligned} \tag{1.75}$$

and their properties

$$\begin{aligned}
&\tfrac{D_t^2(g,g)}{g^2} = \iint u_{tt}dxdx, \quad \tfrac{D_tD_x^3(g,g)}{g^2} = u_{xt} + 3u\int xu_tdx',\\
&\tfrac{D_x^2(g,g)}{g^2} = u, \quad \tfrac{D_x^4(g,g)}{g^2} = u_{2x} + 3u^2,\\
&\tfrac{D_tD_x^2(g,g)}{g^2} = ln(f^2)_{xt}, \quad \tfrac{D_x^6(g,g)}{g^2} = u_{4x} + 15uu_{2x} + 15u^3,\\
&\tfrac{D_t^2(g,g)}{g^2} = \iint u_{tt}dxdx, \quad \tfrac{D_tD_x^3(g,g)}{g^2} = u_{xt} + 3u\int u_tdx',
\end{aligned} \tag{1.76}$$

where

$$u(x,t) = 2(lng(x,t))_{xx}. \tag{1.77}$$

For the KdV equation,

$$u_t + 6uu_x + u_{xxx} = 0. \tag{1.78}$$

The solution is expressed by

$$u(x,t) = 2\frac{\partial^2}{\partial x^2}logg, \tag{1.79}$$

with $g(x,t)$ can be expanded as

$$g(x,t) = 1 + \sum_{n=1}^{\infty} \epsilon^n g_n(x,t), \tag{1.80}$$

where $\epsilon$ indicates a formal expansion parameter. If we look for the one$-$soliton solution, then we set

$$g(x,t) = 1 + \epsilon g_1, \tag{1.81}$$

while for the two-soliton solution, we set

$$g(x,t) = 1 + \epsilon g_1 + \epsilon^2 g_2, \tag{1.82}$$

and so on. the next step is to determine these functions $g_1$, $g_2$, $g_3$...by the use of Hirota$'$s bilinear formalism. The $N-$soliton solution is found from

$$g_1 = \sum_{j=1}^{N} exp(\theta_j), \quad \theta_j = k_j x - c_j t, \tag{1.83}$$

where $k_j$ is the wave number. Analytical study of nonlinear dispersive equations gives rigorous solutions and deep understanding of such waves phenomena. However such analytical treatments are not always practical, that why numerical methods play a significant role in understanding these complicated phenomena via numerical solutions.

# Chapter 2

# Numerical Methods

## 2.1 Introduction

The numerical results give conjectures and motivations for more analytical investigations. Indeed a lot of crucial waves phenomena discovered first numerically such as finite time blows up, fractal scattering and elastic collision of solitary waves. For the space discretization, the typical numerical techniques used are finite differences, finite elements and recently spectral methods and finite volumes. In the next two sections, we describe some numerical techniques used for the two aspects of nonlinear dispersive PDEs computations, namely Generation of solitary wave solutions and Evolution simulations.

## 2.2 Generation of solitary waves

The study of special type localized solutions play significant role in the nonlinear wave phenomena areas. Among these types of solutions, we are interested in the so-called solitary wave solutions ( Solitons ) that preserve their shapes during propagation. If these types of waves are stable as for example solitons in either the KdV or NLS equations, then they can be maintained for long-time solutions; but they keep their importance even in the instable case, such as the 2D NLS ground-state solitary waves in the collapse theory. For the last decades, many papers with developments of much more easy and efficient methods for the computation of these types of nonlinear waves solutions. in this part, we present some efficient methods that do not require much effort, o lot of memory and time to implement even in higher dimensions.

### 2.2.1 Petviashvili technique

This numerical approach was introduced in 1976 by Petviashvili for power−law nonlinearity equations of constant coefficients. The basic idea in this technique is the well known fixed-point iteration with the key of stability which is called a stabilizing factor. In [94] results on the convergence conditions of the first problem solved by this method were developed. It was then extended to other wave equations, see for exemple [5, 74, 86]. Solitary wave solutions

$u(x,t) = \varphi(x - ct)$ of (2.38) can be characterized by the following stationary equation

$$L\varphi = N(\varphi), \tag{2.1}$$

which can be rewritten as

$$\varphi = L^{-1}N(\varphi). \tag{2.2}$$

Unfortunately, if one directly iterates (2.2) to compute the solitary waves solution then this iteration will diverge. To overcome this divergence problem, Petviashvili method idea uses the stabilizing factor. The introduction of this factor is for suppress the iteration function if it grows or pump up it if it decays. Equation (2.2) becomes

$$\varphi_{n+1} = M_n^{\gamma} L^{-1} N(\varphi_n). \tag{2.3}$$

with the stabilizing factor

$$M_n^{\gamma} = \frac{\langle \varphi_n, N(\varphi_n) \rangle}{\langle \varphi_n, \varphi_n \rangle}, \tag{2.4}$$

where $\gamma$ is a constant has to be chosen according to the next theorem

**Theorem 10.** *For the solitary waves of equation* (2.2)*, the Petviashvili approach converges when* $1 < \gamma < \frac{p+1}{p-1}$ *and the fastest convergence appears if* $\gamma = \gamma_{opt} = \frac{p}{p-1}$ *for an initial condition close enough to the exact solution u(x). Here p is the degree of nonlinearity.*

For the proof of this Theorem, see [94, 108].

### 2.2.2 Accelerated imaginary-time evolution technique (AITEM)

The second numerical technique presented here to determine the grond state is the imaginary-time evolution technique.The idea of this approach has been available for both linear and nonlinear equations (see [70, 26]). It is based on the fact that the ground state is turned into diffusive type equation of fictitious time evolution and it requires that after each step of time integration the solution has to be normalized. To keep a fixed power, a ground state would be obtained when the solution develops into a steady state. More recently, this method has been developed into a new one called "accelerated imaginary-time evolution" approach in order to make it more faster. If the solitary wave is sign definite, then the convergence of this technique is directly connected to the linear stability of the later wave and this is the most significant feature in this technique, see [110]. To describe this method, we need to consider a wave equation as an example, we choose here the general multidimensional NLS equation as in [108]

$$\mathrm{i}U_t + \nabla^2 U + F(|U|^2, \mathbf{x})U = 0, \tag{2.5}$$

with a real-valued function $F$. This equation admits a solitary wave of the form

$$U(\mathbf{x}, t) = u(\mathbf{x})e^{\mathrm{i}\omega t}, \tag{2.6}$$

where $\omega$ is the propagation constant, $u(\mathbf{x})$ is a localized function of real-valued which satisfies

$$Lu = \omega u, \tag{2.7}$$

with the operator $L$ defined by

$$L \equiv \nabla^2 + F(u^2, \mathbf{x}). \tag{2.8}$$

From the dispersive equation (2.5) and by replacing $t$ with $-\mathrm{i}t$, we can obtain the following diffusive equation

$$u_t = Lu. \tag{2.9}$$

Then to preserve a fixed power, we need to normalize the solution after any time integration step. the easiest way to integrate equation (2.9) is the use of Euler approach, so the scheme of ITEM is defined as

$$\begin{aligned} u_{n+1} = &\quad \left[\tfrac{P}{\langle \hat{u}_{n+1}, \hat{u}_{n+1}\rangle}\right]^{\frac{1}{2}} \hat{u}_{n+1}; \\ \hat{u}_{n+1} = &\quad u_n + [Lu]_{u=u_n}\, \Delta t, \end{aligned} \tag{2.10}$$

where the propagation constant $\omega$ becomes

$$\omega = \frac{1}{p} \langle u, Lu \rangle .$$

Since the time integration by using the Euler method for the diffusive equation suffers stringent stability restrictions on the time step, the ITEM method would be very slow. Fortunately, there are schemes that can be used to fix this difficulty such as the implicit time-stepping techniques or a preconditioning operator. The later strategy is the known as accelerated ITEM (AITEM), in this technique one deals with the preconditioned imaginary-time equation (2.11) defined below; rather, equation (2.9).

$$u_t = M^{-1}[Lu - \omega u] \tag{2.11}$$

where $M$ define acceleration operator. using again the Euler approach, the AITEM is

$$u_{n+1} = \left[\frac{P}{\langle \hat{u}_{n+1}, \hat{u}_{n+1}\rangle}\right]^{\frac{1}{2}} \hat{u}_{n+1}; \tag{2.12}$$

$$\hat{u}_{n+1} = u_n + M^{-1}(Lu - \omega u)_{u=u_n, \omega=\omega_n} \Delta t, \tag{2.13}$$

$$\omega_n = \frac{\langle M^{-1}u, Lu\rangle}{\langle M^{-1}u, u\rangle}|_{u=u_n}.$$

For the case of multidimensional NLS equation, the solitary wave linearization operator is defined as

$$L' = \nabla^2 - \omega + F(u^2, \mathbf{x}) + 2u^2 F_{u^2}(u^2, \mathbf{x}). \tag{2.14}$$

### 2.2.3 Squared-operator iteration technique

Solitary waves in arbitrary spatial dimensions can be written by

$$Lu(\mathbf{x}) = 0, \tag{2.15}$$

where $u$ is a solitary wave of real-valued vector and $\mathbf{x}$ represents a multidimensional space variable. In this equation, the solitary wave propagation constant is lumped into $L$. Let $L'$ be the linearized operator around the solution $u$ for equation (2.15), this means

$$L(u+u') = L'u' + O(u'^2), \quad u' \ll 1. \tag{2.16}$$

To apply the squared-operator iteration tool ( SOM method); first, one needs to integrate numerically the following squared-operator evolution equation

$$u_t = -M^{-1}L'^{*}M^{-1}Lu. \tag{2.17}$$

Here, $^*$ indicates the Hermitian, $M$ is a Hermitian operator and positive-definite in order to ensure and accelerate the convergence. Choosing a simplest time-stepping approach for equation (2.17) as for instance the forward Euler method, gives the following scheme

$$u_{n+1} = u_n - [M^{-1}L'^{*}M^{-1}Lu]_{u=u_n}\Delta t, \tag{2.18}$$

where the time-step parameter is denoted by $\Delta t$. It is worth pointing out here some remarks, (see [109]for more details).

**Remark 11.** *The remarks that we have on SOM method are:*

1. *In the SOM method, we do not need to normalize the power.*
2. *Unlike the AITEM method the propagation constant in the SOM technique is prefixed.*
3. *Squared-operator equations expressed by* (2.17) *is not the only available one. for example, the following equation*
$$u_t = -M^{-2}L'^{*}Lu, \tag{2.19}$$
*can also be used.*
4. *The forward Euler approach is not the only time-stepping scheme that can be used to deal with equation* (2.17)*, but it is the most efficient one.*
5. *The SOM scheme represented in* (2.18) *converges for all $\Delta t$ less then a certain threshold.*

## 2.3 Evolution simulations

### 2.3.1 Space discretization: spectral method

In recent years, due to theirs advantages, Spectral Methods have great advances and developments. The main idea of spectral Methods is to approximate the function of solution by a finite series of a known basis. The deferent types of the approaches are from which function class of the sum must be selected and the technique should be applied to determine the expansion coefficients. There are three main types: Tau, Galerkin and pseudospectral (known also by collocation) technique. Here, we just concern with the later one. For theoretical review on spectral methods, we recommend [49, 50, 17, 18, 16] and for more practical applications of pseudospectral methods, see [37, 103]. Pseudospectral approaches are mostly well-suited with periodic boundary conditions, so that we consider Fourier collocation method in a periodic setting of one space dimension for simplicity.

### Why spectral methods

In contrast to both finite difference methods and finite element methods, spectral schemes are global, which means they necessary invoke many function values far away from the interesting points. In spectral Methods, the function that we want to differentiate is approximated as the following finite sum of basis functions:

$$u(x) \approx \sum_{k=0}^{N} \alpha_k \phi_k(x), \tag{2.20}$$

with $\phi(x)$ can be for instance trigonometric functions, Legendre or Chebyshev polynomials, this approach allows us to obtain an exact differentiation for these functions. Spectral methods have the following benefits in solving time dependent PDEs:

- Spectral methods give extremely accurate numerical results of exponential convergence.
- The methods are almost free of both dispersive or dissipative errors.
- Spectral methods are of high performance even in many cases that suffer from nonsmoothness or discontinuities and variable coefficients.
- Up to now, spectral methods have appeared to be the highly successful approches in various fields as for instance weather prediction, turbulence modeling, seismic modeling, nonlinear waves. In fact the list of the areas is still growing (see [16, 37] and references therein).
- Nearly all types of spectral methods can be implemented without much efforts, particularly Fourier spectral methods because of Cooley and Tukey algorithm for the Fast Fourier transform (FFT) [28] (see Appendix A).
- The common features of all types of these methods is the requirement of less time and less memory with respect to finite volume (FV), finite element (FE) or finite difference (FD) techniques, since they need low grid points number to achieve high accuracy. This benefit is crucial especially in two or more dimensions.

### Different approaches for spectral methods

According to the selected way to determine the expansion coefficients $\alpha_k$, there are three main used techniques. A common requirement in all of them is to keep the residual as low as possible in the whole domain while making the boundary conditions hold. These approaches are resumed in the following

- **Galerkin** make a new set of the combined original basis functions so that all these new functions satisfy the boundary conditions. Then the residual should be orthogonal to as many of the basis functions of the new set as possible.
- **Tau** the requirement of this technique is that the residual should be orthogonal to as many of the basis functions as possible and $\alpha_k$ has to be chosen such that the boundary conditions are satisfied.

- **Collocation** similar to Galerkin technique, the requirement is that $a_k$ should be chosen so that the boundary conditions are satisfied, but in this case the residual has to be zero at all chosen spatial points (called collocation nodes).

### 2.3.2 Fourier collocation method

Spectral methods involve a way of translating a continuous space and time equation into a discrete setting when we can solve it numerically. In this part, we give a description of Fourier spectral method in space discretization.

#### Fourier transform

Let us denote by $\hat{u}$ the Fourier transform of a function $u \in L^2(\mathbb{R})$, that is defined by

$$\mathcal{F}[u](k) = \widehat{u}(k) = \int_{-\infty}^{+\infty} u(x) e^{-\mathrm{i}kx} dx, \quad k \in \mathbb{R} \tag{2.21}$$

where the corresponding inverse transform is written as

$$\mathcal{F}^{-1}[u](x) = u(x) = \frac{1}{2\pi} \int_{-\infty}^{+\infty} \mathcal{F}[u](k) e^{\mathrm{i}kx} dk, \quad x \in \mathbb{R} \tag{2.22}$$

with $k$ is the wave number. The next theorem shows the connection between the function smoothness and its Fourier transform

**Theorem 12.** *For $u \in L^2(\mathbb{R})$ and $\widehat{u}$ associated Fourier transform, we have the following statements*

1. *For $r \geq 0$, if $u$ has an $r^{th}$ derivative of bounded variation and $r-1$ continuous derivatives in $L^2$, we have*
$$\widehat{u} = O(|k|^{-r-1}) \quad as \ |k| \to \infty.$$

2. *For any $m \geq 0$, if*
$$\widehat{u} = O(|k|^{-m}) \quad as \ |k| \to \infty,$$
*then the function $u$ has infinitly many continuous derivatives in $L^2(\mathbb{R})$. The converse also holds.*

3. *For two postive constants $\alpha$ and $\beta$, such that we can extend $u$ to an analytic function in the complex strip $|Imz| < \alpha$ and for every $y \in (-\alpha, \alpha)$, $\|u(. + \mathrm{i}y)\| \leq \beta$ uniformly, with $\|u(. + \mathrm{i}y)\| \leq \beta$ is the $L^2$ norm along the horizontal line $Imz = y$, then*
$$u_\alpha = e^{\alpha|k|}\widehat{u}(k) \in L^2(\mathbb{R}).$$
*The converse also holds.*

4. *For a strict positive $\alpha$ such that $|u(z)| = o(e^{\alpha|z|})$ as $|z|$ tends to infinity for every $z \in \mathbb{C}$, if we can extend $u$ to entire function, then $\widehat{u}$ has compact support in $[-\alpha, \alpha]$, which means*
$$\widehat{u}(k) = 0, \quad for \ every \ |k| > \alpha.$$
*The converse also holds.*

For the proof of these results, see [103] and references therein.

**Discrete Fourier expansion**

In practical applications, we use the discrete Fourier transform instead of the Continuous Fourier transform. Consider the set of nodes

$$x_j = \frac{2\pi j}{N}, \quad j = 0, ..., N-1, \tag{2.23}$$

for each integer $N > 0$. The corresponding discrete Fourier coefficients are given by

$$\widetilde{u} = \frac{1}{N} \sum_{j=0}^{N-1} u(x_j) e^{-\mathrm{i}kx_j}, \quad k = -\frac{N}{2}, ..., \frac{N}{2} - 1, \tag{2.24}$$

for a function $u \in [0, 2\pi]$, using the orthogonality property

$$\frac{1}{N} \sum_{j=0}^{N-1} u(x_j) e^{-\mathrm{i}px_j} = \left\{ \begin{array}{ll} 1 & \text{if} \quad p = N_m, \quad m = 0 \pm 1, \pm 2, ..., \\ \\ 0 & \text{otherwise} \end{array} \right\}. \tag{2.25}$$

The inverse formula is given by

$$u(x_j) = \sum_{k=-N/2-1}^{N/2} \widetilde{u}_k e^{\mathrm{i}kx_j}, \quad j = 0, ..., N-1. \tag{2.26}$$

Thus, the trigonometric interpolant of $u$ is

$$I_N u(x) = \sum_{k=-N/2-1}^{N/2} \widetilde{u}_k e^{\mathrm{i}kx}, \tag{2.27}$$

which means that $I_N u(x_j) = u(x_j)$ for $j = 0, 1, ..., N-1$. The polynomial (2.27) is called the discrete Fourier series of $u$. Hence the discrete Fourier transform (DFT) can be defined as the mapping between $u(x_j)$ and $\widetilde{u}_k$, for $j = 0, 1, ..., N-1$ and $k = -N/2, ..., N/2 - 1$. The DFT can be implemented by the algorithm of Fast Fourier Transform (FFT) (see Appendix A, for details).
In the the following, we find discrete version of theorem (12)

**Theorem 13.** *For a function $u$ that has a bounded variation first derivative in $L^2(\mathbb{R})$, $v$ is the discrete function defined by $v_j = u(x_j)$ on the interval $I$, then for $k \in [\frac{\pi}{h}, \frac{\pi}{h}]$ or for any constant $L$ such that $k \in [-L, L]$, the next estimates hold uniformly*

1. *If $u$ has a $r^{th}$ bounded variation derivative in $L^2(\mathbb{R})$ for some positive $r$ and $r-1$ continuous derivatives, then*

$$|\widehat{v}(k) - \widehat{u}(k)| = O(h^{r+1}) \quad \text{as } h \to 0$$

2. *If $u$ has many infinitely continuous derivatives in $L^2(\mathbb{R})$, then*

$$|\widehat{v}(k) - \widehat{u}(k)| = O(h^p) \quad \text{as } h \to 0$$

*for any $p \geq 0$*

3. *If $u$ can be extended to an analytic function for two strict positive numbers $\alpha$ and $\beta$, such that $|Imz| < \alpha$ and for any $y \in (-\alpha, \alpha)$, $\|u(. + \mathrm{i}y)\| \leq \beta$ uniformly, Then*

$$|\widehat{v}(k) - \widehat{u}(k)| = O(e^{-\pi(\alpha-\epsilon)/h}) \quad as\ h \to 0$$

*for any $\epsilon > 0$.*

4. *If $|u(z)| = o(e^{\alpha(z)})$ as $|z| \to \infty$ for a strict positive $\alpha$ and for every complex value $z \in \mathbb{C}$ and if one can extend it to an entire function, then, provided $h \leq \frac{\pi}{\alpha}$*

$$\widehat{v}(k) = \widehat{u}(k)$$

For more details on these results, see [53, 100, 103].

**Differentiation**

In a spectral method there are two manners to accomplishe differentiation:

**1-** In transform space, differentiation consists only multiplying any Fourier coefficient by $\mathrm{i}k$, with $k$ represents the corresponding wavenumber, i.e., Let

$$Su = \sum_{k=-\infty}^{\infty} \widehat{u}_k \phi_k$$

be the Fourier series of $u$, its truncated Fourier series is defined for an integer $m$ by

$$P_N u(x) = \sum_{k=-m}^{m} \widehat{u}_k e^{\mathrm{i}kx}, \tag{2.28}$$

so the Fourier series of $u'$ is given by

$$Su' = \sum_{k=-\infty}^{\infty} \mathrm{i}k\widehat{u}_k \phi_k, \tag{2.29}$$

Consequently, we find that there is commute between truncation and differentiation, i.e.,

$$(P_N u)' = P_N u', \tag{2.30}$$

**2-**In physical space, differentiation is based on the values of $u$ at the the grid points (2.23). To compute $u'j$ at the Fourier nodes $x_j$, first we need to evaluate the DFT according to (2.24) and then perform the differentiation in transform space as explained before; and finally, according to (2.26) transform back to the former space.
The approximate derivative values $(D_N u)_j$ at the grid points $x_j$ are hence given by

$$(D_N u)_j = \sum_{k=-N/2}^{N/2-1} \widetilde{u}_k^{(1)} e^{2\mathrm{i}k_j \pi/N}, \quad j = 0, 1, ..., N-1, \tag{2.31}$$

with

$$\widetilde{u}_k^{(1)} = \mathrm{i}k\widetilde{u}_k = \frac{\mathrm{i}k}{N}\sum_{l=0}^{N-1} u(x_l)e^{-2\mathrm{i}kl\pi/N}, \quad k = -N/2, ..., N/2-1. \tag{2.32}$$

The above procedure allows to compute the first derivative of $(I_N u)$, i.e.,

$$D_N u = (I_N u)',$$

where $D_N u$ is known as the Fourier interpolation derivative to the function $u$. In the same way, we can compute the $m^{th}$ derivative, but $(\mathrm{i}k)$ should be replaced by $(\mathrm{i}k)^m$. It is worth noticing that

$$D_N u \neq P_N u'.$$

Differentiation and Interpolation do not commute, i.e.,

$$(I_N u)' \neq I_N u'.$$

### 2.3.3 Aliasing error

Let $u$ be a continuous function, the Fourier expansion is typically defined by

$$u(x) = \sum_{k=-\infty}^{\infty} \widehat{u}(x)e^{\mathrm{i}\pi kx}.$$

Every Fourier mode $e^{\mathrm{i}\pi(k+wN)x}$ in a distinct set of $N$- equi-distant points in $[-1,1]$ for $w = ...-1, 0, 1, ...$, appears identical, see Figure 2.1. The function $u$ is sampled by a DFT at such grid point and these modes become indistinguishable. Let us assume that $N$ is odd, i.e., $N = 2m+1$, for $k \in [-m, m]$,

$$\widetilde{u} = \sum_{k=-\infty}^{\infty} \widehat{u}(k+wN),$$

the trigonometric interpolating that defined as in (2.27)

$$I_N u(x) = \sum_{k=-m}^{m} \widetilde{u}(k)e^{\mathrm{i}\pi kx},$$

does not take the exact values between grid point, but not at these points. The difference between the interpolating and the truncation (that defined as in (2.28)) is called the aliasing error, i.e.,

$$R_N u(x) = I_N u(x) - P_N u(x) = \sum_{k=-m}^{m} \sum_{\substack{w=-\infty \\ w\neq 0}}^{\infty} \widehat{u}(k+wN)e^{\mathrm{i}\pi kx}.$$

The next theorem shows the accuracy of Fourier spectral differentiation

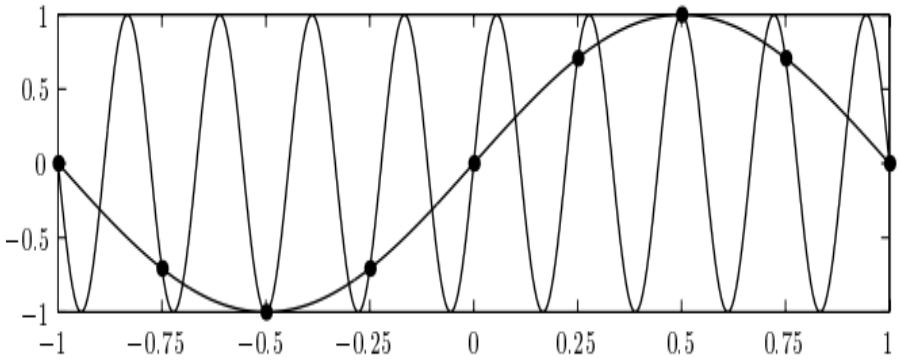


Figure 2.1: Example of Aliasing effect for $sin\pi x$ and $sin9\pi x$.

**Theorem 14.** *For a function $u$ that has a $m^{th}$ bounded variation derivative with $m \geq 1$, and for a $m^{th}$ spectral derivative $w$ of $u$ on the grid $h\mathbb{Z}$. The next estimates hold uniformly for every $x \in h\mathbb{Z}$*

1. *If $u$ has a $r^{th}$ bounded variation derivative in $L^2(\mathbb{R})$ for some positive $r$ such that $r \geq m+1$ and $r-1$ continuous derivatives, then*

$$|w_j - u^m(x_j)| = O(h^{r-m}) \quad as\ h \to 0$$

2. *If $u$ has many infinitely continuous derivatives in $L^2(\mathbb{R})$, then*

$$|w_j - u^m(x_j)| = O(h^p) \quad as\ h \to 0$$

   *for all $p \geq 0$*

3. *If $u$ can be extended to an analytic function for two strict positive numbers $\alpha$ and $\beta$, such that $|Imz| < \alpha$ and for any $y \in (-\alpha, \alpha)$, $\|u(. + \mathrm{i}y)\| \leq \beta$ uniformly, Then*

$$|w_j - u^m(x_j)| = O(e^{-\pi(\alpha-\epsilon)/h}) \quad as\ h \to 0$$

   *for all $\epsilon > 0$*

4. *If $|u(z)| = o(e^{\alpha(z)}$ as $|z| \to \infty$ for a strict positive $\alpha$ and for every complex value $z \in \mathbb{C}$ and if one can extend it to an entire function, then, provided $h \leq \frac{\pi}{\alpha}$*

$$w_j = u^m(x_j)$$

   .

This Theorem has been also illustrated and discussed in [103].

### 2.3.4 Gibbs phenomenon

To understand this phenomenon, let us discuss the following Example

**Example 15.** *Consider the periodically extended function*

$$u(x) = \left\{ \begin{array}{ll} x & 0 \leq x \leq \pi, \\ \\ x - 2\pi & \pi < x \leq 2\pi, \end{array} \right\} \tag{2.33}$$

*The Fourier series expansion coefficients are given by*

$$\widehat{u}_n = \left\{ \begin{array}{ll} \mathrm{i}(-1)^{|n|}/n & n \neq 0, \\ \\ 0 & n = 0. \end{array} \right\} \tag{2.34}$$

In Figure 2.2, we can notice the strong oscillations that appear around the discontinuity and they do not decay even for an increasing resolution, but we observe also the slow convergence of the approximation away from the discontinuity see Figure 2.2 (right). At the most, this convergence is linear, accompanying to the expansion coefficients decay. In Figure 2.2, we see that the error of the discontinuity does not disappear for an increasing resolution. So, inspite of the convergence of the approximation in the mean, this convergence is not uniform. To see the convergence of the approximation in the mean, we can use Parseval's identity to estimate the $L^2-$error.

$$\|u - P_N u\|_{L^2[0,2\pi]} = 2\pi \left( \sum_{|n|>N} \frac{1}{n^2} \right)^{1/2} \simeq \frac{1}{\sqrt{N}}.$$

Although the smoothness and periodicity of the function away from the discontinuity, the presence of the discontinuity dominates the global rate of convergence. Therefore, in this example we find two main aspects of the problem: the non uniform convergence close to the discontinuity, and the slow convergence far from the discontinuity. These two aspects characterize the so-called Gibbs phenomenon. For more details see also [43]

## 2.4 Time discretization methods

In this section, we present some well known standard time discretization methods for stiff systems and discuss their stability conditions.

### 2.4.1 Runge-Kutta methods

Runge-Kutta techniques are multistep time discretizations with single-step. Their three versions are

- A second$-$order Runge-Kutta (RK2) technique can be written as follows

$$u^{n+1} = u^n + \frac{1}{2}\Delta t[f(u^n, t^n) + f(u^n + \Delta t f(u^n, t^n), t^n + \Delta t)] \tag{2.35}$$

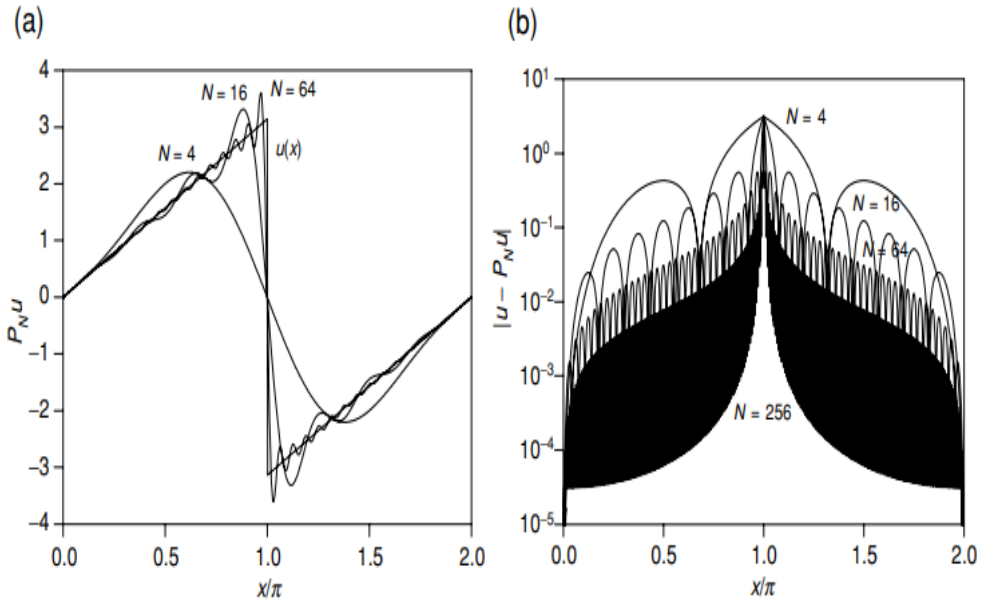


Figure 2.2: On the left, the Gibbs phenomenon is illustrated from the approximation of a discontinuous function by the continuous Fourier series. On the right, we show the pointwise error of this approximation for an increasing resolution.

- A famous third−order Runge-Kutta (RK3) is of the form

$$\begin{aligned} R_1 &= f(u^n, t^n), \\ R_2 &= f(u^n + \tfrac{1}{2}\Delta t R_1, t^n + \tfrac{1}{2}\Delta t), \\ R_3 &= f(u^n + \tfrac{3}{4}\Delta t R_2, t^n + \tfrac{3}{4}\Delta t), \\ u^{n+1} &= u^n + \tfrac{1}{9}\Delta t[2R_1 + 3R_2 + 4R_3]. \end{aligned} \tag{2.36}$$

- The standard fourth-order Runge-Kutta (RK4) technique is

$$\begin{aligned} R_1 &= f(u^n, t^n), \\ R_2 &= f(u^n + \tfrac{1}{2}\Delta t R_1, t^n + \tfrac{1}{2}\Delta t), \\ R_3 &= f(u^n + \tfrac{1}{2}\Delta t R_2, t^n + \tfrac{1}{2}\Delta t), \\ R_4 &= f(u^n + \Delta t R_3, t^n + \Delta t), \\ u^{n+1} &= u^n + \tfrac{1}{6}\Delta t[R_1 + 2R_2 + 2R_3 + R_4]. \end{aligned} \tag{2.37}$$

### 2.4.2 Integrating factor methods

In the theory of ODEs, multiply both sides of an equation by an integrating factor and use some change of variables are a first basic idea, see for instance [72]. A similar idea has been developed in PDEs theory. the method involves to use a change of variable to help us to get the exact solution of the linear part and then choose a suitable numerical scheme to solve the transformed, nonlinear part. This method was introduced by Lawson [75] in 1967 and then it has been used for PDEs by Milewski and Tabak [85], Fornberg and Driscoll [38], Cox and Matthews [29]... Now we apply this method on the following semi-linear problems

$$u_t = Lu + N(u,t), \tag{2.38}$$

we start by defining the following transformation

$$v = e^{-Lt}u, \tag{2.39}$$

here $e^{-Lt}$ is called the integrating factor. By differentiating (2.39), we have

$$v_t = -e^{-Lt}Lu + e^{-Lt}u_t. \tag{2.40}$$

From (2.38), we get that

$$e^{-Lt}u_t - e^{-Lt}Lu = v_t = e^{-Lt}N(u). \tag{2.41}$$

Then,

$$v_t = e^{-Lt}N(e^{Lt}v) \tag{2.42}$$

Equation (2.42) can be solved by choosing a time-stepping method, for example RK4.

### 2.4.3 Sliders methods

We can say that sliders schemes idea is an extension of implicit-explicit methods idea (that is an explicit multistep scheme to integrate the nonlinear part and an implicit formula to deal with the linear part of the problem, see [22] for the application of these methods on KdV equation) because sliders techniques consist to split the problem into linear and nonlinear part. But in addition to that split, the linear equation is also divided into three regions in Fourier space: high, medium, and low wavenumbers, and we use a convenient numerical scheme in each part. Unfortunately, these methods are not stable when not purely dispersive equations are considered. to generalize the conception, Driscoll introduced a very similar principle by making different schemes to deal with the fast and slow modes.

### 2.4.4 Exponential time-differencing methods

We focus here only in one formula of these methods based on Runge−Kutta scheme which is the exponential time-differencing fourth order Runge–Kutta ETDRK4 scheme, since unlike the others formula of the ETD, ETDRK4 work successfully even if the matrix $L$ is not diagonal. related ideas of the ETD scheme in the ODE context were developed in 1928 ( see [35]) and

then they have been used in many reviews ( see for example [11, 21, 29]). In their paper, Cox and Matthews gave the ETDRK4 scheme which is based on ETD methods in combination with the fourth-order Runge–Kutta time-stepping. Since the basic idea in the ETD is to integrate (2.38) exactly over a time step of length $h$, with respect to $t$.

$$u_{n+1} = e^{Lh}u_n + \int_0^h e^{L(h-\sigma)}N(u(t_n+\sigma), t_n+\sigma)d\sigma.$$

Then, the ETDRK4 schemes are given as follows: if we set

$$\begin{aligned}
a_n &= u_n E_2 + (E_2 - I)N(u_n, t_n)L^{-1}, \\
b_n &= u_n E_2 + (E_2 - I)N(a_n, t_n + h/2)L^{-1}, \\
c_n &= a_n E_2 + (E_2 - I)(2N(b_n, t_n + \tfrac{h}{2}) - N(u_n, t_n))L^{-1}, \\
\phi_1 &= (L^2h^2 - 3Lh + 4)E_1 - Lh - 4, \\
\phi_2 &= (Lh - 2)E_1 + Lh + 2, \\
\phi_3 &= (-Lh + 4)E_1 - L^2h^2 - 3Lh - 4;
\end{aligned} \tag{2.43}$$

we get

$$\begin{aligned}
u_{n+1} &= u_n E_1 + h^{-p}L^{-p-1}[\phi_1 N(u_n, t_n) + 2\phi_2(N(a_n, t_n + h/2) \\
&+ N(b_n, t_n + h/2)) + \phi_3 N(c_n, t_n + h)],
\end{aligned} \tag{2.44}$$

with $E_1 = e^{hL}$, $E_2 = e^{hL/2}$.

### 2.4.5 Convergence

Here, we present some convergence theoretical results of the used methods

$$\begin{aligned}
&\tfrac{\partial u(x,t)}{\partial t} = L(x,t)u(x,t) + f(x,t), \quad x \in D, \;\; t \geq 0, \\
&B(x)u(x,t) = 0 \qquad x \in \partial D, \;\; t > 0, \\
&u(x,0) = g(x) \qquad x \in D,
\end{aligned} \tag{2.45}$$

with $D$ and $\partial D$ are spatial domain and its boundary, respectively. $L$ is a linear differential operator and $B$ is a boundary operator. The semi−discrete approximations of this initial-boundary value problems is of the form

$$\frac{\partial u_N(x,t)}{\partial t} = L_N(x,t)u_N(x,t) + f_N(x,t) \tag{2.46}$$

**Definition 16.** *The spectral approximations* (2.46) *will be stable if*

$$\|e^{L_N t}\| \leq K(t), \tag{2.47}$$

*where* $\|e^{L_N t}\| = \max\limits_{u \in H} \frac{\|e^{L_N t} - u\|}{\|u\|}$ *and* $K$ *is a finite function.*

we say that a spectral approximation is convergent if

$$\|u(t) - u_N(t)\| \to 0 \quad \text{as} N \to \infty, \tag{2.48}$$

**Definition 17.** *A spectral approximation can be consistent if*

$$\begin{aligned} \|Lu - L_N u\| &\to 0 \\ \|Lu - P_N u\| &\to 0 \end{aligned} \tag{2.49}$$

*here $P_N$ is the truncated Fourier series of u, for every u in a dense subspace of H and $N \to \infty$.*

The following Theorem is called Lax-Richtmyer theorem, which make a connection between consistency, stability and convergence.

**Theorem 18.** *a consistent approximation of a linear well-posed initial-value problem is stable if and only if it is convergent.*

**Definition 19.** *Let L be a linear operator and $L^*$ is its adjoint. L is a normal operator if*

$$LL^* = L^*L$$

*and the same for the finite dimensional approximation of L, i.e,*

$$L_N L_N^* = L_N^* L_N.$$

The next theorem show one of the stability condition according to Von Neumann

**Theorem 20.** *A sufficient condition for a normal operator L to be stable is*

$$Re(\lambda_N) < C,$$

*where C is a N−independent finite constant and $\lambda_N$ is an eigenvalue of $L_N$.*

In the case when the operators $L_N$ are not normal, the Von Neumann stability condition would be not sufficient but still necessary to ensure stability.

**Theorem 21.** *Let A be any family of $m \times m$ matrices, the following arguments imply each other*

1. *There are $S(w)$ symmetric matrices such that $S(w)A(w)+A^*(w)S(w) \leq 0$ and $I \leq S(w)$, $\|S(w)\| \leq C$ for a constant C.*
2. *$\|exp[A(w)t]\| \leq C$ for every $t \geq 0$.*
3. *$|Re(\lambda)|\|(\lambda I - A(w))^{-1}\| \leq C'$, for some constant $C'$ and every $\lambda$ such that $Re(\lambda) > 0$.*
4. *There are matrices $S(w)$ such that 1. is satisfied with $\|S(w)\| \leq K(w)C'$, where $C'$ is the same constant in 3. and $K(w)$depends only on the number m and not the matrices family $A(w)$*

**Theorem 22.** *If a family of matrices $A(w)$ satisfy the conditions of Kreiss matrix theorem, then all the eigenvalues of $A(w)$ have negative real parts.*

### 2.4.6 Stability regions

**Definition 23.** *Numerical approximation is said to be A-stable if it is only stable for every $\lambda$ in the nonpositive half-plane.*

Due to Dahlquist[31], we have the next proposition

**Proposition 24.** *For linear multi-step approaches, we have the following properties*

- *There is no explicit A-stable method.*
- *An A-stable implicit method can be at best second-order accurate.*

**Remark 25.** *Let us present two remarkable properties of the stability of methods*

- *In many cases of applications, weaker requirements than A-stability are sufficient*
- *Most methods such as Runge-Kutta or all linear explicit multi-step methods have stability regions that are bounded away from the origin in every directions.*

# Chapter 3

# Numerical Study for Blow-up in Solutions of the Generalized 1-D and 2-D Benjamin-Ono Equation

## 3.1 Introduction

In this chapter, we give a full description to the solutions dynamics of the generalized of a dispersive wave equation in the presence of perturbations. Let us first consider the following well-known dispersive wave equations

$$u_{tt} = u_{xx} - u \ \textbf{(KG)}, u_t = u_{xxx} \ \textbf{(KDV)}, u_t = H(u_{xxx}) \ \textbf{(BO)},$$

$$u_t = iu_{xx} \ \textbf{(S)}, \ u_t \ - u_x = u_{xxt} \ \textbf{(RLW)}. \ \textbf{(*)}$$

These PDEs are respectively the Klein-Gordon (KG), KDV, BO, Shrödinger (S) and the regularised long wave (RLW) equations, If we write $u(x,t) = \exp(i(kx - wt))$, their corresponding dispersion relations are respectively given by

$$w^2 = k^2 + 1, w = k^3, w = sign(k)k^2, w = k^2, w = k/(1 + k^2)$$

and they enable one to solve these PDEs, analytically involving Fourier integrals, and numerically by computing them with the discrete fast Fourier transform FFT. Note that these dispersion relations, and particularly $\frac{dw}{dk}$ give a complete description of the evolution of each wave equation.
For the numerical Fourier spectral-based approximations, one proceeds as follows: a given initial condition is converted to Fourier space via the FFT to give the coefficients $a(k, 0)$. Then the solution is advanced in Fourier space with respect to the time variable $t$ to get $a(k, t) = a(k, 0) \exp(-iw(k)t$. An inverse FFT brings us back to $u(x, t)$. The errors incurred here are those in approximating the Fourier integrals with the FFT. These errors can be rendered small by taking many points in the FFT and choosing a sufficiently large space interval so that the waves do not touch the boundaries, particularly for a problem with a strong dispersion.

Here we plot the solution of the five PDEs with the same initial condition, on the same space

interval. The solutions are plotted at different times $t$, for example for a PDE with a strong dispersion, such as the KDV, we could go only to about $t = 1$ before the waves reached the edge of the computational domain; while for weak dispersion cases such as the KG and RLW, we could go up to $t = 10$ or $t = 20$ for $u(x, 0) = \cos(x), x \in [-20, 20]$; and to $t = 20$ or $t = 25$ for $u(x, 0) = sech(x), x \in [-40, 40]$ (see Figure 3.1).

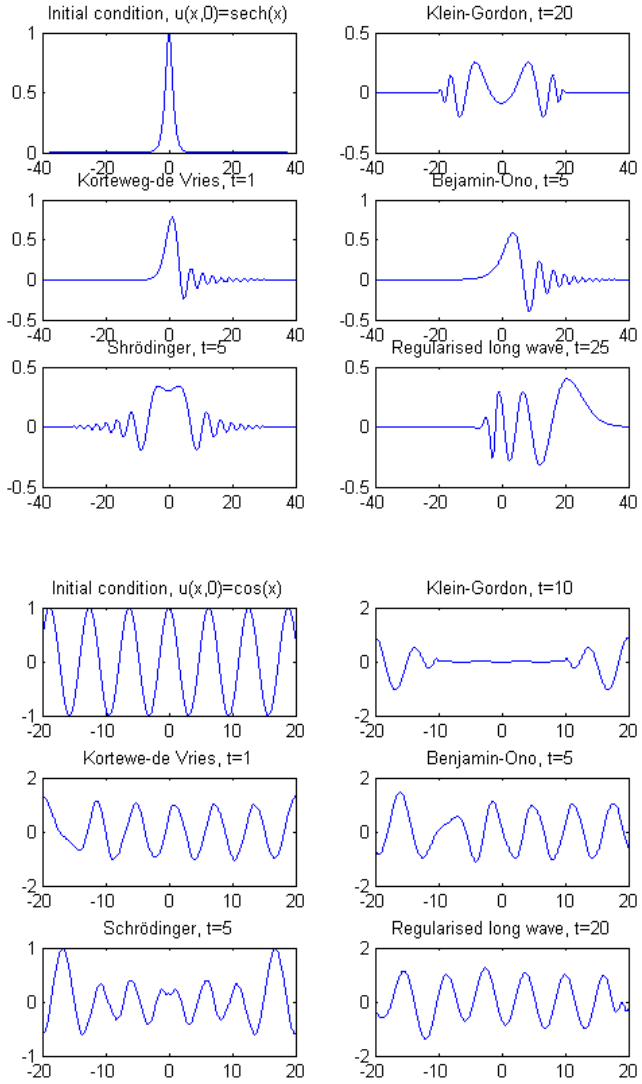


Figure 3.1: Numerical wave evolution of equations (*): Top for $u(x, 0) = sech(x)$, and bottom for $u(x, 0) = cos(x)$.

Inspired by these results, we are interested to study the dispersive decay of long time solutions for small localized data and explore the blow-up phenomenon of the generalized BO equation with different types of nonlinearities in both one and two dimension.

## 3.2 Generalized 1-D Benjamin-Ono equations

This section is concerned with a detailed numerical study to the dynamics of solutions of generalized Benjamin-Ono equations (gBO) in one dimension with critical and supercritical nonlinearity. Three numerical procedures are presented, the first two methods use the Fourier collocation scheme for the spatial discretization with an efficient time integration of high accuracy in order to integrate the direct gBO equations and their rescaled equations, while the third one is a fixed point algorithm to construct the approximate solitary wave solutions of the equations.

The Benjamin-Ono eqution defined by (1.7) has the following explicit known soliton solutions

$$Q_{BO} = \frac{4c}{1+(cx)^2}, \quad c \in \mathbb{R}^* \tag{3.1}$$

where $c$ is the wave speed. A natural generalization of (1.7) equation is

$$u_t + u^n u_x - H u_{xx} = 0. \qquad t \in \mathbb{R}, x \in \mathbb{R} \tag{3.2}$$

Equations (3.2) appear in many applications specially for $n = 2$ (the modified Benjamin-Ono equation (mBO)), see for instance [14]. This generalized equations show the important fact that the dispersive effect is identified by a nonlocal operator and it is weaker than that presented by the celebrated generalized KdV equations.
The following quantities are formally invariant under the flow associated to gBO

$$M(u) = \int_{\mathbb{R}} u^2 dx. \tag{3.3}$$

$$E(u) = \frac{2}{(n+1)(n+2)} \int u^{n+2} dx - \int u H u_x dx. \tag{3.4}$$

The introduction of a stronger nonlinearity in BO has the effect that solutions to gBO equations may blow-up in a finite time for $n \geq 2$. Recall that the Cauchy problem for (3.2) with $n = 2$ is locally well-posed in the energy space $H^{\frac{1}{2}}(\mathbb{R})$ by the work of Kenig and Takaoka [68]. See also [102, 87, 88, 66], for previous related works on the Benjamin-Ono equation, and the modified Benjamin-Ono equation. For such solutions, the quantities $M(u(t))$ and $E(u(t))$ are conserved.

Now, we show a careful numerical investigation of solutions stability in the critical and supercritical cases. To do so we follow the dual approach applied in [59]: a direct integration for both the gBO equations (3.2) and their rescaled equations (3.9). In all cases, we employ Fourier collocation method for the spatial dependence but for the time dependence we use a different fourth order schemes: a Runge-Kutta method to deal with gBO equations (3.2) and ETD (exponential time differencing) scheme for the dynamically rescaled gBO equation (3.9). The rescaling code is used to test the other one.

### 3.2.1 Numerical discretisation

In the studies of nonlinear dispersive wave equations in a bounded domain, a smooth, localized initial data play an important role in the decomposition into solitary waves and an expected blow-up in finite time. So an initial localized condition with a number of numerical tools that have been developed in this thesis provide a precise illustration of several aspects of the gBO equations's dynamics. The main approache will be a Petviashvili-type methods in order to compute numerically the approximate solitary wave solutions to the equations, a direct integration and a dynamical rescaling for the gBO equations with a spatial Fourier transform method for the spatial dependence and fourth order methods for the time integration, taking into account the well known soliton solutions (3.1)

#### Direct numerical integration

For the direct integration of (3.2), we use Fourier spectral methods, which have excellent approximation properties for smooth, localized functions as the ones considered here. Thanks to the finite numerical precision and a large enough computational domain, the rapidly decreasing initial data can be seen as periodic functions. For gBO there is an additional reason to use Fourier spectral methods, that is the conveniences of define the term $Hu_{xx}$ in Fourier space where the gBO equations have the following form

$$\hat{u_t} = N(u) + L(\hat{u}), \tag{3.5}$$

where $N(u) = -\frac{\mathrm{i}K}{n+1}\widehat{u^{n+1}}$ and $L = \mathrm{i}|K|K$ ($K$ is the wave number). Equation (3.5) allow us to apply many efficient high-order schemes for the time integration, see for instance [55, 45, 29]. As in [59], we use an implicit Runge-Kutta of fourth order (IRK4) scheme and solve its nonlinear equations by a simplified Newton scheme.
Motivated by ([59, 60]), we compute the time dependent quantity

$$\Delta = \left| \frac{E(t)}{E(0)} - 1 \right| \tag{3.6}$$

to control the numerical accuracy of the solution, it was indicated in [58, 61] that this quantity more accurate than the $L_\infty$ norm of the difference between exact and numerical solution. We basically choose large enough computational domain, $x \in L[-\pi, \pi]$ to guarantee the periodicity of the used initial data with a sufficient number of Fourier modes as well as a small enough time step to ensure that the solution is considered with machine precision before the blow-up time.

#### Dynamic rescaling

For the critical case $n = 2$, the results in [83] indicate that an expected blow-up of solutions for initial data with minimal mass blow-up (the mass of the unique ground state solution of $DQ + Q = Q^3$). In addition it is more convenient to treat the fact that the maximum which eventually develops into the blow-up is moving as the case of gKdV (for the information of the method and the results in the gKdV case, we refer the reader to [59]and references therein).

Thus we also shift by the location of the maximum $x_m(t)$ the $x$ coordinate. In the case $n \geq 2$, we expecte that the quantity $x_m$ tends to infinity at blow-up. The transformed coordinates

$$\eta = \frac{x - x_m}{L}, \frac{d\tau}{dt} = \frac{1}{L^2}, U = L^{\frac{1}{n}} u. \tag{3.7}$$

That give

$$\begin{aligned}
&u = UL^{\frac{1}{n}},\\
&u^n = (UL^{-\frac{1}{n}})^n = U^n L^{-1},\\
&u_x = (UL^{-\frac{1}{n}})_x = (UL^{-\frac{1}{n}})_\eta \tfrac{d\eta}{dx} = U_\eta L^{-\frac{1}{n}} \tfrac{1}{L},\\
&u_{xx} = (U_\eta L^{-\frac{1}{n}} \tfrac{1}{L})_x = (U_\eta L^{-\frac{1}{n}} \tfrac{1}{L})_\eta \tfrac{d\eta}{dx} = U_{\eta\eta} L^{-\frac{1}{n}} \tfrac{1}{L^2},\\
&u_t = (UL^{-\frac{1}{n}})_t = (UL^{-\frac{1}{n}})_\tau \tfrac{d\tau}{dt} + (UL^{-\frac{1}{n}})_\eta \tfrac{d\eta}{dt}\\
&\quad = U_\tau L^{-\frac{1}{n}} \tfrac{1}{L^2} - \tfrac{1}{n} UL^{-\frac{1}{n}-1} \tfrac{L_\tau}{L^2} - L^{-\frac{1}{n}} U_\eta \tfrac{1}{L^2} \tfrac{L_\tau}{L^2}(x - x_m) - U_\eta L^{-\frac{1}{n}} \tfrac{1}{L^2} \tfrac{x_{m,\tau}}{L},
\end{aligned} \tag{3.8}$$

which keep the gBO invariant for constant $L$ and $x_m$, from (3.2) we have

$$U_\tau - \alpha(\frac{1}{n} U + \eta U_\eta) - vU_\eta + U^n U_\eta - HU_{\eta\eta} = 0, \tag{3.9}$$

where

$$\alpha = (\ln L)_\tau, v = \frac{x_{m,\tau}}{L}. \tag{3.10}$$

Note that, we have to choose $L$ and $v$ in a convenient way. We also choose $\eta$ such that the maximum of $|U|$is located at $\eta = 0$ this means $U_\eta(\eta_0, \tau) = 0$. By differentiating with respect to $\eta$, we find that

$$U_{\tau\eta} - \alpha(\frac{1}{n} U_\eta + U_\eta + \eta U_{\eta\eta}) - vU_{\eta\eta} + nU^{n-1} U_\eta^2 + U^n U_{\eta\eta} - HU_{\eta\eta\eta}, \tag{3.11}$$

which implies

$$v = -\alpha\eta_0 + U(\eta_{0,}\tau)^n - \frac{HU_{\eta\eta\eta}(\eta_{0,}\tau)}{U_{\eta\eta}(\eta_{0,}\tau)}. \tag{3.12}$$

On the other hand, The scaling function $L$ may be chosen to keep each norm constant, for example the $L_\infty$ norm

$$L^{\frac{1}{n}} = \frac{\|U\|_\infty}{\|u\|_\infty}. \tag{3.13}$$

Thus, we get from (3.7)

$$\alpha = -\frac{nHU_{\eta\eta}(\eta_{0,}\tau)}{U(\eta_{0,}\tau)}. \tag{3.14}$$

We can also choose $L$ as

$$L^{\frac{1}{n}-\frac{1}{2}} = \frac{\|U\|_2}{\|u\|_2}, \tag{3.15}$$

since

$$\|u\|_2^2 = \int u^2 dx = \int (UL^{-\frac{1}{n}})^2 L d\eta = \|U\|_2^2 L^{-\frac{2}{n}+1}. \tag{3.16}$$

Another way is to choose $L$ such that the $L_2$ norm of $U_\eta$ being constant, namely

$$L^{\frac{1}{n}+\frac{1}{2}} = \frac{\|U_\eta\|_2}{\|u_x\|_2}, \tag{3.17}$$

since

$$\begin{aligned} \|u_x\|_2^2 &= \int u_x^2 dx = \int (UL^{-\frac{1}{n}})_x^2 dx = \int (UL^{-\frac{1}{n}})_\eta^2 (\tfrac{d\eta}{dx})^2 L d\eta = \int U_\eta^2 L^{-\frac{2}{n}} \tfrac{1}{L^2} L d\eta \\ &= \int U_\eta^2 L^{-\frac{2}{n}-1} d\eta = \|U_\eta\|^2 L^{-\frac{1}{n}-\frac{1}{2}}. \end{aligned} \tag{3.18}$$

We obtain from (3.9) in this case

$$a = \frac{2n}{(2+n)(1+n)\,\|U_\eta\|} \int_{\mathbb{R}} U^{n+1} U_{\eta\eta\eta} d\eta. \tag{3.19}$$

As in the case of NLS and KdV equation, this approach showed to be numerically much more stable than setting the $L_\infty$ norm to be constant, see [99, 59] and references therein.
Under the coordinate transformation (3.7) and from the conserved energy of gBO equation (3.4), we have that

$$\begin{aligned} E[U] &= \tfrac{2}{(n+1)(n+2)} \textstyle\int_{\mathbb{R}} (UL^{-\frac{1}{n}})^{n+2} L d\eta - \int_{\mathbb{R}} UL^{-\frac{1}{n}} H U_\eta L^{-\frac{1}{n}} \tfrac{1}{L} L d\eta \\ &= \tfrac{1}{L^{\frac{2}{n}}} \textstyle\int_{\mathbb{R}} \tfrac{2}{(n+1)(n+2)} (U^{n+2} - UHU_\eta) d\eta. \end{aligned} \tag{3.20}$$

### 3.2.2 Numerical tests

In contrast to the gKdV equations case, the gBO equations for $n \geq 2$ do not have explicitly known solutions, the reason is that the later equations are not completely integrable. Thus we use the soliton (3.1) of the BO equation (the case $n = 1$) as initial data with $c = 2$ to numerically test the propagation of the solution. The test is executed for $x \in 50[-\pi, \pi]$ with $N = 2^{14}$ Fourier modes and $N_t = 1000$ time steps for $t \leq 10$ and find that The relative computed energy is in this case of order $10^{-14}$ ,i.e., machine precision. Unfortunately, due to a Gibbs phenomenon, the Fourier coefficients do not decrease. The reason is that the soliton of BO decreases algebraically as $x^{-2}$ for $|x| \to \infty$. This numerical problematic has a consequence that the numerical precision will be limited and it cannot be addressed even with a large computational domain.
We also use the initial data (3.1) to test the code with dynamical rescaling, the code is implemented until $\tau = t = 10$ with $N^t = 10^5$, whereas all other parameters are as before. The relative computed energy is in this case around the order of $10^{-8}$. The consistency of results with both codes provides an additional test of the accuracy (see Figure 3.2).

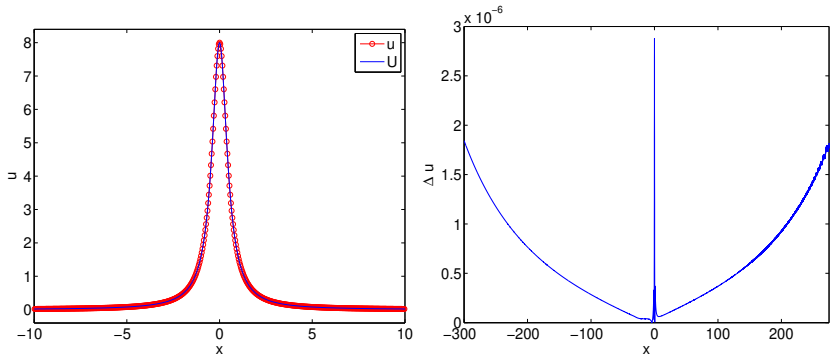


Figure 3.2: Solution to the gBO equation (3.2) for $n = 2$ and the initial data (3.1) in red, and the solution to the rescaled gBO equation (3.9) in blue on the left; on the right we show the difference between both solutions.

### 3.2.3 Numerical construction of solitons

solitary waves play a crucial role in the study of nonlinear wave phenomena. For the computation of this kind of waves, various analytical and numerical methods have been developed. Among them, we find the Newton's method, the shooting method, Accelerated Imaginary-time Evolution Methods,..., etc. In this subsection one of the most efficient and simple methods to implement the approximate soliton is presented. Recall that a solitary-wave solutions of (3.2) are solutions $u$ of the form $u(x,t) = Q_c(x - ct)$, which satisfy

$$DQ_c + cQ_c - \frac{1}{n+1}Q_c^{n+1} = 0, \tag{3.21}$$

for some profile $Q$ and speed $c$ where $D = H\partial_x$. We numerically solve the above equation for $c = 1$ (see Figure 3.3) by the use of a spectral method due to Petviashvili. equation(3.33) can be written

$$HQ_x + Q = Q^{n+1}, \tag{3.22}$$

or

$$MQ = Q^{n+1}, \tag{3.23}$$

where $M = H\partial_x + 1$. This equation may be rewritten as

$$Q = M^{-1}Q^{n+1}. \tag{3.24}$$

Hence a natural iterative scheme is

$$Q_{p+1} = M^{-1}Q_p^{n+1}. \tag{3.25}$$

Unfortunately, if we directly iterate equation (3.24), this iteration solution will usually diverge. However, the following iterative scheme with stabilizing factor

$$S_p = \frac{\langle Q_p, MQ_p\rangle}{\langle Q_p, Q_p^{n+1}\rangle},$$

(here $\langle .,. \rangle$ is the standard inner product in the space of square-integrable functions) defined by:

$$Q_{p+1} = S_p^{\lambda} M^{-1} Q_p^{n+1}, \ \lambda = const \tag{3.26}$$

possesses much better convergence properties.

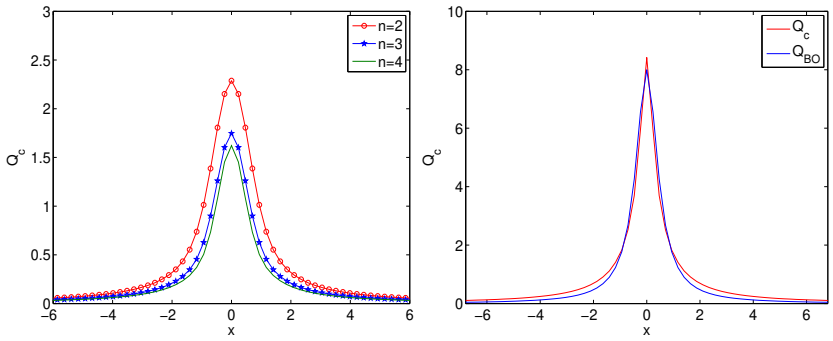


Figure 3.3: Solitary waves (3.21) for $c = 1$ and different values of $n$ on the left; on the right approximate soliton of the gBO equation for $c = 1$, $n = 1$ in red and the corresponding BO soliton in blue.

Throughout the rest of this section, we consider as initial data a perturbations of the Gaussian of the form

$$u(x, 0) = \lambda \exp(-x^2/0.5), \ \lambda \geq 0. \tag{3.27}$$

### 3.2.4 $L_2$ critical case $n = 2$

For $n = 2$, we first run the code for direct integration of modified Benjamin-Ono equation until $t = 5$ for $\lambda = 2$, $L = 50$ and $2^{14}$ Fourier modes with $N_t = 10^4$ time steps. The solution mass in this case is smaller than the corresponding approximate soliton mass. As can be seen in Figure 3.4, the solution is radiated away due to the propagation of the dispersive oscillations and it appears that the $L_\infty$ decreases monotonically. The relative energy is conserved to the order of $10^{-14}$. So in this case there is no indication of blow-up.

The situation is totally different for initial data with $\lambda = 3$. This time the code is carried out with $L = 20$, $N = 2^{14}$ and $N_t = 2^5$ time steps for $t \leq 12$. In this case, we have positive initial energy and the solution mass is larger than the corresponding approximate soliton mass. It can be seen from Figure 3.5, that there are some dispersive oscillations spreading to the left and the solution gets more and more peaked and finally looks to blow up in a given time. As shown in Figure3.6, the blow-up can be also indicated from both the $L_\infty$ norm of the solution and its Fourier coefficients. We stop the code at $t = 10.32$ when the relative energy conservation drops below $10^{-3}$ since there are no more reliable results. In this case although the initial energy is positive, we have a blow-up.

### 3.2.5 $L_2$ supercritical case $n = 3$

For $n = 3$, as in the critical case we perturb the Gaussian (3.27) with $\lambda = 1.5$ for which the initial energy is positive, we execute the code with $N^{13}$ Fourier modes and $N_t = 2$ time steps

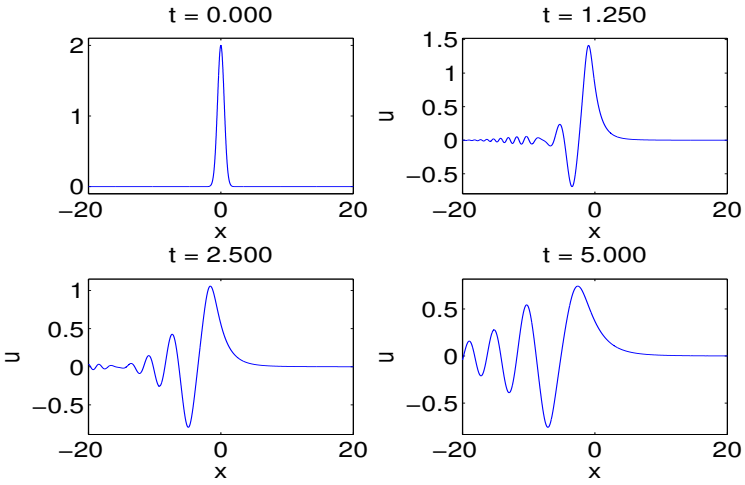


Figure 3.4: Solution to the modified BO equation (3.2) for $n = 2$ and the perturbed initial data (3.27) with $\lambda = 2$ for several values of time.

on a large computational domain $x \in [-\pi, +\pi]$ for $t \leq 2$. Here the mass of the solution is smaller than the corresponding approximate soliton mass. As presented in Figure3.7, a tail of dispersive oscillations is developed towards $-\infty$. the $\Delta$ is conserved to the order of $10^{-14}$. There is basically no indication of blow-up.

The situation is completely different if we run the code for $\lambda = 2.9$, $2^{15}$ Fourier modes and $N_t = 20000$ on $x \in 10[-\pi, +\pi]$ until the code breaks at $t = 0.039$ because there is no more convergent iteration. Here the mass of the solution is larger than the corresponding approximate soliton mass and the initial energy is negative. At $t = 0.037$ the energy conservation drops below $10^{-3}$ which indicates the appearance of blow-up (see Figure 3.8 and Figure 3.9).

## 3.3 Generalized 2-D Benjamin-Ono equation

In this section, we present a numerical study of the blow-up phenomenon for the BO-generalized KP version with different types of nonlinearities. A dynamic rescaling can be used to identify the type of the singularity and explore the investigation of observed blow-ups. For the numerical experimentations, an exponential time-differencing fourth-order Runge-Kutta method combined with a space-scheme based on the Fourier spectral method is used.

Recently, the study of the generalization of the BO equation for weak transverse perturbations has become more meaningful for researchers in many fields. To our Knowledge, there is no class of $(1+2)$-dimensional BO equations known to be integrable. However, there are some interesting results concerning a larger class of these equations, see [41], [79] and [95] for a more recent review. The KP-BO equations describe the motion of long, weakly nonlinear internal waves in a deep stratified fluid with weak transverse effects (see [42] for more details). By using different techniques, these equations have been studied by several authors, for example:

- In [52], the authors have developed a proof for the solution's local well-posedness by the

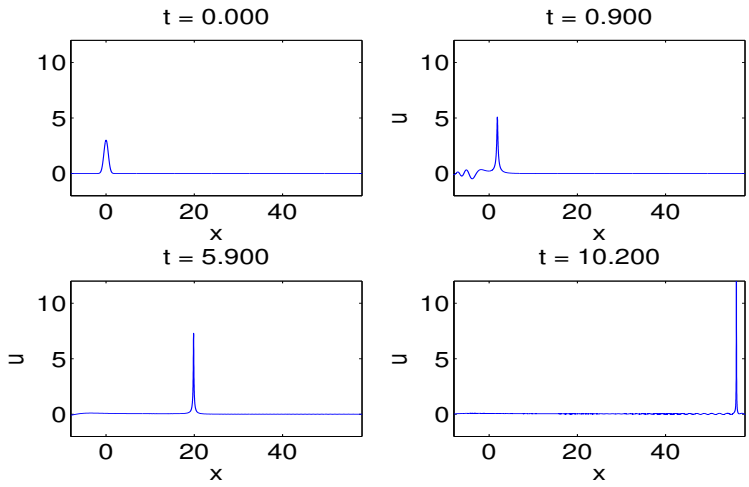


Figure 3.5: Solution to the modified BO equation (3.2) for $n = 2$ and the perturbed initial data (3.27) with $\lambda = 3$ for several values of time.

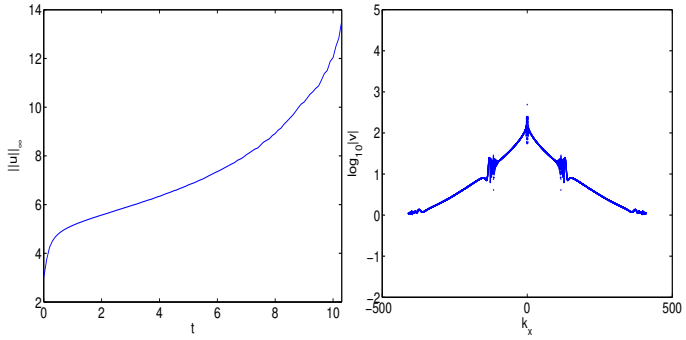


Figure 3.6: $L_\infty$ norm of the solution to the gBO equation (3.2) with for $n = 2$ and the perturbed initial data (3.27) with $\lambda = 3$ on the left, and the modulus of the Fourier coefficients of the solution for $t = 10.32$ on the right.

use of a method due to Kato [56], and investigated its blows-up in finite time, for suitable conditions as in [97].

- Esfahani has claimed in [33] the existence of solitary waves, by a suitable application of the anisotropic Sobolev embedding theorem.

- More recently, by the use of the so-called minimax theory techniques and the Lizorkin's theorem. The existence, regularity and analyticity properties of their solitary waves, were established in [95] .

- For the case when $n = 1$, some interesting results were shown, for example analytical stability issues for (3.28) can be found in [42], the existence of global solutions and scattering was proved for small, smooth and localized initial data (see [41]) and the local Cauchy problem of the gKP-BO was studied in [79].

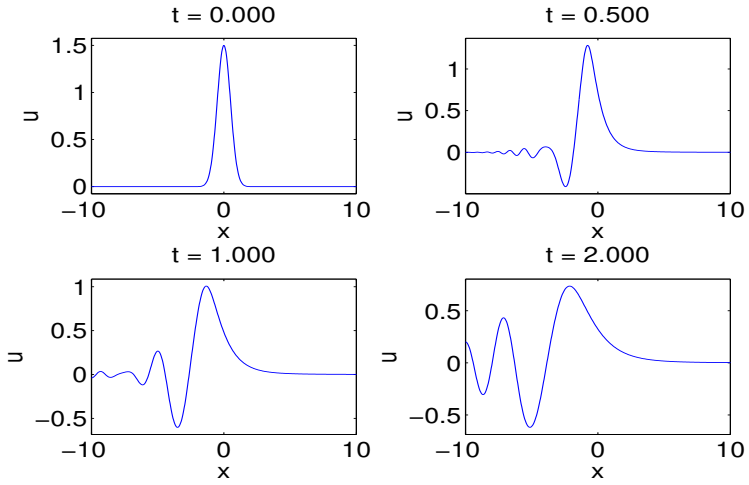


Figure 3.7: Solution to the modified BO equation (3.2) for $n = 3$ and the perturbed initial data (3.27) with $\lambda = 1.5$ for several values of time.

In the following of this section we consider a class of the two dimensional generalized BO equations (shortly denoted by GKP-BO) written as:

$$(u_t - \mathrm{H}u_{xx} + u^n u_x)_x = \lambda u_{yy}, \quad \lambda = \pm 1. \tag{3.28}$$

with $n = \frac{n_1}{n_2}$, $n_1$, $n_2 \in \mathbb{N}^*$, or in the integrated form as

$$u_t - \mathrm{H}u_{xx} + u^n u_x = \lambda \partial_x^{-1} u_{yy}, \quad \lambda = \pm 1. \tag{3.29}$$

$\lambda = 1$ for (GKPI-BO) while $\lambda = -1$ for (GKPII-BO).
Here $\partial_x^{-1}$ is determined via the Fourier transform as

$$\widehat{\partial_x^{-1} f}(k_x, k_y) = \frac{1}{\mathrm{i}k_x} \widehat{f}(k_x, k_y). \tag{3.30}$$

Equations (3.29) satisfy the following conservation quantities

$$M[u] = \|u\|_2. \tag{3.31}$$

and

$$E[u] = \int_{\mathbb{R}^2} [-\frac{1}{2} u_x H u - \frac{1}{(n+1)(n+2)} u^{n+2} + \frac{\lambda}{2} (\partial_x^{-1} u_y)^2] \, dxdy. \tag{3.32}$$

In addition GKP-BO also have localized travelling wave solutions in the $x$-direction that take the form $u(x; y; t) = Q(x - ct; y)$, where the nontrivial $Q(z; y)$ satisfies

$$-cQ_{zz} + \frac{1}{n+1} Q_{zz}^{n+1} - HQ_{zzz} - \lambda Q_{yy} = 0. \tag{3.33}$$

Due to the antiderivative term in (3.29), $\forall t > 0$ the solutions satisfy the constraint

$$\int_{\mathbb{R}} u_{yy} dx = 0. \tag{3.34}$$

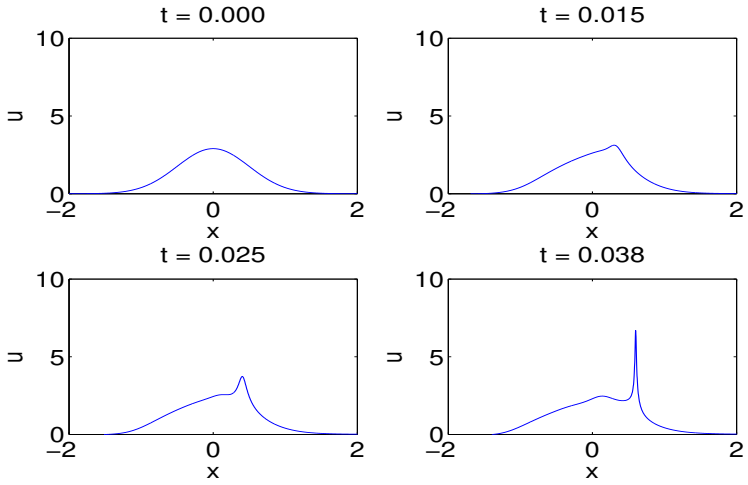


Figure 3.8: Solution to the modified BO equation (3.2) for $n = 3$ and the perturbed initial data (3.27) with $\lambda = 2.9$ for several values of time.

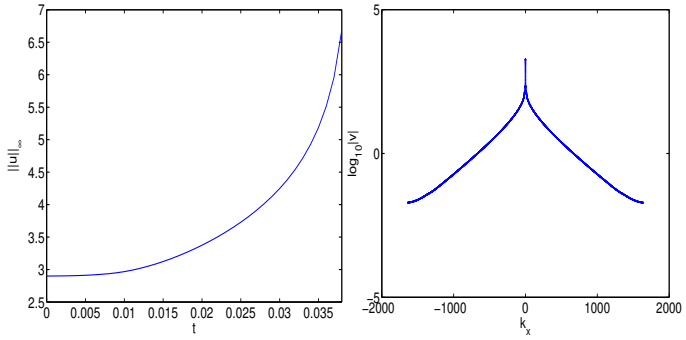


Figure 3.9: $L_\infty$ norm of the solution to the gBO equation (3.2) for $n = 3$ and the perturbed initial data (3.27) with $\lambda = 2.9$ on the left, and the modulus of the Fourier coefficients of the solution for $t = 0.039$ on the right.

Furthermore a singularity at the $x$ frequency $k_x = 0$ delimits the achievable precision in the solutions of the GKP-BO equations. It was proved that the solutions to a Cauchy problem will not be smooth in time for $t = 0$ if they do not satisfy the constraint (3.34). Numerically, these solutions develop an infnite trench as was reported in [62]. This nonregularity represented numerically when $t \to 0$, presents a problem as it delimits the manageable accuracy. To avoid such problems, we consider initial data that are $x$-derivatives of rapidly decreasing functions satisfying (3.34). In this section, we consider the following initial data

$$u_0(x, y) = \beta \exp\left(-(x^2 + y^2)\right), \beta \textit{ is a constant.} \tag{3.35}$$

### 3.3.1 Dynamic rescaling

Equation (3.29) is symmetric under the following rescaling

$$\xi = \frac{x - x_m}{L}, \quad \eta = \frac{y - y_m}{L^{\frac{3}{2}}}, \quad \frac{d\tau}{dt} = \frac{1}{L^2}, \quad U = L^{\frac{1}{n}} u. \tag{3.36}$$

with a dynamic rescaling $L = L(t)$. Thus we write (3.29) as

$$U_\tau - a\left(\frac{1}{n}U + \xi U_\xi + \frac{3}{2}\eta U_\eta\right) - v_\xi U_\xi - v_\eta U_\eta + U^n U_\xi - HU_{\xi\xi} = \lambda \int_{-\infty}^{\xi} U_{\eta\eta} dz, \tag{3.37}$$

with

$$a = \frac{L_\tau}{L}, v_\xi = \frac{x_{m,\tau}}{L}, v_\eta = \frac{y_{m,\tau}}{L}, \tag{3.38}$$

where $x_m$, $y_m$ are the maximum or the minimum location and the index $\tau$ denotes the $\tau$-derivative. Equations (3.37) and (3.38) are obtained from the following equations

$$\begin{aligned}
&u = UL^{-\frac{1}{n}},\\
&u^n = (UL^{-\frac{1}{n}})^n = U^n L^{-1},\\
&u_x = (UL^{-\frac{1}{n}})_x = (UL^{-\frac{1}{n}})_\xi \tfrac{d\xi}{dx} = U_\eta L^{-\frac{1}{n}} \tfrac{1}{L},\\
&u_{xx} = (U_\xi L^{-\frac{1}{n}} \tfrac{1}{L})_x = (U_\xi L^{-\frac{1}{n}} \tfrac{1}{L})_\xi \tfrac{d\xi}{dx} = U_{\xi\xi} L^{-\frac{1}{n}} \tfrac{1}{L^2},\\
&u_y = (UL^{-\frac{1}{n}})_y = (UL^{-\frac{1}{n}})_\eta \tfrac{d\eta}{dy} = U_\eta L^{-\frac{1}{n}} \tfrac{1}{L^{3/2}},\\
&u_{yy} = (U_\eta L^{-\frac{1}{n}} \tfrac{1}{L^{3/2}})_y = (U_\eta L^{-\frac{1}{n}} \tfrac{1}{L^{3/2}})_\eta \tfrac{d\eta}{dy} = U_{\eta\eta} L^{-\frac{1}{n}} \tfrac{1}{L^3},\\
&\partial_x^{-1} u_{yy} = \partial_\xi^{-1} U_{\eta\eta} L^{-\frac{1}{n}} \tfrac{1}{L^3} L = \partial_\xi^{-1} U_{\eta\eta} L^{-\frac{1}{n}} \tfrac{1}{L^2},
\end{aligned} \tag{3.39}$$

$$\begin{aligned}
u_t &= (UL^{-\frac{1}{n}})_t = (UL^{-\frac{1}{n}})_\tau \tfrac{d\tau}{dt} + (UL^{-\frac{1}{n}})_\xi \tfrac{d\xi}{dt} + (UL^{-\frac{1}{n}})_\eta \tfrac{d\eta}{dt}\\
&= U_\tau L^{-\frac{1}{n}} \tfrac{1}{L^2} - \tfrac{1}{n} U L^{-\frac{1}{n}-1} \tfrac{L_\tau}{L^2} - L^{-\frac{1}{n}} U_\xi \tfrac{1}{L^2} \tfrac{L_\tau}{L^2}(x - x_m) - U_\xi L^{-\frac{1}{n}} \tfrac{1}{L^2} \tfrac{x_{m,\tau}}{L}\\
&-\tfrac{3}{2} L^{-\frac{1}{n}} U_\eta \tfrac{1}{L^2} \tfrac{L_\tau}{L^{5/2}}(y - y_m) - U_\eta L^{-\frac{1}{n}} \tfrac{1}{L^2} \tfrac{y_{m,\tau}}{L^{3/2}},
\end{aligned} \tag{3.40}$$

An asymptotic blow-up can be described by equation (3.37). It is expected that if $\tau \to \infty$, the functions $U$, $v_\eta$, $v_\xi$ and $a$ will be independent of $\tau$ ( that are denoted by a superscript $\infty$), hence (3.37) becomes

$$\begin{aligned}
&U_\tau^\infty - a^\infty \left(\tfrac{1}{n} U^\infty + \xi {U_\xi}^\infty + \tfrac{3}{2}\eta {U_\eta}^\infty\right) - v_\xi^\infty U_\xi^\infty -\\
&\qquad v_\eta^\infty U_\eta^\infty + (U^\infty)^n {U_\xi}^\infty - HU_{\xi\xi}^\infty = \lambda \int_{-\infty}^{\xi} U_{\eta\eta}^\infty dz.
\end{aligned} \tag{3.41}$$

For the numerical implementation, $L$, $v_\xi$ and $v_\eta$ have to be chosen in a convenient way. A possible choice is to assume that the single global minimum of $U$ to be $U^0_\eta = U^0_\xi = 0$, for $\xi = \eta = 0$. This implies

$$\begin{pmatrix} U^0_{\xi\xi} & U^0_{\xi\eta} \\ U^0_{\xi\eta} & U^0_{\eta\eta} \end{pmatrix} \begin{pmatrix} v_\xi \\ v_\eta \end{pmatrix} = \begin{pmatrix} (U^0)^n U^0_{\xi\xi} - HU^0_{\xi\xi} + \lambda U^0_{\eta\eta} \\ (U^0)^n U^0_{\xi\eta} - HU^0_{\xi\xi\eta} + \lambda U^0_{\eta\eta\eta} \end{pmatrix}. \tag{3.42}$$

From the coordinate transformation (3.36), we have that

$$\| u \|_2^2 = \int u^2 dxdy = \int (UL^{-\frac{1}{n}})^2 LL^{3/2} d\xi d\eta = \int U^2 L^{-\frac{2}{n}} L^{5/2} d\xi d\eta. \tag{3.43}$$

this yields

$$\| u \|_2^2 = L^{\frac{-2}{n}+\frac{5}{2}} \| U \|_2^2 . \tag{3.44}$$

Hence the $L_2$ critical case is $n = \frac{4}{5}$. We have also that

$$\| u_x \|_2^2 = \int u_x^2 dxdy = \int \left( (UL^{-\frac{1}{n}})_\xi \frac{d\xi}{dx} \right)^2 LL^{3/2} d\xi d\eta = U_\xi^2 L^{-\frac{2}{n}} \frac{1}{L^2} LL^{3/2} = L^{\frac{1}{2}-\frac{2}{n}} \| U_\xi \|_2^2, \tag{3.45}$$

this implies the invariance under (3.36) when $n = 4/5$. Since the blow-ups phenomenon in [52] are established for $\| u_y \|_2^2$, so we consider

$$\| u_y \|_2^2 = \int u_y^2 dxdy = \int \left( (UL^{-\frac{1}{n}})_\eta \frac{d\eta}{dy} \right)^2 LL^{3/2} d\xi d\eta = U_\xi^2 L^{-\frac{2}{n}} \frac{1}{L^3} LL^{3/2} = L^{-(\frac{1}{2}+\frac{2}{n})} \| U_\eta \|_2^2 . \tag{3.46}$$

Fixing $||U_\eta||$ to be constant gives

$$a = \frac{2n}{(2+n)(1+n)\,\|U_\eta\|} \int_{\mathbb{R}^2} U^{n+1} U_{\eta\eta\xi} d\xi d\eta. \tag{3.47}$$

This can be taken for the numerical implementation. The physical time $t$ and scaling factor $L(\tau)$ can be computed by using the trapezoidal rule. The numerical computation accuracy can be controlled by (3.44) or by

$$\begin{aligned} E[U] &= \textstyle\int_{\mathbb{R}^2} [-\frac{1}{2}(U_\xi L^{-\frac{1}{n}} \frac{1}{L}) H(UL^{-\frac{1}{n}}) - \frac{1}{(n+1)(n+2)} (UL^{-\frac{1}{n}})^{n+2} + \frac{\lambda}{2} (\partial_\xi^{-1} LU_\eta L^{-\frac{1}{n}} L^{-3/2})^2] LL^{3/2} d\xi d\eta \\ &= \textstyle\frac{1}{L^{\frac{2}{n}-\frac{3}{2}}} \int_{\mathbb{R}^2} [-\frac{1}{2} U_\xi HU - \frac{1}{(n+1)(n+2)} U^{n+2} + \frac{\lambda}{2} (\partial_\xi^{-1} U_\eta)^2] d\xi d\eta. \end{aligned} \tag{3.48}$$

Note that the energy is invariant under the rescaling (3.36) and the case $n = \frac{4}{3}$ is energy critical.

### 3.3.2 Numerical discretisation

Due to the periodicity, the Fourier spectral methods are the most convenient approaches for space variable approximations. For the integration of the resulting semi discrete stiff systems, a fourth order exponential time differencing (ETD) scheme is applied.
The $2d$ Fourier transform is defined by:

$$\hat{u}(k_x, k_y) = \int_{-\infty}^{\infty} \int_{-\infty}^{\infty} e^{-i(k_x x + k_y y)} u(x, y) dx dy. \tag{3.49}$$

In Fourier space, equation (3.29) is equivalent to

$$\hat{u}_t = \mathrm{N}(\hat{u}) + \mathrm{M}\hat{u}. \tag{3.50}$$

where $\mathrm{N}(\hat{u}) = -\mathrm{i}k_x \widehat{\frac{u^{n+1}}{n+1}}$, and $\mathrm{M} = -\mathrm{i}\,\mathrm{sgn}(k_x)k_x^2 + \lambda\frac{\mathrm{i}k_y^2}{k_x}$. In the numerical approximation of the above equation, we apply a discrete Fourier transform which can be computed by a FFT, while for the time integration, as was shown in [61, 92] the ETD schemes are most efficient methods for this type of equations (see also [55]) but we use here a modified version of these approaches, called by the *exponential time-differencing fourth order Runge Kutta* (ETDRK4) scheme, which is also convenient for the stiff systems. This explicit method is very appropriate as it can avoid a pollution of the Fourier coefficients and allows us to use small time steps to maintain the numerical stability.
The ETDRK4 schemes are based on ETD methods combined with the fourth-order Runge–Kutta time-stepping. The basic idea in the ETD is to integrate (3.50) exactly over a time step of length h with respect to t. If we write $\widehat{u}(t_p) = \widehat{u}_p$, and $\widehat{u}(t_{p+1}) = \widehat{u}_{p+1}$, then we get

$$\widehat{u}_{p+1} = e^{Mh}\widehat{u}_p + \int_0^h e^{M(h-\sigma)} N(\widehat{u}(t_p + \sigma), t_p + \sigma) d\sigma. \tag{3.51}$$

Now, we use the ETDRK4 schemes that illustrated in (2.43) and (2.44).

The following computations are carried out with the number of Fourier modes $N_x$ and $N_y$, that should be high enough in order to achieve a good precision, and a space computational domain large enough, to ensure periodicity of the solution. Note that the number of Fourier modes depends on the size of the domain, and will increase for the high wave numbers when a blow-up occurs.

### 3.3.3 Numerical experimentations

As in the case of one dimension, we use the following $\Delta$ in order to control the accuracy of the computations,

$$\Delta = \left| \frac{E(t)}{E(o)} - 1 \right|. \tag{3.52}$$

The Fourier coefficients can be also used as reliable indicator for the accuracy tests.

**1- $L_2$-critical case:** in this part, we study the solutions of equation (3.29) with $\lambda = 1$ for $n = \frac{4}{5}$. This nonlinearity is not very relevant for applications, but it is mathematically interesting. Here we consider the problem with different initial data.
We first study the GKPI-BO using initial data (3.35) with $\beta = 1$ such that the inital energy is positive. The calculation is performed on $[-5, 5]^2$ with $N_x = Ny = 2^9$ and a time step $\Delta t = 0.0005$. The relative computed energy is conserved up to $10^{-8}$ after 1000 iterations. From the results shown in Figure 3.10 there is no ascertainment of a blow-up, and this is even more obvious from the norms shown in Figure 3.10 (bottom), both $\|u\|_\infty$ and $\|u_y\|_2$ appear to be monotonically decreasing. The situation is not different for initial data with negative energy, i.e. if we set $u_0(x, y) = 12exp(-(x^2 + y^2))$, use the same computation domain and $N_x = 2^{10}$, $Ny = 2^{10}$ and a smaller time step for numerical stability reason, $\Delta t = 0.00001$. As can be seen in 3.11, $\|u\|_\infty$ decreases monotonically and after a some time it increases then decreases, whereas the $\|u_y\|_2$ appears to increase without showing any blow-up and the relative computed energy reached $10^{-6}$ after 10000 iterations. Note that in this case even the corresponding Fourier coefficients tend to increase (see 3.11 top right).

**2- $L_2$ supercritical case:** we seek solutions of (3.29) with $\lambda = 1$ considering two cases:
**case 1:** we take $n = 1$ with positive energy. More exactly, with the initial data $u_0(x, y) = 3exp(-(x^2 + y^2))$. The calculation is performed with $[-20, 20] \times [-5, 5]$, $N_x = Ny = 2^{10}$ and $\Delta t = 0.0001$. The relative computed energy is conserved up to $10^{-11}$ and in this situation there is no blow-up (see Figure 3.12). The norms for this solution shown in Figure 3.12 (bottom) indicate that $\|u\|_\infty$ decreases monotonically and after a some time it increases then starts to decrease again, whereas $\|u_y\|_2$ appears to increase. These results are qualitatively the same as the ones for the critical case (Figure 3.11 bottom).
However if we take $u_0(x, y) = 12exp(-(x^2 + y^2))$ i.e. subject to a negative energy, on $[-5, 5]^2$ and $N_x = 2^{12}$, $Ny = 2^{10}$ and a very small time step $\Delta t = 0.000001$, we get a blow-up (see Figure 3.13). The relative computed energy reaches a value arround $10^{-2}$.

**case 2:** for $n = 2$ and initial data (3.35) with $\beta = 1$, $N_x = N_y = 2^{10}$, $\Delta t = 0.0001$, $L_x = 10$, $L_y = 4$, after 1000 iterations, we get a $\Delta$ of an order better than $10^{-9}$, i.e. there is no blow-up, as can be seen in Figure 3.14 that the initial hump has been completely radiated away.
The situation is completely different if $\beta = 6$, when the initial energy becomes negative. The calculation is performed for $L_x = L_y = 5$, $N_x = 2^{11}$, $N_y = 2^{12}$ with 5000 iterations. As can be seen in Figure 3.15, that the initial minimum appears to blow-up in a point after getting more and more peaks, the code breaks down when $\Delta > 10^{-3}$.
We have point out that the numerical experimentations were explored for both $\lambda = 1$ and $\lambda = -1$. Here we present the results for $\lambda = 1$ (see Figure 3.10- Figure 3.15) and $\lambda = -1$ (3.16-3.19). Note that the obtained results are qualitatively similar for both $\lambda = 1$ and $\lambda = -1$. The results of this section were published in [12].

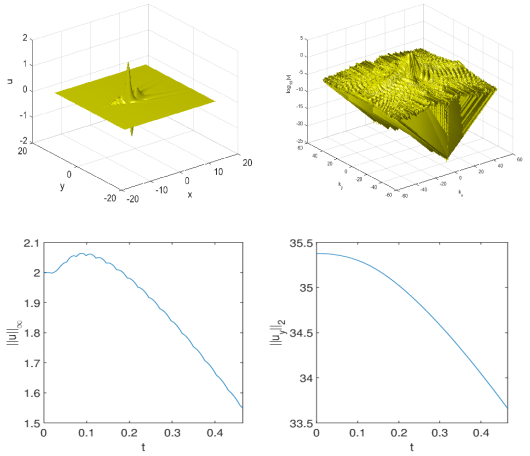

Figure 3.10: From top to bottom and left to right, the solution, its Fourier coefficients, $\|u\|_\infty$ and $\|u_y\|_2$ for (3.28), $\lambda = 1$ with $n = \frac{4}{5}$ and $u_0(x, y) = exp(-(x^2 + y^2))$.

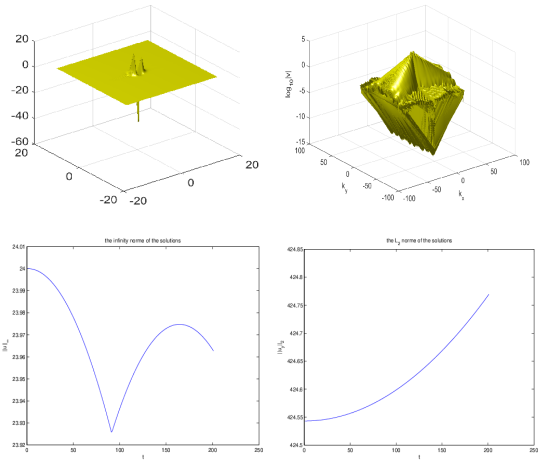

Figure 3.11: From top to bottom and left to right, the solution, its Fourier coefficients, $\|u\|_\infty$ and $\|u_y\|_2$ for (3.28), $\lambda = 1$ with $n = \frac{4}{5}$ and $u_0(x, y) = 12exp(-(x^2 + y^2))$.

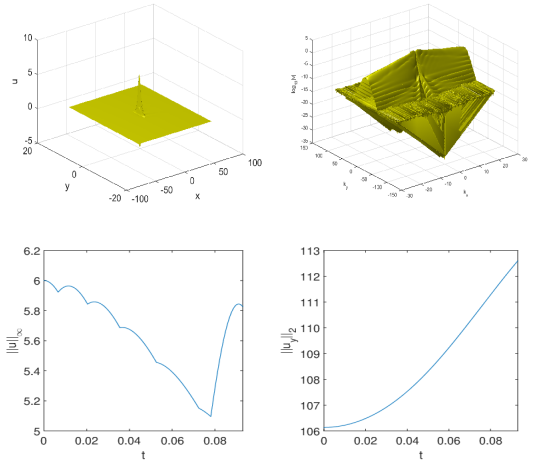

Figure 3.12: From top to bottom and left to right, the solution, its Fourier coefficients, $\|u\|_\infty$ and $\|u_y\|_2$ for (3.28), $\lambda = 1$ with $n = 1$ and $u_0(x, y) = 3exp(-(x^2 + y^2))$.

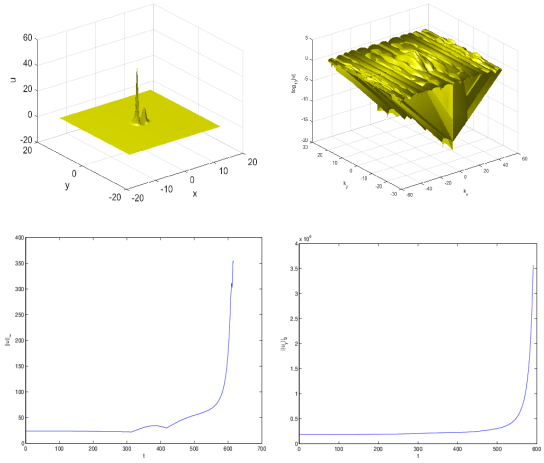

Figure 3.13: From top to bottom and left to right, the solution, its Fourier coefficients, $\|u\|_\infty$ and $\|u_y\|_2$ for (3.28), $\lambda = 1$ with $n = 1$ and $u_0(x, y) = 12exp(-(x^2 + y^2))$.

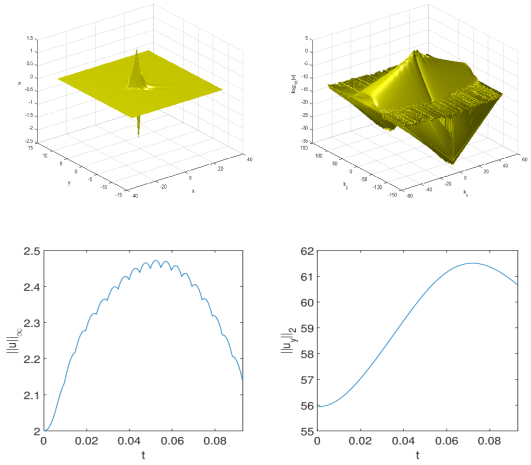


Figure 3.14: From top to bottom and left to right, the solution, its Fourier coefficients, $\|u\|_\infty$ and $\|u_y\|_2$ for (3.28), $\lambda = 1$ with $n = 2$ and $u_0(x, y) = exp(-(x^2 + y^2))$.

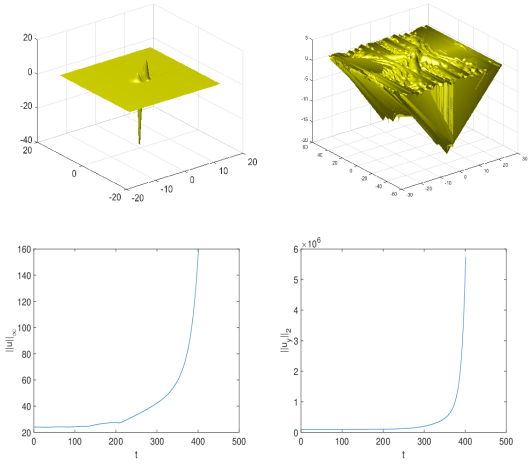


Figure 3.15: From top to bottom and left to right, the solution, its Fourier coefficients, $\|u\|_\infty$ and $\|u_y\|_2$ for (3.28),$\lambda = 1$ with $n = 2$ and $u_0(x, y) = 6exp(-(x^2 + y^2))$.

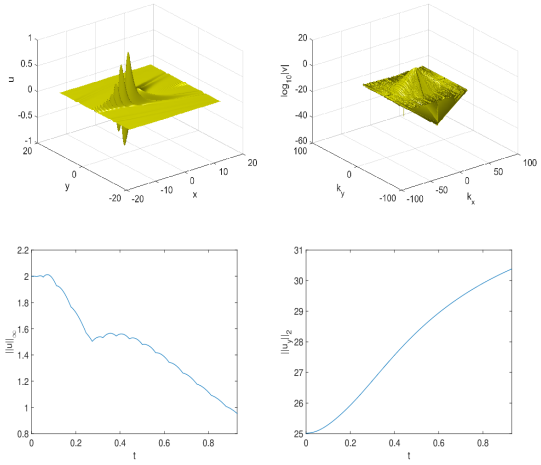

Figure 3.16: From top to bottom and left to right, the solution, its Fourier coefficients, $\|u\|_\infty$ and $\|u_y\|_2$ for (3.28),$\lambda = -1$ with $n = \frac{4}{5}$ and $u_0(x, y) = exp(-(x^2 + y^2))$.

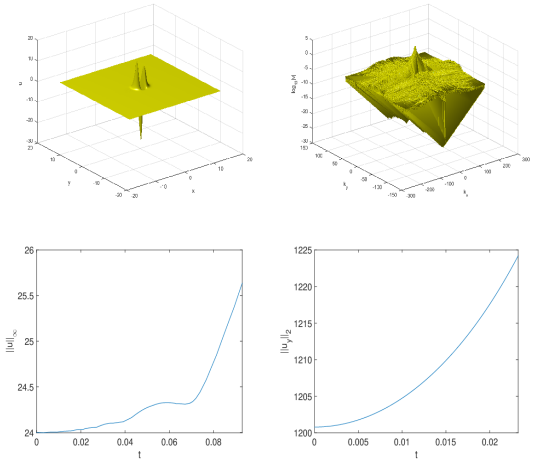

Figure 3.17: From top to bottom and left to right, the solution, its Fourier coefficients, $\|u\|_\infty$ and $\|u_y\|_2$ for (3.28), $\lambda = -1$ with $n = \frac{4}{5}$ and $u_0(x, y) = 12exp(-(x^2 + y^2))$.

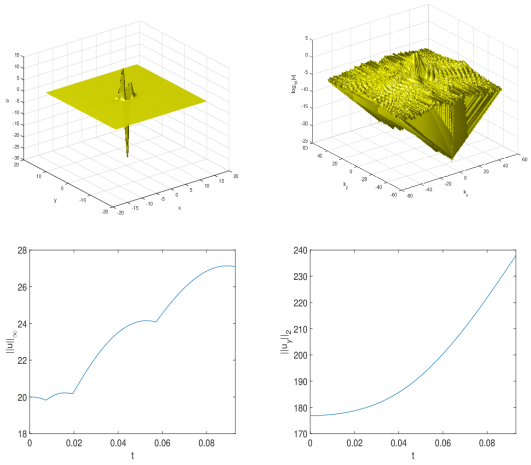

Figure 3.18: From top to bottom and left to right, the solution, its Fourier coefficients, $\|u\|_\infty$ and $\|u_y\|_2$ for (3.28), $\lambda = -1$ with $n = 1$ and $u_0(x, y) = 3exp(-(x^2 + y^2))$.

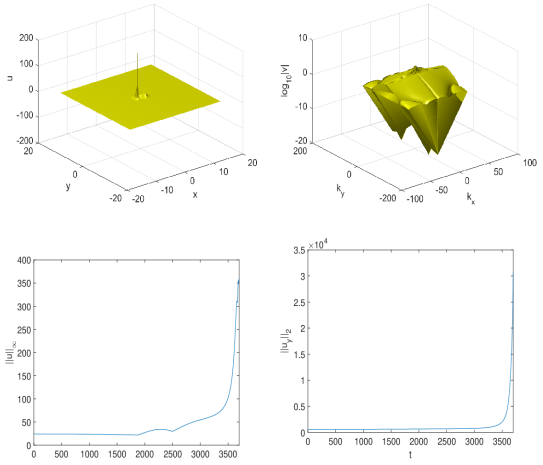

Figure 3.19: From top to bottom and left to right, the solution, its Fourier coefficients, $\|u\|_\infty$ and $\|u_y\|_2$ for (3.28), $\lambda = -1$ with $n = 1$ and $u_0(x, y) = 12exp(-(x^2 + y^2))$.

## 3.4 Conclusion

In this chapter we have two sections, in the first one, we investigated the behavior of the solutions to gBO equations in one dimension for $n = 2$ and $n = 3$, and we conclude that:
1-If $n = 2$,

- Localized smooth initial data with mass smaller than the mass of the approximate soliton are radiated away for positive initial energy.
- Localized smooth initial data with a mass larger than the mass of the approximate soliton present blow-up for both positive and negative initial energy.

2- If $n = 3$

- Localized smooth initial data with mass smaller than the mass of the approximate soliton are radiated away for positive initial energy.
- Localized smooth initial data with a mass larger than the mass of the approximate soliton present blow-up for negative initial energy.

In the second section, we studied the GKP-BO equations's solutions for $n = \frac{4}{5}$, $n = 1$ and $n = 2$. The numerical results are resumed in the Figures 3.10-3.15, for $\lambda = 1$. where we plot the solution, its corresponding Fourier coefficients, $\|u\|_\infty$ and $\|u_y\|_2$ to visualise the blowing up behavior according to each case. We remarque that the two cases $\lambda = 1$ and $\lambda = -1$ lead to similar qualitative results but with a slight difference in the plotted curves and conclude that:
1- If $n = \frac{4}{5}$, no blow-up occurs. This is shown in Figure 3.10. and Figure 3.11 for $\lambda = 1$ and in Figure 3.16. and Figure 3.17 for $\lambda = -1$ and by $\|u\|_\infty$ which increases monotonically and after a some time it increases.
2- For $n = 1$ and $n = 2$, if we take initial data with positive energy, we get almost the same situation as for the critical case (see Figure 3.12 & Figure 3.14 for $\lambda = 1$ and Figure **??** for $\lambda = -1$). However for a negative initial energy we can exhibit a blow-up and this can be seen in Figure 3.13 and Figure 3.15 for $\lambda = 1$ and in Figure 3.19 for $\lambda = -1$. Hence the blow-up phenomenon's behaviour depends on both an initial data satisfying the constraint (3.34) and the energy's sign ($> 0$ or $< 0$), and this is quite relevant so that when the energy is positive we get no blow-up, whereas for the negative case a blow-up occurs.

# Chapter 4

# Rotation-Modified Benjamin Equation

## 4.1 Introduction

In this chapter, we are concerned with the so-called Rotation-Modified Benjamin equation (RMBenjamin). Physically, this equation was introduced by Durán [32] as a model of internal wave propagation in rotating two-fluids. The vertical displacement of the interface between two-layer can be characterized by the RMBenjamin equation, where the lower and upper layers are respectively bounded below and above by a rigid horizontal plane (see Figure 4.1). The

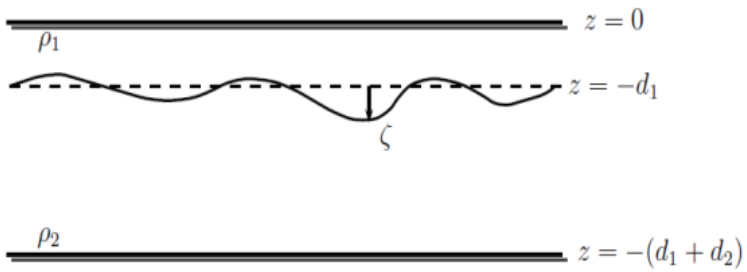


Figure 4.1: Model for propagation of internal wave in a two-layer interface, where $d_i$, $i = 1, 2$ is the depths, $\rho_i$, $i = 1, 2$ is the densities and $\zeta$ is the vertical displacement of the interface from a level of rest.

RMBenjamin equation takes the following form

$$(u_t + \alpha u_x + uu_x - \beta \mathcal{H} u_{xx} - \delta u_{xxx})_x = \gamma u,\ t \geq 0,\ x \in \mathbb{R}, \tag{4.1}$$

where $u = u(x, t)$, $x \in \mathbb{R}$ and $t \geq 0$. $\alpha$ and $\delta$ are positive while $\beta \neq 0$. $\gamma$ is a positive real parameter, measures the rotation effect, $\beta$ and $\delta$ are used to control the effects of the general dispersive whereas $\alpha$ depends on the fluids's densities. Here $\mathcal{H}$ is the Hilbert operator defined by (1.2.4).
There is several well-know related equations to the RMBenjamin equation, like the Ostrovsky equation

$$(u_t + uu_x - \delta u_{xxx})_x = \gamma u, \tag{4.2}$$

that describes the propagation of nonlinear dispersive shallow long water waves in a fluid with rotation force. The associated Cauchy problem has been investigated by many authors, see for example [47, 104, 107]. Isaza and Mejía showed in their paper [48] the sharp local well-posedness for the corresponding initial value problem in the Sobolev space $H^s$ for $s > -3/4$ if $\delta < 0$. By using the Fourier restriction norm method, Tsugawa [104] proved the local well-posedness of the Cauchy problem for (4.2) in the anisotropic Sobolev space $H^{a,s}$ for $s > -\frac{a}{2} - \frac{3}{4}$ and $0 \leq a \leq 1$. Recently, Wang and Yan [106] used the Strichartz estimates rather than the Cauchy Schwarz inequalities to investigate the local well-posedness of (4.2) with negative dispersion. Almost following the same method, Yan et al [107] established the proof of the local well-posedness in the case of positive dispersion in $H^s$ for $s = -3/4$.

Setting $\alpha = 0$ and $\delta = 0$, one obtains the rotation-modified Benjamin-Ono(RMBO) equation

$$(u_t + uu_x - \beta \mathcal{H} u_{xx})_x = \gamma u, \tag{4.3}$$

which models the internal long wave propagation in a deep fluid subject to rotation effects. The well-posedness of the related Cauchy problem has been proved by Linares and Milanes [77] in the space

$$X_s = \{u \in H^s(\mathbb{R}); \partial_x^{-1} u \in H^s(\mathbb{R})\},$$

with the associated norm

$$\|u\|_{X_s} = \|u\|_{H^s(\mathbb{R})} + \|\partial_x^{-1} u\|_{H^s(\mathbb{R})},$$

for $s > 3/2$.
In the absence of a Coriolis forces, equation (4.1) reduces to the Benjamin equation [10]

$$u_t + \alpha u_x + uu_x - \beta H u_{xx} - \delta u_{xxx} = 0, \tag{4.4}$$

that was modeled to describe the intermediate wave propagation in the stratified fluid with the existence of a considerable capillarity on the surface. For this equation, a sharp well posedness results were established in [25] and [24], they showed that the corresponding Cauchy problem is global and local well-posed when $s \geq -3/4$, whereasit is ill-posed for $s < -3/4$.

In the case $\alpha = 0$, for the study of Cauchy problem see for example [52] and [71]. See also [8, 78, 7, 23] for more explications on the study of existence, nonexistence results, stability and asymptotics investigations of the corresponding solitary waves. In fact (4.1) can be regarded as a perturbation of (4.4) by a nonlocal term. Two more things are also worth noting in this case ($\alpha = 0$).
**1-** The case $\beta = 0$ induces the well known Korteweg-de Vries equation (KdV) which has been investigated in great detail, the associated Cauchy problem has been widely studied, the reader can see for example [69], [27] and [67]. By using the Bourgain spaces Kenig et al [67] proved the local well-posedness in $H^s(\mathbb{R})$ if $s > -3/4$; this local result provided successfully the proof of a global one in [27, 69].
**2-** The case $\delta = 0$ and $\beta \neq 0$ generates the celebrated Benjamin-Ono equation, see [36], [46], [57] and [63], where much was shown about its mathematical aspects concerning complete integrability, conserved quantities, local and global well-posedness, existence and asymptotics of the solitary wave solutions.

## 4.2 Well-posedness of the RMBenjamin equation

In this section, we mainly investigate the Cauchy problem for the RMBenjamin equation. By using a sharp bilinear estimate, we prove the well-posedness of the problem in $H^s$ for $s > -\frac{3}{4}$. Let us define some used functions for this section

$$m(\eta) = \frac{\gamma}{\eta} + \alpha\eta - \beta\eta|\eta| + \delta\eta^3, \quad m(\eta_j) = \frac{\gamma}{\eta_j} + \alpha\eta_j - \beta\eta_j|\eta_j| + \delta\eta_j^3, \tag{4.5}$$

$$\lambda = \tau - m(\eta), \quad \lambda_j = \tau_j - m(\eta_j), \text{ for } j = 1, 2. \tag{4.6}$$

Throughout the rest of this section, we may assume that $\gamma$, $\delta > 0$, $\beta < 0$ or $0 < \beta < 4\delta^{3/4}\gamma^{1/4}$. Let $a = max\left\{1, \frac{2|\beta|}{3|\delta|}\right\}$, $\tau = \tau_1 + \tau_2$, $\eta = \eta_1 + \eta_2$, $\eta_{max} = max\{\eta, \eta_1, \eta_2\}$ and $\eta_{med} = med\{\eta, \eta_1, \eta_2\}$ as well as $\eta_{min} = min\{\eta, \eta_1, \eta_2\}$. Also, $\varphi$ stands for a $C_0^\infty$ function supported in $[-2, +2]$ and equals to 1 over the interval $[-1, +1]$, where $\varphi_\rho = \varphi(\frac{t}{\rho})$,
Let us now formulate our main results for this section.

**Theorem 26** ([13]). *Let $s \geq -\frac{3}{4} + 3\epsilon$, then there is $b \in (\frac{1}{2}, 1)$, such that we have*

$$\|\partial_x(uv)\|_{X_{s,b-1}} \leq C\|u\|_{X_{s,b}}\|v\|_{X_{s,b}} \tag{4.7}$$

**Theorem 27** ([13]). *Let $s \geq -\frac{3}{4} + 3\epsilon$, $b \in (\frac{1}{2}, 1)$, then the problem (4.1) is locally well-posed in $H^s(\mathbb{R})$. i.e., for $u_0 \in H^s(\mathbb{R})$ there exists $T = T(\|u\|_{H^s} > 0)$, such that the problem has a unique solution $u \in C([0, T], H^s) \cap X_{s,b}$. In addition the solution map $T : u_0 \to u$ is an analytic map from $H^s(\mathbb{R})$ to $C([0, T]; H^s(\mathbb{R}))$.*

To prove these results, we need some preliminaries.

### 4.2.1 Preliminary estimates

For convenience, we write

$$P^N F = \int_{|\eta|\geq N} e^{\mathrm{i}x\eta}\widehat{F}d\eta, \quad P_N F = \int_{|\eta|\leq N} e^{\mathrm{i}x\eta}\widehat{F}d\eta, \quad \forall N > 0$$

and

$$f = \mathscr{F}^{-1}F, \quad \mathscr{F}f_\sigma(\eta, \tau) = \frac{F(\eta, \tau)}{\langle\lambda\rangle^\sigma}$$

The solution of (4.1) is formally written in the following form

$$u(x, t) = S(t)u_0(x) = \frac{1}{2\pi}\int_\infty^{-\infty} e^{\mathrm{i}(\eta x - m(\eta))t}u_0 d\eta. \tag{4.8}$$

Now, Let us give some useful lemmas that will be used later

**Lemma 28.** *Let $m(.)$ is given by 4.5 with $\alpha = 0$ (a change of variable allows us to assume $\alpha = 0$) as well as $m(0) = 0$, then*

$$|m''(\eta)| \geq -2\beta + 8\gamma^{\frac{1}{4}}\delta^{\frac{3}{4}}, \ \ \eta \neq 0.$$

**Lemma 29.** *Let $f \in L^2$, we get*

$$\|S(t)f\|_{L_t^q L_x^p} \leq \|f\|_{L^2}, \tag{4.9}$$

*for $q = \frac{4}{\theta}$, $p = \frac{2}{1-\theta}$, $\theta \in [0,1]$.*

*Proof.* For the proof of these two lemmas; 29 and 28, see lemma 1 and theorem 2 in [32]. □

**Lemma 30.** *Let $\rho \in [0,1]$, $-\frac{1}{2} < b' \leq 0 \leq b \leq b'+1$ and $s \in \mathbb{R}$, then the following two inequalities hold*

$$\|\varphi(\frac{t}{\rho})S(t)u_0\|_{X_{s,b}(\mathbb{R}^2)} \leq C\rho^{\frac{1}{2}-b}\|u_0\|_{H^s(\mathbb{R})}, \tag{4.10}$$

$$\left\|\varphi(\frac{t}{\rho})\int_0^t S(t-\tau)F(\tau)d\tau\right\|_{X_{s,b}(\mathbb{R}^2)} \leq C\rho^{1+b'-b}\|F\|_{X_{s,b'}(\mathbb{R}^2)}. \tag{4.11}$$

*Proof.* For the proof of this lemma, see [65]. □

**Lemma 31.** *Let $\theta \in [0,1]$, $N \geq 2$, if $r > \frac{\theta}{2}$, then*

$$\|D_x^\theta P^N f_r\|_{L_x^{\frac{2}{1-\theta}} L_t^2} \leq C\|F\|_{L_\eta^2 L_\tau^2}.$$

**Lemma 32.** *Let $r > \frac{1}{3}$, $N \geq 2$ and $0 < c < +\infty$, then it holds that*

$$\|f_r\|_{L_x^4 L_t^4} \leq C\|F\|_{L_\eta^2 L_\tau^2}. \tag{4.12}$$

*If $r > \frac{1}{2}$, then we get*

$$\|P_c f_r\|_{L_x^2 L_t^\infty} \leq C\|F\|_{L_\eta^2 L_\tau^2}. \tag{4.13}$$

**Lemma 33.** *For $b > \frac{1}{2}$, $N \geq 2$, then*

$$\|f\|_{L_x^2 L_t^2} \leq C\|F\|_{X_{0,0}}, \tag{4.14}$$

$$\|f\|_{L_x^2 L_t^4} \leq C\|F\|_{X_{0,\frac{1}{2}b}}, \tag{4.15}$$

$$\|D_x^{\frac{1}{4}} P^N f\|_{L_x^\infty L_t^4} \leq C\|F\|_{X_{0,b}}, \tag{4.16}$$

$$\|D_x^{\frac{1}{8}} P^N f\|_{L_x^4 L_t^4} \leq C\|F\|_{X_{0,\frac{3}{4}b}}. \tag{4.17}$$

*Proof.* For the proof of lemmas 31; 32 and 33, the reader can be referred to [105] and [52] □

**Lemma 34.** *Let $\alpha$, $\beta$, $\gamma$, $\delta$ and $m(.)$ be as in 4.5. If $|\eta_{min}| \geq 1$ or $|\eta_{min}|^2|\eta_{max}||\eta_{med}| \geq 1$ and $|\eta_{max}| \sim |\eta_{med}| \geq 2a$, so one of the following three possibilities must hold,*

$$|\lambda| := max\{|\lambda|,\ |\lambda_1|,\ |\lambda_2|\} \geq |\eta_1\eta_2\eta|, \tag{4.18}$$

$$|\lambda_2| := max\{|\lambda|,\ |\lambda_1|,\ |\lambda_2|\} \geq |\eta_1\eta_2\eta|, \tag{4.19}$$

$$|\lambda_1| := max\{|\lambda|,\ |\lambda_1|,\ |\lambda_2|\} \geq |\eta_1\eta_2\eta|. \tag{4.20}$$

*Proof.* From equation (4.6), we find that

$$\begin{aligned} L(\eta) &= -\lambda + \lambda_1 + \lambda_2 \\ &= -\tau + m(\eta) + \tau_1 - m(\eta_1) + \tau_2 - m(\eta_2) \\ &= m(\eta) - m(\eta_1) - m(\eta_2) \\ &= 3\delta\eta\eta_1\eta_2 - \beta(|\eta|\eta - |\eta_1|\eta_1 - |\eta_2|\eta_2) - \gamma(\tfrac{\eta_1^2+\eta_2^2+\eta_1\eta_2}{\eta\eta_1\eta_2}), \end{aligned} \tag{4.21}$$

using the symmetry property, we may assume that $|\eta_1| < |\eta_2|$. Hence we can simplify (4.21) according to the following four regions:

$$\begin{aligned} D_1 &= \{(\tau_1, \eta_1, \tau_2, \eta_2) \in \mathbb{R}^4; \eta_1 < 0, \eta_2 < 0\}, \\ D_2 &= \{(\tau_1, \eta_1, \tau_2, \eta_2) \in \mathbb{R}^4; \eta_1 > 0, \eta_2 > 0\}, \\ D_3 &= \{(\tau_1, \eta_1, \tau_2, \eta_2) \in \mathbb{R}^4; \eta_1 > 0, \eta_2 < 0\}, \\ D_4 &= \{(\tau_1, \eta_1, \tau_2, \eta_2) \in \mathbb{R}^4; \eta_1 < 0, \eta_2 > 0\}. \end{aligned}$$

Then, we have that

$$\begin{aligned} L_{D_1}(\eta) &= 3\delta\eta_1\eta_2\eta - \beta(-(\eta_1+\eta_2)^2 + \eta_1^2 + \eta_2^2) - \gamma\tfrac{\eta_1^2+\eta_2^2+\eta_1\eta_2}{\eta_1\eta_2\eta} \\ &= 3\delta\eta_1\eta_2(\eta + \tfrac{2\beta}{3\delta}) - \gamma\tfrac{\eta_1^2+\eta_2^2+\eta_1\eta_2}{\eta_1\eta_2\eta}. \end{aligned}$$

$$\begin{aligned} L_{D_2}(\eta) &= 3\delta\eta_1\eta_2\eta - \beta((\eta_1+\eta_2)^2 - \eta_1^2 - \eta_2^2) - \gamma\tfrac{\eta_1^2+\eta_2^2+\eta_1\eta_2}{\eta_1\eta_2\eta} \\ &= 3\delta\eta_1\eta_2(\eta - \tfrac{2\beta}{3\delta}) - \gamma\tfrac{\eta_1^2+\eta_2^2+\eta_1\eta_2}{\eta_1\eta_2\eta}. \end{aligned}$$

$$\begin{aligned} L_{D_3}(\eta) &= 3\delta\eta_1\eta_2\eta - \beta(-(\eta_1+\eta_2)^2 - \eta_1^2 + \eta_2^2) - \gamma\tfrac{\eta_1^2+\eta_2^2+\eta_1\eta_2}{\eta_1\eta_2\eta} \\ &= 3\delta\eta\eta_1(\eta_2 + \tfrac{2\beta}{3\delta}) - \gamma\tfrac{\eta_1^2+\eta_2^2+\eta_1\eta_2}{\eta_1\eta_2\eta}. \end{aligned}$$

$$\begin{aligned} L_{D_4}(\eta) &= 3\delta\eta_1\eta_2\eta - \beta((\eta_1+\eta_2)^2 + \eta_1^2 - \eta_2^2) - \gamma\tfrac{\eta_1^2+\eta_2^2+\eta_1\eta_2}{\eta_1\eta_2\eta} \\ &= 3\delta\eta\eta_1(\eta_2 - \tfrac{2\beta}{3\delta}) - \gamma\tfrac{\eta_1^2+\eta_2^2+\eta_1\eta_2}{\eta_1\eta_2\eta}. \end{aligned}$$

We only treat with the restriction of $L$ on $D_1$, the proof of the others three cases can be obtained by a similar argument . From (4.21), we find that

$$\begin{aligned} |L| &= |-\lambda+\lambda_1+\lambda_2| \\ &\leq |\lambda|+|\lambda_1|+|\lambda_2| \\ &\leq 3\,max\{|\lambda|,|\lambda_1|,|\lambda_2|\}. \end{aligned}$$

If the maximum of $(\lambda,\lambda_i)$ is denoted by $\lambda_{max}$ for $i=1,2$, we get

$$|\lambda_{max}| \geq \frac{1}{3}|L|.$$

On the other hand, we have

$$|L| \geq 3\delta|\eta_1||\eta_2|\left|\left(\eta+\frac{2\beta}{3\delta}\right)\right| - \gamma|\eta_1||\eta_2||\eta|\left(\frac{|\eta_1^2+\eta_2^2+\eta_1\eta_2|}{(\eta_1\eta_2\eta)^2}\right), \tag{4.22}$$

$$\left|\left(\eta+\frac{2\beta}{3\delta}\right)\right| \geq |\eta|-a \geq |\eta|-\frac{1}{2}|\eta| \geq \frac{1}{2}|\eta|, \tag{4.23}$$

and

$$\frac{|\eta_1^2+\eta_2^2+\eta_1\eta_2|}{(\eta_1\eta_2\eta)^2} \leq \frac{1}{(\eta_2\eta)^2}+\frac{1}{(\eta_1\eta)^2}+\frac{1}{\eta_1\eta_2\eta^2} \leq \frac{3}{\eta_{min}^2\eta_{max}\eta_{med}} \leq \frac{3}{\eta_{min}^4} \leq C. \tag{4.24}$$

□

Equations (4.22), (4.23) and (4.24) yield

$$|L| \geq C|\eta_1||\eta_2||\eta|,$$

then the proof of lemma (34) is completed

**Lemma 35.** *For $\eta \neq 0$, let $m(\eta)=\frac{1}{\eta}+\eta|\eta|+\eta^3$ and $0 \leq s \leq \frac{1}{2}$ as well as*

$$\mathscr{F}(K^s(u,v)(\eta,\tau)) = \int_{\eta\tau} |m'(\eta-\eta_1)-m'(\eta_1)|^s \mathscr{F}u(\eta,\tau)\mathscr{F}v(\eta_1,\tau_1)d\eta_1 d\tau_1.$$

*Then, we have that*

$$\|K^s(u,v)\|_{L^2_{xt}} \leq C\|u\|_{X_{0,\frac{2+2s}{3}(b+)}}\|v\|_{X_{0,\frac{2+2s}{3}(b+)}}.$$

*Proof.* The proof of this lemma can be reached by the use of a similar argument as in the proof of lemma 2.9 in [107]. □

### 4.2.2 Proof of the bilinear estimate

Let us discuss a bilinear estimate associated to the nonlinear term in (4.1), that is the crucial step to prove the well-posedness by the use of Picard iteration.

*Proof.* By the use of duality and the identity of Plancheral, (4.7) follows if we show

$$\int_{\mathbb{R}^2} \overline{w}\partial_x(uv)dxdt \leq C[\|u\|_{X_{s,b+}}\|v\|_{X_{s,b+}}]\|w\|_{X_{-s,(1-b)-}}, \tag{4.25}$$

with $b = \frac{1}{2}$. If we define

$$\begin{aligned} F(\eta,\tau) &= \langle\eta\rangle^{-s}\langle\lambda\rangle^{(1-b)-}\widehat{w}(\eta,\tau), \\ F_1(\eta_1,\tau_1) &= \langle\eta_1\rangle^{s}\langle\lambda_1\rangle^{b+}\widehat{u}(\eta_1,\tau_1), \\ F_2(\eta_2,\tau_2) &= \langle\eta_2\rangle^{s}\langle\lambda_2\rangle^{b+}\widehat{v}(\eta_2,\tau_2), \end{aligned}$$

thus (4.25) is equivalent to

$$\int_{\mathbb{R}^2}\int_{\eta\tau} \frac{|\eta_1+\eta_2|\langle\eta\rangle^s F(\eta,\tau)\prod_{j=1}^{2}F_j(\eta_j,\tau_j)}{\langle\lambda_j\rangle^{(1-b)-}\prod_{j=1}^{2}\langle\eta_j\rangle^s\langle\lambda_j\rangle^{b+}}d\eta_1 d\tau_1 d\eta d\tau \leq C\|F\|_{L^2_{\eta\tau}}\left(\prod_{j=1}^{2}\|F_j\|_{L^2_{\eta\tau}}\right). \tag{4.26}$$

By symmetry property, we may assume that $|\eta_1| \leq |\eta_2|$ and $F(\eta,\tau) \geq 0$, $F_j(\eta_j,\tau_j) \geq 0$. $j = 1, 2$. Let us define

$$M(\eta_1,\tau_1,\eta,\tau) := \frac{|\eta|\langle\eta\rangle^s}{\langle\lambda\rangle^{(1-b)-}\prod_{j=1}^{2}\langle\eta_j\rangle^s\langle\lambda_j\rangle^{b+}}, \tag{4.27}$$

and

$$I = \int_{\mathbb{R}^2}\int_{\eta\tau} M(\eta_1,\tau_1,\eta,\tau)F(\eta,\tau)\prod_{j=1}^{2}F_j(\eta_j,\tau_j)d\eta_1 d\tau_1 d\eta d\tau. \tag{4.28}$$

Also define

$$\Lambda := \{(\eta_1,\tau_1,\eta,\tau)\in\mathbb{R}^4 :\ \eta = \eta_1+\eta_2,\ \tau = \tau_1+\tau_2,\ |\eta_1| \leq |\eta-\eta_1|\},$$

and

$$\begin{aligned} \Lambda_1 &:= \{(\eta_1,\tau_1,\eta,\tau)\in\Lambda :\ |\eta-\eta_1| \leq 2a\}, \\ \Lambda_2 &:= \{(\eta_1,\tau_1,\eta,\tau)\in\Lambda :\ |\eta_1| \geq 2a,\ 2|\eta_1| \leq |\eta-\eta_1|\}, \\ \Lambda_3 &:= \{(\eta_1,\tau_1,\eta,\tau)\in\Lambda :\ |\eta_1| \leq 2a,\ |\eta-\eta_1| \geq 4a,\ 2|\eta_1| \leq |\eta-\eta_1|\}, \\ \Lambda_4 &:= \{(\eta_1,\tau_1,\eta,\tau)\in\Lambda :\ |\eta| \geq \tfrac{1}{2}|\eta-\eta_1|,\ |\eta-\eta_1| \geq 4a,\ |\eta-\eta_1| \leq 2|\eta_1|\}, \\ \Lambda_5 &:= \{(\eta_1,\tau_1,\eta,\tau)\in\Lambda :\ |\eta| \leq 2a,\ |\eta-\eta_1| \geq 4a,\ |\eta-\eta_1| \leq 2|\eta_1|\}. \end{aligned}$$

Let $I_j$ be the restriction of $I$ on the regions $\Lambda_j$, for $j = 1, 2, 3, 4, 5$.

- in region $\Lambda_1$, we have that $|\eta_1| \leq |\eta - \eta_1| \leq 2a$ and $|\eta| \leq 2|\eta - \eta_1| \leq 4a$, so we obtain

$$M(\eta, \tau, \eta_1, \tau_1) \leq \frac{C}{\langle\lambda\rangle^{(1-b)-} \prod_{j=1}^{2} \langle\lambda_j\rangle^{b+}}. \tag{4.29}$$

In view of the Hölder and Cauchy–Schwarz inequality, lemma 32 as well as the Plancherel identity, we get

$$\begin{aligned} I_1 \leq & \; C \int_{\mathbb{R}^2} \int_{\eta\tau} \tfrac{F(\eta,\tau) F_1(\eta_1,\tau_1) F_2(\eta-\eta_1,\tau-\tau_1)}{\langle\lambda\rangle^{(1-b)-} \langle\lambda_1\rangle^{b+} \langle\lambda_2\rangle^{b+}} d\eta_1 d\tau_1 d\eta d\tau \\ \leq & \; \left\| \tfrac{F(\eta,\tau)}{\langle\lambda\rangle^{(1-b)-}} \right\|_{L^2_{\eta\tau}} \left\| \int_{\eta\tau} \tfrac{F_1(\eta_1,\tau_1) F_2(\eta-\eta_1,\tau-\tau_1)}{\langle\lambda_1\rangle^{b+} \langle\lambda_2\rangle^{b+}} d\eta_1 d\tau_1 \right\|_{L^2_{\eta\tau}} \\ \leq & \; \|F(\eta,\tau)\|_{L^2_{\eta\tau}} \left\| \mathscr{F}^{-1} \tfrac{F_1(\eta_1,\tau_1)}{\langle\lambda_1\rangle^{b+}} \right\|_{L^4_{xt}} \left\| \mathscr{F}^{-1} \tfrac{F_2(\eta-\eta_1,\tau-\tau_1)}{\langle\lambda_2\rangle^{b+}} \right\|_{L^4_{xt}} \\ \leq & \; \|F\|_{L^2_{\eta\tau}} \|F_1\|_{L^2_{\eta\tau}} \|F_2\|_{L^2_{\eta\tau}} . \end{aligned}$$

- in region $\Lambda_2$, since $2|\eta_1| \leq |\eta - \eta_1|$, we find that $\frac{1}{2}|\eta - \eta_1| \leq |\eta| \leq \frac{3}{2}|\eta - \eta_1|$, which means that $|\eta| \sim |\eta - \eta_1|$. Next, we study the three cases (4.18)-(4.20), respectively.
1- If (4.18) is valid, so that $|\lambda| \geq |\eta - \eta_1|^2 |\eta_1|$. Since $s \geq -\frac{3}{4} + 3\epsilon$, we obtain

$$\begin{aligned} M(\eta, \tau, \eta_1, \tau_1) \leq & \; C \tfrac{|\eta||\eta_1|^{-s}}{\langle\lambda\rangle^{(1-b)-} \prod_{j=1}^{2} \langle\lambda_j\rangle^{b+}} \leq C \tfrac{|\eta|^{2\epsilon} |\eta_1|^{-s+(b-1)+}}{\prod_{j=1}^{2} \langle\lambda_j\rangle^{b+}} \\ \leq & \; C \tfrac{|\eta|^{2\epsilon} |\eta_1|^{-s+(b-1)+}}{\prod_{j=1}^{2} \langle\lambda_j\rangle^{b+}} \leq C \tfrac{|\eta|^{\frac{1}{4}}}{\prod_{j=1}^{2} \langle\lambda_j\rangle^{b+}} \leq C \tfrac{|\eta-\eta_1|^{\frac{1}{4}}}{\prod_{j=1}^{2} \langle\lambda_j\rangle^{b+}}. \end{aligned} \tag{4.30}$$

By similar argument as before (by using Plancherel, Cauchy–Schwarz and Hölder) with lemma 33, we get,

$$\begin{aligned} I_2 \leq & \; C \int_{\mathbb{R}^2} \int_{\eta\tau} \tfrac{F_1(\eta_1,\tau_1) \mathcal{X}_{|\eta-\eta_1|\geq 4a} |\eta-\eta_1|^{\frac{1}{4}} F_2(\eta-\eta_1,\tau-\tau_1)}{\langle\lambda_1\rangle^{b+} \langle\lambda_2\rangle^{b+}} F(\eta,\tau) d\eta_1 d\tau_1 d\eta d\tau \\ \leq & \; \|F(\eta,\tau)\|_{L^2_{\eta\tau}} \left\| \mathscr{F}^{-1} \tfrac{F_1(\eta_1,\tau_1)}{\langle\lambda_1\rangle^{b+}} \right\|_{L^2_x L^4_t} \left\| P^{4a} D_x^{\frac{1}{4}} \mathscr{F}^{-1} \tfrac{F_2(\eta-\eta_1,\tau-\tau_1)}{\langle\lambda_2\rangle^{b+}} \right\|_{L^4_t L^\infty_x} \\ \leq & \; \|F\|_{L^2_{\eta\tau}} \|F_1\|_{L^2_{\eta\tau}} \|F_2\|_{L^2_{\eta\tau}} . \end{aligned}$$

2- If (4.19) is valid and since $s \geq -\frac{3}{4} + 3\epsilon$ and $\langle\lambda\rangle^{(b-1)+} \langle\lambda_2\rangle^{(-b)-} \leq \langle\lambda_2\rangle^{(b-1)+} \langle\lambda\rangle^{(-b)-}$ as well as

$$
\begin{aligned}
|m'(\eta)-m'(\eta_1)| = & \left|-\tfrac{1}{\eta^2}+\tfrac{1}{\eta_1^2}+|\eta|-|\eta_1|+3(\eta^2-\eta_1^2)\right| \\
= & \ 3|\eta^2-\eta_1^2|\left|1+\tfrac{1}{3\eta^2\eta_1^2}+\tfrac{1}{3(|\eta|+|\eta_1|)}\right| \\
\geq & \ C|\eta^2-\eta_1^2| \\
\geq & \ C|\eta|^2,
\end{aligned}
$$

then, we deduce that

$$
\begin{aligned}
M(\eta,\tau,\eta_1,\tau_1) \leq & \ C\tfrac{|\eta||\eta_1|^{-s}}{\langle\lambda_2\rangle^{(1-b)-}\langle\lambda\rangle^{b+}\langle\lambda_1\rangle^{b+}} \leq C\tfrac{|\eta|^{2\epsilon}||\eta_1|^{-s+(b-1)+}}{\langle\lambda\rangle^{b+}\langle\lambda_1\rangle^{b+}} \\
\leq & \ C\tfrac{|\eta|^{\frac{1}{4}}}{\langle\lambda\rangle^{b+}\langle\lambda_1\rangle^{b+}} \leq C\tfrac{|m'(\eta)-m'(\eta_1)|^{\frac{1}{2}}}{\langle\lambda\rangle^{b+}\langle\lambda_1\rangle^{b+}}.
\end{aligned} \tag{4.31}
$$

By utilizing the following transformed variables

$$
\eta'=\eta-\eta_1, \quad \tau'=\tau-\tau_1, \quad \eta_1'=-\eta_1, \quad \tau_1'=-\tau_1, \quad \eta'-\eta_1'=\eta, \quad \tau-\tau_1'=\tau,
$$

$$
\lambda'=\tau'-m(\eta')=\lambda_2, \quad \lambda_1'=\tau_1'-m(\eta_1')=-\lambda_1, \quad \lambda_2'=\tau'-\tau_1'-m(\eta-\eta_1')=\lambda,
$$

$$
F'(\eta',\tau')=F_2(\eta-\eta_1,\tau-\tau_1),\ F_1'(\eta_1',\tau_1')=F_1(-\eta_1,-\tau_1),\ F_2'(\eta'-\eta_1',\tau'-\tau_1')=F(\eta,\tau),
$$

, we obtain

$$
M(\eta,\tau,\eta_1,\tau_1) \leq C\frac{|m'(\eta'-\eta_1')-m'(\eta_1')|^{\frac{1}{2}}}{\langle\lambda_2'\rangle^{b+}\langle\lambda_1'\rangle^{b+}}.
$$

Again, by using Plancherel identity, Cauchy-Schwarz and Hölder inequalities together with (4.31) as well as lemma 35, we infer that

$$
\begin{aligned}
I_2 \leq & \ C\int_{\mathbb{R}^2}\int_{\eta\tau}\tfrac{|m'(\eta'-\eta_1')-m'(\eta_1')|^{\frac{1}{2}}F'(\eta',\tau')F_1'(\eta_1',\tau_1')F_2(\eta'-\eta_1',\tau'-\tau_1')}{\langle\lambda_2'\rangle^{b+}\langle\lambda_1'\rangle^{b+}}d\eta_1 d\tau_1 d\eta d\tau \\
\leq & \ \|\mathscr{F}^{-1}F(\eta',\tau')\|_{L^2_{xt}}\left\|K^{\frac{1}{2}}\left(\mathscr{F}^{-1}\left(\tfrac{F_2'(\eta'-\eta_1',\tau'-\tau_1')}{\langle\lambda_2'\rangle^{b+}}\right),\mathscr{F}^{-1}\left(\tfrac{F_1'(\eta_1',\tau_1')}{\langle\lambda_1'\rangle^{b+}}\right)\right)\right\|_{L^2_{xt}} \\
\leq & \ C\|F'\|_{L^2_{\eta,\tau}}\|F_1'\|_{L^2_{\eta,\tau}}\|F_2'\|_{L^2_{\eta,\tau}}.
\end{aligned}
$$

3- If (4.20) is valid, this case can be established as the previous one.

- for region $\Lambda_3$. we also have $|\eta|\sim|\eta-\eta_1|$. but, we only deal with the most interesting case $-\frac{3}{4}+3\epsilon\leq s<0$, so we conclude that

$$
M(\eta,\tau,\eta_1,\tau_1) \leq \frac{C|\eta|}{\langle\lambda\rangle^{(1-b)-}\prod_{j=1}^{2}\langle\lambda_j\rangle^{b+}}. \tag{4.32}
$$

Consider the two cases $|\eta_1|<1$ and $|\eta_1|\geq 1$.
The case $|\eta_1|\geq 1$ is handled like the one in the previous region.
For the case when $|\eta_1|<1$, by using lemmas 31 and 32 it follows that

$$\begin{aligned} I_3 \leq & \ C\int_{\mathbb{R}^2}\int_{\eta\tau}\frac{F(\eta,\tau)F_1(\eta_1,\tau_1)|\eta-\eta_1|F_2(\eta-\eta_1,\tau-\tau_1)}{\langle\lambda\rangle^{(1-b)-}\langle\lambda_1\rangle^{b+}\langle\lambda_2\rangle^{b+}}d\eta_1 d\tau_1 d\eta d\tau \\ \leq & \ \left\|\frac{F(\eta,\tau)}{\langle\lambda\rangle^{(1-b)-}}\right\|_{L^2_{\eta\tau}}\left\|\int_{\eta\tau}\frac{F_1(\eta_1,\tau_1)F_2(\eta-\eta_1,\tau-\tau_1)}{\langle\lambda_1\rangle^{b+}\langle\lambda_2\rangle^{b+}}d\eta_1 d\tau_1\right\|_{L^2_{\eta\tau}} \\ \leq & \ \left\|\mathscr{F}^{-1}\frac{F(\eta,\tau)}{\langle\lambda\rangle^{(1-b)-}}\right\|_{L^2_{xt}}\left\|P_1\mathscr{F}^{-1}\frac{F_1(\eta_1,\tau_1)}{\langle\lambda_1\rangle^{b+}}\right\|_{L^2_xL^\infty_t}\left\|P^{4a}D_x\mathscr{F}^{-1}\frac{F_2(\eta-\eta_1,\tau-\tau_1)}{\langle\lambda_2\rangle^{b+}}\right\|_{L^2_tL^\infty_x} \\ \leq & \ \|F\|_{L^2_{\eta\tau}}\|F_1\|_{L^2_{\eta\tau}}\|F_2\|_{L^2_{\eta\tau}}. \end{aligned}$$

- in region $\Lambda_4$, since $\frac{1}{2}|\eta-\eta_1|\leq|\eta|\leq 2|\eta-\eta_1|$ and $|\eta_1|\leq|\eta-\eta_1|\leq 2|\eta_1|$, this implies that $|\eta|\sim|\eta_1|\sim|\eta-\eta_1|$. The three scenarios (4.18), (4.19) and (4.20) have to be considered.
1- If (4.18) is valid, then $|\lambda|\geq|\eta|^3$, it follows that

$$\begin{aligned} M(\eta,\tau,\eta_1,\tau_1)\leq & \ C\frac{|\eta-\eta_1|^{-s}|\eta|}{\langle\lambda\rangle^{(1-b)-}\langle\lambda_1\rangle^{b+}\langle\lambda_2\rangle^{b+}}\leq C\frac{|\eta-\eta_1|^{-s+3(b-1)+3\epsilon+1}}{\langle\lambda_1\rangle^{b+}\langle\lambda_2\rangle^{b+}} \\ \leq & \ C\frac{|\eta_1|^{\frac{1}{8}}|\eta-\eta_1|^{\frac{1}{8}}}{\langle\lambda_1\rangle^{b+}\langle\lambda_2\rangle^{b+}}. \end{aligned} \tag{4.33}$$

Then

$$\begin{aligned} I_4 \leq & \ C\int_{\mathbb{R}^2}\int_{\eta\tau}\frac{F(\eta,\tau)\mathcal{X}_{|\eta_1|\geq 2a}|\eta_1|^{\frac{1}{8}}F_1(\eta_1,\tau_1)\mathcal{X}_{|\eta-\eta_1|\geq 4a}|\eta-\eta_1|^{\frac{1}{8}}F_2(\eta-\eta_1,\tau-\tau_1)}{\langle\lambda_1\rangle^{b+}\langle\lambda_2\rangle^{b+}}d\eta_1 d\tau_1 d\eta d\tau \\ \leq & \ \|F(\eta,\tau)\|_{L^2_{\eta\tau}}\left\|\int_{\eta\tau}\frac{\mathcal{X}_{|\eta|\geq 2a}|\eta_1|^{\frac{1}{8}}F_1(\eta_1,\tau_1)\mathcal{X}_{|\eta-\eta_1|\geq 4a}|\eta-\eta_1|^{\frac{1}{8}}F_2(\eta-\eta_1,\tau-\tau_1)}{\langle\lambda_1\rangle^{b+}\langle\lambda_2\rangle^{b+}}d\eta_1 d\tau_1\right\|_{L^2_{\eta\tau}} \\ \leq & \ \|F(\eta,\tau)\|_{L^2_{\eta\tau}}\left\|D_x^{\frac{1}{8}}P^{2a}\mathscr{F}^{-1}\frac{F_1(\eta_1,\tau_1)}{\langle\lambda_1\rangle^{b+}}\right\|_{L^4_tL^4_x}\left\|D_x^{\frac{1}{8}}P^{4a}\mathscr{F}^{-1}\frac{F_2(\eta-\eta_1,\tau-\tau_1)}{\langle\lambda_2\rangle^{b+}}\right\|_{L^4_tL^4_x} \\ \leq & \ \|F\|_{L^2_{\eta\tau}}\|F_1\|_{L^2_{\eta\tau}}\|F_2\|_{L^2_{\eta\tau}}, \end{aligned}$$

which follows by Cauchy, Plancherel and Hölder as well as lemma 33.
2- If (4.19) is valid, so that $\langle\lambda_2\rangle^{(-b)-}\leq|\eta|^{-3b-3\epsilon}$ which implies

$$\begin{aligned} M(\eta,\tau,\eta_1,\tau_1)\leq & \ C\frac{|\eta|^{-s+1-3b-3\epsilon}}{\langle\lambda\rangle^{(1-b)-}\langle\lambda_1\rangle^{b+}}\leq C\frac{|\eta|^{\frac{1}{4}}}{\langle\lambda_1\rangle^{b+}\langle\lambda\rangle^{(1-b)-}} \\ \leq & \ C\frac{|\eta_1|^{\frac{1}{8}}|\eta|^{\frac{1}{8}}}{\langle\lambda_1\rangle^{b+}\langle\lambda\rangle^{(1-b)-}}. \end{aligned} \tag{4.34}$$

By using the same argument as before, and because $(1-b)->\frac{3}{8}$, so we can use (4.17) in lemma 33. Then we conclude that

$$
\begin{aligned}
I_4 \leq & \ C\int_{\mathbb{R}^2}\int_{\eta\tau}\frac{\mathcal{X}_{|\eta_1|\geq 2a}|\eta_1|^{\frac{1}{8}}F_1(\eta_1,\tau_1)\mathcal{X}_{|\eta|\geq 2a}|\eta|^{\frac{1}{8}}F(\eta,\tau)F_2(\eta-\eta_1,\tau-\tau_1)}{\langle\lambda_1\rangle^{b+}\langle\lambda\rangle^{(1-b)-}}d\eta_1 d\tau_1 d\eta d\tau \\
\leq & \ \|F_2(\eta-\eta_1,\tau-\tau_1)\|_{L^2_{\eta\tau}}\left\|\int_{\eta\tau}\frac{\mathcal{X}_{|\eta_1|\geq 2a}|\eta_1|^{\frac{1}{8}}F_1(\eta_1,\tau_1)\mathcal{X}_{|\eta|\geq 2a}|\eta|^{\frac{1}{8}}F(\eta,\tau)}{\langle\lambda_1\rangle^{b+}\langle\lambda\rangle^{(1-b)-}}d\eta_1 d\tau_1\right\|_{L^2_{\eta\tau}} \\
\leq & \ \|F_2(\eta-\eta_1,\tau-\tau_1)\|_{L^2_{\eta\tau}}\left\|D_x^{\frac{1}{8}}P^{2a}\mathscr{F}^{-1}\frac{F_1(\eta_1,\tau_1)}{\langle\lambda_1\rangle^{b+}}\right\|_{L^4_tL^4_x}\left\|D_x^{\frac{1}{8}}P^{2a}\mathscr{F}^{-1}\frac{F(\eta,\tau)}{\langle\lambda\rangle^{(1-b)-}}\right\|_{L^4_tL^4_x} \\
\leq & \ \|F\|_{L^2_{\eta\tau}}\|F_1\|_{L^2_{\eta\tau}}\|F_2\|_{L^2_{\eta\tau}}.
\end{aligned}
$$

3- If (4.20) is valid, so this case can be proceeded as the previous one.

- in region $\Lambda_5$, we consider the two cases: $s\geq 0$, $-\frac{3}{4}\leq s<0$, respectively.

  1- If $s\geq 0$, we have that

$$
\begin{aligned}
M(\eta,\tau,\eta_1,\tau_1)\leq & \ C\frac{|\eta|^{1+s}|\eta_1|^{-2s}}{\langle\lambda\rangle^{(1-b)-}\langle\lambda_1\rangle^{b+}\langle\lambda_2\rangle^{b+}} \\
\leq & \ \frac{C}{\langle\lambda\rangle^{(1-b)-}\langle\lambda_1\rangle^{b+}\langle\lambda_2\rangle^{b+}}.
\end{aligned}
\tag{4.35}
$$

  This case can be proved in a similar way as (4.29).

  2- If $-\frac{3}{4}+3\epsilon\leq s<0$, considering $|\eta|\geq 1$ or $|\eta||\eta_1|^{\frac{1}{2}}|\eta-\eta_1|^{\frac{1}{2}}\geq 1$ and $|\eta|<1$ or $|\eta||\eta_1|^{\frac{1}{2}}<1|\eta-\eta_1|^{\frac{1}{2}}<1$, respectively.

  – When $|\eta|\geq 1$, (4.18), (4.19) and (4.20) are needed to deal .
  1- If (4.18) is valid, then $|\lambda|\geq|\eta||\eta-\eta_1|^2$, and because $0>s\geq-\frac{3}{4}+3\epsilon$, we obtain that

$$
\begin{aligned}
M(\eta,\tau,\eta_1,\tau_1)\leq & \ C\frac{|\eta||\eta-\eta_1|^{\frac{3}{2}-6\epsilon}}{\langle\lambda\rangle^{(1-b)-}\langle\lambda_1\rangle^{b+}\langle\lambda_2\rangle^{b+}} \\
\leq & \ C\frac{|\eta|^{\frac{1}{2}+\epsilon}|\eta-\eta_1|^{\frac{1}{2}-4\epsilon}}{\langle\lambda_1\rangle^{b+}\langle\lambda_2\rangle^{b+}} \\
\leq & \ C\frac{|\eta|^{\frac{1}{2}}|\eta-\eta_1|^{\frac{1}{2}}}{\langle\lambda_1\rangle^{b+}\langle\lambda_2\rangle^{b+}}.
\end{aligned}
\tag{4.36}
$$

  On the other hand,

$$
\begin{aligned}
|m'(\eta-\eta_1)-m'(\eta_1)|= & \ \left|-\tfrac{1}{(\eta-\eta_1)^2}+\tfrac{1}{\eta_1^2}+|\eta-\eta_1|-|\eta_1|+3((\eta-\eta_1)^2-\eta_1^2)\right| \\
= & \ 3|(\eta-\eta_1)^2-\eta_1^2|\left|1+\tfrac{1}{3(\eta-\eta_1)^2\eta_1^2}+\tfrac{1}{3((|\eta-\eta_1)|+|\eta_1|)}\right| \\
\geq & \ C|(\eta-\eta_1)^2-\eta_1^2| \\
\geq & \ C|\eta-\eta_1||\eta|.
\end{aligned}
\tag{4.37}
$$

From (4.37), (4.36) and by using a similar argument as before (Plancherel, Cauchy Schwarz and Hölder) with lemma 35, we conclude that

$$\begin{aligned} I_5 \leq & \; C\int_{\mathbb{R}^2}\int_{\eta\tau}\frac{F(\eta,\tau)|m'(\eta_1)-m'(\eta-\eta_1)|^{\frac{1}{2}}F_1(\eta_1,\tau_1)F_2(\eta-\eta_1,\tau-\tau_1)}{\langle\lambda\rangle^{(1-b)-}\langle\lambda_1\rangle^{b+}\langle\lambda_2\rangle^{b+}}d\eta_1 d\tau_1 d\eta d\tau \\ \leq & \; \|F(\eta,\tau)\|_{L^2_{\eta\tau}}\left\|\int_{\eta\tau}\frac{|m'(\eta_1)-m'(\eta-\eta_1)|^{\frac{1}{2}}F_1(\eta_1,\tau_1)F_2(\eta-\eta_1,\tau-\tau_1)}{\langle\lambda_1\rangle^{b+}\langle\lambda_2\rangle^{b+}}d\eta_1 d\tau_1\right\|_{L^2_{\eta\tau}} \\ \leq & \; \|F(\eta,\tau)\|_{L^2_{\eta\tau}}\left\|K^{\frac{1}{2}}\left(\mathscr{F}^{-1}\left(\frac{F_1(\eta_1,\tau_1)}{\langle\lambda_1\rangle^{b+}}\right),\mathscr{F}^{-1}\left(\frac{F_2(\eta-\eta_1,\tau-\tau_1)}{\langle\lambda_2\rangle^{b+}}\right)\right)\right\|_{L^2_{xt}} \\ \leq & \; C\|F\|_{L^2_{\eta,\tau}}\|F_1\|_{L^2_{\eta,\tau}}\|F_2\|_{L^2_{\eta,\tau}}. \end{aligned}$$

2- If (4.19) is valid, we obtain $|\lambda_2| \geq |\eta||\eta_1|^2$, hence

$$\begin{aligned} M(\eta,\tau,\eta_1,\tau_1) \leq & \; C\frac{|\eta|^{\frac{1}{2}+\epsilon}|\eta_1|^{\frac{1}{2}-4\epsilon}}{\langle\lambda\rangle^{b+}\langle\lambda_1\rangle^{b+}} \\ \leq & \; C\frac{|\eta_1|}{\langle\lambda\rangle^{b+}\langle\lambda_1\rangle^{b+}}. \end{aligned} \tag{4.38}$$

On the other hand,

$$\begin{aligned} |m'(\eta)-m'(\eta_1)| = & \; \left|-\tfrac{1}{\eta^2}+\tfrac{1}{\eta_1^2}+|\eta|-|\eta_1|+3(\eta^2-\eta_1^2)\right| \\ = & \; 3|\eta^2-\eta_1^2|\left|1+\tfrac{1}{3\eta^2\eta_1^2}+\tfrac{1}{3(|\eta|+|\eta_1|)}\right| \\ \geq & \; C|\eta^2-\eta_1^2| \\ \geq & \; C|\eta_1|^2. \end{aligned} \tag{4.39}$$

Thus from (4.38) and (4.39), we have that

$$M(\eta,\tau,\eta_1,\tau_1) \leq \; C\frac{|m'(\eta)-m'(\eta_1)|^{\frac{1}{2}}}{\langle\lambda\rangle^{b+}\langle\lambda_1\rangle^{b+}} \tag{4.40}$$

This case can be studied similarly to (4.31).
3- If (4.20) is valid, as the previous one, this case can be proved.

– When $|\eta||\eta_1|^{\frac{1}{2}}|\eta-\eta_1|^{\frac{1}{2}}<1$, we have

$$\begin{aligned} M(\eta,\tau,\eta_1,\tau_1) \leq & \; C\tfrac{|\eta|^{1+s}|\eta_1|^{-s}|\eta-\eta_1|^{-s}}{\langle\lambda\rangle^{(1-b)-}\langle\lambda_1\rangle^{b+}\langle\lambda_2\rangle^{b+}} \\ \leq & \; C\tfrac{|\eta-\eta_1|^{-1-2s}}{\langle\lambda\rangle^{(1-b)-}\langle\lambda_1\rangle^{b+}\langle\lambda_2\rangle^{b+}} \\ \leq & \; C\tfrac{|\eta-\eta_1|^{\frac{1}{2}}}{\langle\lambda\rangle^{(1-b)-}\langle\lambda_1\rangle^{b+}\langle\lambda_2\rangle^{b+}} \\ \leq & \; C\tfrac{|\eta-\eta_1|}{\langle\lambda\rangle^{(1-b)-}\langle\lambda_1\rangle^{b+}\langle\lambda_2\rangle^{b+}} \\ \leq & \; C\tfrac{|m'(\eta-\eta_1)-m'(\eta_1)|^{\frac{1}{2}}}{\langle\lambda\rangle^{(1-b)-}\langle\lambda_1\rangle^{b+}\langle\lambda_2\rangle^{b+}}. \end{aligned} \tag{4.41}$$

$$\begin{aligned} I_5 \leq & \; C\int_{\mathbb{R}^2}\int_{\eta\tau}\tfrac{F(\eta,\tau)|m'(\eta_1)-m'(\eta-\eta_1)|^{\frac{1}{2}}F_1(\eta_1,\tau_1)F_2(\eta-\eta_1,\tau-\tau_1)}{\langle\lambda\rangle^{(1-b)-}\langle\lambda_1\rangle^{b+}\langle\lambda_2\rangle^{b+}}d\eta_1 d\tau_1 d\eta d\tau \\ \leq & \; \left\|\tfrac{F(\eta,\tau)}{\langle\lambda\rangle^{(1-b)-}}\right\|_{L^2_{\eta\tau}}\left\|\int_{\eta\tau}\tfrac{|m'(\eta_1)-m'(\eta-\eta_1)|^{\frac{1}{2}}F_1(\eta_1,\tau_1)F_2(\eta-\eta_1,\tau-\tau_1)}{\langle\lambda_1\rangle^{b+}\langle\lambda_2\rangle^{b+}}d\eta_1 d\tau_1\right\|_{L^2_{\eta\tau}} \\ \leq & \; \left\|\tfrac{F(\eta,\tau)}{\langle\lambda\rangle^{(1-b)-}}\right\|_{L^2_{\eta\tau}}\left\|K^{\frac{1}{2}}\left(\mathscr{F}^{-1}\left(\tfrac{F_1(\eta_1,\tau_1)}{\langle\lambda_1\rangle^{b+}}\right),\mathscr{F}^{-1}\left(\tfrac{F_2(\eta-\eta_1,\tau-\tau_1)}{\langle\lambda_2\rangle^{b+}}\right)\right)\right\|_{L^2_{xt}} \\ \leq & \; C\|F\|_{L^2_{\eta,\tau}}\|F_1\|_{L^2_{\eta,\tau}}\|F_2\|_{L^2_{\eta,\tau}}. \end{aligned}$$

Which is treated similarly to (4.36).

This ends the proof. □

### 4.2.3 Proof of Theorem 27

Let us now demonstrate the second result stated in theorem 27.

*Proof.* For $u_0\in H^s$ $(s>-\frac{3}{4})$, let us define the following set

$$\mathcal{S}=\{u\in X_{s,b}:\|u\|_{X_{s,b}}\leq 2C\|u_0\|_{Hs}\},$$

and the operator

$$\Theta_{u_0}(u)=\Theta(u)=\varphi(t)S(t)u_0-\frac{1}{2}\varphi_\rho(t)\int_0^t S(t-t')(\partial_x u^2)(t')dt.$$

To applying the fixed point theorem, one needs to show that $\Theta$ is a contraction mapping on the set $\mathcal{S}$. First, we prove that $\Theta(\mathcal{S})\subset\mathcal{S}$. Using theorem 26 and lemma 29 as well as lemma 30, we deduce that

$$\|\Theta(u)\|_{X_{s,b}}\leq C\|u_0\|_{H^s}+C\rho^{b'-b}\|u\|^2_{X_{s,b}}\leq C\|u_0\|_{H^s}+C\rho^{b'-b}\|u\|_{H^s}\|u\|_{X_{s,b}}.$$

Hence, when we fix $\rho$ for which $C\rho^{b'-b}\|u\|_{H^s} \leq \frac{1}{2}$, yields $\Theta(\mathcal{S}) \subset \mathcal{S}$.
On the other hand, for $u$, $v \in \mathcal{S}$, a similar argument as above, gives

$$\|\Theta(u) - \Theta(v)\|_{X_{s,b}} \leq C\rho^{b'-b}(\|u\|_{H^s} + \|v\|_{H^s})\|u - v\|_{X_{s,b}} \leq \frac{1}{2}\|u - v\|_{X_{s,b}}.$$

Hence, we can say that $\Theta$ is a contraction mapping on $\mathcal{S}$ with the constant $C = \frac{1}{2}$. Therefore, the fixed point theorem can be applied for $T < \frac{\rho}{2}$ to prove the existence and uniqueness of the solution to the Cauchy problem (4.1), this completes the proof of theorem 27. □

The results of this section exist in [13].

## 4.3 Conclusion

In this chapter, we are interested in a nonlinear dispersive model for the internal waves propagation in a two-layer system with the presence of rotational, surface tension and gravity forces. An mathematical aspect of the proposed model is studied in this chapter, which is the local well-posedness of the related Cauchy problem to this nonlinear dispersive model using a sharp bilinear estimate. As shown above in Theorem 27 that RMBenjamin equation is locally well-posed in $H^s$ for $s > -\frac{3}{4}$ this means that we obtain the same results as the local well-posedness for the standard Benjamin equation i.e., RMBenjamin without the rotation term. Hence we can conclude that the addition of rotational forces does not have any effect on the Cauchy problem of the equation. In fact we expect similar results for $s \leq -\frac{3}{4}$.

# Conclusion and Perspectives

## Conclusion

In this thesis, we were mainly interested in the study of some analytical methods for nonlinear dispersive wave equations, together with their numerical approaches. In particular we studied an integro-differential equation, in both one and two dimensions. By applying a powerful analytical method that is the inverse scattering transform technique, we get the corresponding solitons in one dimension and we present the behavior of the numerical solutions of the associated generalized integro-differential equation, in a perturbation scenario in both dimensions where no analytical results exist and we give a description to the appearance of blow-up phenomena.

When theories fail, numerical simulations stay the only tool for investigation of such problem solutions. Numerical simulations have been also used in the case of the existence properties, since in this case they allow us to validate the theoretical results and give conjectures for future researches. From the obtained results, we conclude that, by using the energy conservation, fourth order time stepping approaches behave efficiently in the deal of stiff systems where the stifness caracter is related to the linear part.

On the other hand, we investigated some important mathematical aspects associated to the considered integro-differential equation with a nonlocal rotational term (RMBenjamin) in one dimension; such as the well posedness of the corresponding Cauchy problem and geometric properties. Furthermore the well posedness of the rotational equation was shown in $H^s$ with $s > -3/4$, i.e the case where there is no nonlocal rotational term. In addition, we can point out that the corresponding approximation solitary wave depend on the degree of the nonlinearity.

## Perspectives

In view of its importance, the study of nonlinear dispersive wave equations has become a wide field either analytically or numerically, many open questions arise, we cite the following points:

- The investigation of the existence, nonexistence, stability and unstability of solitary wave solutions for RMBenjamin equation.
- The study of the solution behavior of the proposed integro-differential equation in both dimensions with a small dispersion limit; that is called semiclassical limit.
- Development of other new numerical schemes that can be more effective for the stiff systems in combination with Fourier spectral method.

- Seek other cases for the ill posedness of the proposed integro-differential equation with the existence of nonlocal rotational term

# Appendix A

**Fast Fourier Transforms**

The recursive algorithm known as Fast Fourier Transform (FFT) is used to evaluate the DFT and its inverse. Thus the FFT is written in a conventional manner to evaluate the following formulas

$$\widetilde{u}_k = \sum_{j=0}^{N-1} u_j e^{2\pi \mathrm{i} jk/N}, \quad k = 0, 1, ..., N-1. \tag{42}$$

$$\widetilde{u}_k = \sum_{j=0}^{N-1} u_j e^{-2\pi \mathrm{i} jk/N}, \quad k = 0, 1, ..., N-1. \tag{43}$$

After its introduction by Cooley and Tukey (1965), the FFT rapidly became a widely used method. The Cooley-Tukey algorithm allows to implement the sums (43) by $5Nlog_2N$ real operations rather than $8N^2$ real operations. Moreover, the error of the calculation with FFT is less than the straightforward sum due to round-off. up to now, numerous versions of the FFT are Known, For example Temperton (1983) in his paper introduced a version allows $N$ to be as

$$N = 2^p 3^q 4^r 5^s 6^t, \tag{44}$$

with the operation count

$$N(5p + 9(1/3)q + 8(1/2)r + 13(3/5)s + 13(1/3)t - 6). \tag{45}$$

In Fourier spectral methods applications, the following two sums must be evaluated

$$\widetilde{u}_k = \frac{1}{N} \sum_{j=0}^{N-1} u_j e^{-2\pi \mathrm{i} jk/N}, \quad k = -\frac{N}{2}, ..., \frac{N}{2} - 1, \tag{46}$$

and

$$u_j = \sum_{k=-N/2}^{N/2-1} \widetilde{u}_k e^{-2\pi \mathrm{i} jk/N}, \quad j = 0, 1, ..., N-1. \tag{47}$$

It is Clearly from (46) that, for two integers $p$ and $k$, we have

$$\widetilde{u}_{k+pN} = \widetilde{u}_k$$

If $(u_0, u_1, ..., u_{N-1})$ is fed into FFT in order to evaluate (43), it returns the following array

$$(N\widetilde{u}_0, N\widetilde{u}_1, ..., N\widetilde{u}_{-N/2}, ..., N\widetilde{u}_{-1}). \tag{48}$$

Conversely, the array $(u_0, u_1, ..., u_{N-1})$ is returned when (48) is fed into FFT. It is worth to mention that, in many spectral methods applications the direct apply of the complex FFT (42), eqreffft1 is needlessly expensive. But Orszag (1971) and Brachet et al.(1983) have addressed these issues in their papers.

# Appendix B

**Some used identities and inequalities**
Here, we recall by the identities and inequalities that be used in this thesis;

- **Plancherel identity**

  **Definition 36.** *For $L^2(\mathbb{R}^n)$ function $u$, we have that $\hat{u} \in L^2(\mathbb{R})$. Moreover, the operator $\mathcal{F}$ is unitary from $L^2(\mathbb{R}^n)$ to $L^2(\mathbb{R}^n)$ and*

  $$\|u\|_{L^2(\mathbb{R}^n)} = \|\mathcal{F}u\|_{L^2(\mathbb{R}^n)}.$$

- **Cauchy-Schwarz inequality**

  **Definition 37.** *Let $u$ and $v$ two vectors $u$ and $v$ of an inner product space, the Cauchy-Schwarz inequality states that the following is true*

  $$|\langle u, v\rangle| \leq \langle u, u\rangle \langle v, v\rangle,$$

  *where is the inner product.*

- **Hölder inequality**

  **Definition 38.** *For a measure space $(\mathcal{S}, \Sigma, \mu)$ and for two numbers $p$ and $q$ in $[1, \infty)$ such that $\frac{1}{p} + \frac{1}{q} = 1$, we have that*

  $$\|uv\|_1 \leq \|u\|_p \|v\|_q,$$

  *where $u$ and $v$ are measurable functions of real or complex valued.*

- **Young inequality**

  **Definition 39.** *Let $a$ and $b$ be two nonnegative real numbers and let $p$ and $q$ be two real numbers greater than 1 with $\frac{1}{p} + \frac{1}{q} = 1$, then*

  $$ab \leq \frac{a^p}{p} + \frac{b^q}{q}.$$

# Bibliography


[1] M.J. Ablowitz and P.A. Clarkson, Solitons, Nonlinear Evolution Equations, and Inverse Scattering, Cambridge University Press, Cambridge, (1991).

[2] M.J. Ablowitz and A.S. Fokas, The inverse scattering transform for the Benjamin-Ono equation: a pivot to multidimensional problems, Stud. App. Math. 68 (1983), 1–10.

[3] M.J. Ablowitz and A.S. Fokas, Introduction and Applications of Complex Variables, Cambridge University Press, second edition, (2003).

[4] M.J. Ablowitz, A.S. Fokas and R. Anderson, The direct linearizing transform and the Benjamin-Ono equation, Physics Letters A. 93 (8) (1983), 375–378.

[5] M.J. Ablowitz and Z.H. Musslimani, Spectral renormalization method for computing self-localized solutions to nonlinear systems, Opt. Lett. 30 (2005), 2140–2142.

[6] M.J. Ablowitz and H. Segur, Solitons and the Inverse Scattering Transform, Society for Industrial and Applied Mathematics, Philadelphia, (1981).

[7] J.P Albert, J.L. Bona and J.M. Restrepo, Solitary wave solutions of the Benjamin equation, SIAM J. Appl. Math. 59 (1997): 2139–2161.

[8] J. Angulo, Existence and stability of solitary wave solution of the Benjamin equation, J. Differentional Equations. 152 (1999): 136–159.

[9] K. A. Bagrinovskii and S. K. Godunov, Difference schemes for multi-dimensional problems, Dokl. Acad. Nauk. 115 (1957), pp. 431–433

[10] T.B. Benjamin, Internal waves of permanent form in fluids of great depth, J. Fluid. Mech. 29 (1967): 559–592.

[11] G. Beylkin, J. M. Keiser, and L. Vozovoi, A new class of time discretization schemes for the solution of nonlinear PDEs, J. Comput. Phys. 147 (1998): 362–387

[12] F. Bousbia and F.Z. Nouri, A numerical study for blow-up in solutions of the generalized 2-D Benjamin-Ono equation, IAENG International Journal of Applied Mathematics. 50(2020): 170–176.

[13] F. Bousbia and F.Z. Nouri, Cauchy problem for the rotational-modified Benjamin equation, International Journal of Applied Mathematics et Statistics. 59, no. 4, 2020..

[14] J. L. Bona, Private communication.

[15] J.L. Bona and H. Kalisch, Singularity formation in the generalized Benjamin-Ono equation, Disc. Cont. Dyn. Syst. 11, (2004): 27–45.

[16] J. P. Boyd, Chebyshev and Fourier Spectral Methods, Springer-Verlag, New York (1989).

[17] C. Canuto, M. Y. Hussaini, A. Quarteroni, and T. A. Zang, Spectral methods, Scientific Computation, Springer-Verlag, Berlin, (2006). Fundamentals in single domains.

[18] C. Canuto, M. Y. Hussaini, A. Quarteroni, and T. A. Zang, Spectral methods, Scientific Computation, Springer, Berlin, (2007). Evolution to complex geometries and applications to fluid dynamics.

[19] K.M. CASE, Properties of the Benjamin-Ono equation, J. Math. Phys. 20 (1979): 972–977.

[20] K.M. CASE, Benjamin-Ono-related equations and their solutions, Proc. Nat. Acad.Sci. USA. 76 (1979): 1–3.

[21] J. Certaine, The solution of ordinary differential equations with large time constants, in Mathematical Methods for Digital Computers, A. Ralston and H. S. Wilf, eds., Wiley, New York, (1960): 128–132.

[22] T. F. Chan and T. Kerkhoven, Fourier methods with extended stability intervals for the Korteweg–de Vries equation, SIAM J. Numer. Anal. 22 (1985): 441–454.

[23] H. Chen and J.L. Bona, Existence and asymptotic properties of solitary-wave solutions of the Benjamin-type equations, Adv. Diff. Eqns. 3 (1998): 51–84.

[24] W. Chen, Z. Guo and J. Xiao, Sharp well-posedness for the Benjamin equation, Nonlinear Anal. 74 (2011): 6209–6230.

[25] W. Chen and J. Xiao, A sharp bilinear estimate for the Bourgain-type space with application to the Benjamin equation, Comm. in Part. Diff. Eqns. 13(2010): 1739–1762.

[26] M.L. Chiofalo, S. Succi, and M.P. Tosi, Ground state of trapped interacting BoseEinstein condensates by an explicit imaginary-time algorithm, Phys. Rev. E. 62 (2000): 7438–7444.

[27] J. Colliander, M. Keel, G. Staffilani, H. Takaoka and T. Tao, Global well-posedness for KdV in Sobolev spaces of negative index, Electron. J. Differential Equations (2001): 1–7.

[28] J. W. Cooley and J. W. Tukey, An algorithm for the machine calculation of complex Fourier series, Math. Comput. 19 (1965): 297–301

[29] S. M. Cox and P. C. Matthews, Exponential time differencing for stiff systems, J. Comput. Phys. 176 (2002): 430–455.

[30] M. Darwich, On the stability of the solitary waves to the rotation Benjamin-Ono equation, Math Meth Appl Sci. 42 (2019): 219–228.

[31] G. Dahlquist, Convergence and stability in the numerical integration of ordinary differential equations, Math. Scand. 4 (1956): 33-53.

[32] A. Durán, On a model for internal waves in rotating, fluids Appl Math Nonlinear Sci. 3 (2018): 627–648.

[33] A. Esfahani, Remarks on solitary waves of the generalized two dimensional Benjamin-Ono equation,Applied Mathematics and Computation. 218 (2011) 308–323.

[34] A. Esfahani and S. Levandosky, Solitary waves of a coupled KdV system with a weak rotation, J. Differential Equations, https://doi.org/10.1016/j.j de.2018.06.023. (2018).

[35] L. N. G. Filon, On a quadrature formula for trigonometric integrals, Proc. Roy. Soc. Edinburgh Sect. A. 49 (1928–1929): 38–47.

[36] A.S. Fokas and M.J. Ablowitz, The inverse scattering transform for the Benjamin Ono equation: a pivot to multidimensional problems, Stud. Appl. Math. 68 (1983): 1–10.

[37] B. Fornberg, A practical Guide to pseudospectral Methods, vol. 1 of Cambridge Monographs on Applied and Computational Mathematics, Cambridge University Press, Cambridge, (1996).

[38] B. Fornberg and T. A. Driscoll, A fast spectral algorithm for nonlinear wave equations with linear dispersion, J. Comput. Phys. 155 (1999): 456–467.

[39] J. Fröhlich, E.H. Lieb and M. Loss, Stability of coulomb systems with magnetic fields I. The one electron atom, Commun. Math. Phys (1986): 251–270.

[40] R. H. Hardin and F. Tappert, Applications of the split-step Fourier method to the numerical solution of nonlinear and variable coefficient wave equations, SIAM,

[41] B. Harrop-Griffiths and J.L. Marzuola, Small data global solutions of the Camassa- Choi equation, Nonlinearity. 31 (2018): 1868–1904.

[42] K.R. Helfrich and W.K. Melville, Long nonlinear internal waves, Ann. Rev. Fluid Mech. 38 (2006): 395–425.

[43] J. Hesthaven, S. Gottliebs and D. Gottliebs, Spectral Methods for Time-Dependent Problems, Cambridge, (2010).

[44] . R. Hirota, The Direct Method in Soliton Theory, Cambridge University Press, Cambridge, (2004).

[45] M. Hochbruck, A. Ostermann, Exponential Runge-Kutta methods for semilinear parabolic problems, SIAM J. Numer. Anal. 43 (2005): 1069–1090.

[46] A.D. Ionescu and C.E. Kenig, Global well-posedness of the Benjamin-Ono equation in low regularity spaces, J. Amer. Math. Soc. 20 (2007): 753–798.

[47] P. Isaza and J. Mejía, Cauchy problem for the Ostrovsky equation in spaces of low regularity, J. Differential Equations. 230 (2006): 661–681.

[48] P. Isaza and J. Mejía, Global Cauchy problem for the Ostrovsky equation, Nonlinear Anal. TMA 67(2007): 1482–1503.

[49] D. Gottlieb, L. Lustman, and E. Tadmor, Stability analysis of spectral methods for hyperbolic initial-boundary value problems, SIAM 1. Numer.Anal. 24 (1987): 241–58.

[50] D. Gottlieb and S. A. Orszag, Numerical Analysis of Spectral Methods, SIAM, Philadelphia (1977).

[51] B. Gou, Y. Han, Remarks on the generalized Kadomtsev-Petviashvili equations and two-dimensional Benjamin-Ono equations, Proc. Royal Soc. London Sec. A. 452 (1996) 1585–1595.

[52] B. Guo and Z. Huo, The well-posedness of the Korteweg-de Vries-Benjamin-Ono equation, J. Math. Anal. Appl. 295(2004): 444–458.

[53] P. Henrici, Applied and Computational Complex Analysis, v. 3 , Wiley, (1986).

[54] D.J. Kaup and Y. Matsuno, The inverse scattering for the Benjamin-Ono equation, Stud. Appl. Math. 101 (1998): 73–98.

[55] A. K. Kassam and L. N. Trefethen, Fourth order time-stepping for stiff pdes, SIAM J. Sci. Comput. 26 (2005): 1214–1233.

[56] T. Kato, Quasi-linear equations of evolution, with applications to partial differential equations. Springer Lecture Notes in Mathematics. 448 (1975): 25–70.

[57] C.E. Kenig and K.D. Koenig, On the local well-posedness of the Benjamin Ono and modified Benjamin-Ono equations, Math. Res. Lett. 10 (2003): 879–895.

[58] C. Klein, Fourth order time-stepping for low dispersion Korteweg-de Vries and nonlinear Schrodinger equations, ETNA 29 (2008): 116–135.

[59] C. Klein and R. Peter, *Numerical study of blow-up in solutions to generalized Korteweg-de Vries equations*, (2013).

[60] C. Klein and R. Peter, Numerical study of blow-up in solutions to generalized Kadomtsev-Petviashvili equations, Discrete and Continuous Dynamical Systems, B. 19(6): 1689–1717. doi: 10.3934/dcdsb.2014.19.1689.

[61] C. Klein and K. Roidot, Fourth order time-stepping for Kadomtsev-Petviashvili and Davey-Stewardson equations, SIAM J. Sci. Comput. 33 (2011): 3333–3356

[62] C. Klein, C. Sparber, and P. Markowich, Numerical study of oscillatory regimes in the Kadomtsev- Petviashvili equation, J. Nonl. Sci. 17 (2007): 429–470.

[63] C.E. Kenig and Y. Martel, Asymptotic stability of solitons for the Benjamin-Ono equation, Revista Matematica Iberoamericana. 25 (2009): 909–970.

[64] C. E. Kenig, Y. Martel and L. Robbiano, Local well-posedness and blow-up in the energy space for a class of $L^2$ critical dispersion generalized Benjamin-Ono equations, Ann. Inst. H. Poincaré, Anal. Non Lin., 28 (2011): 853–887.

[65] C.E. kenig, G. Ponce and L. Vega, The Cauchy problem for the Korteweg-de Vries equation in Sobolev spaces of negative indices, Duke Math. J. 71 (1993): 1–21.

[66] C. E. Kenig, G. Ponce and L. Vega, On the generalized Benjamin-Ono equation, Trans. Amer. Math. Soc. 342 (1994): 155–172

[67] C.E. kenig, G. Ponce and L. Vega, A bilinear estimate with applications to the KdV equation, J. Amer. Math. Soc. 9 (1996): 573–603.

[68] C. E. Kenig and H. Takaoka, Global wel l-posedness of the modified Benjamin-Ono equation with initial data in $H^{\frac{1}{2}}$, Int. Math. Res. Not., Art. ID 95702 (2006): 1–44.

[69] N. Kishimoto, Well-posedness of the Cauchy problem for the Korteweg-de Vries equation at the critical regularity, Diff. Int. Eqns. 22(2009): 447–464.

[70] S.E. Koonin, Computational Physics, Addison-Wesley, Redwood City, CA, (1986).

[71] H. Kozono, T. Ogawa and H. Tanisaka, Well-posedness for the Benjamin equations, J. Korean Math. Soc. 38 (2001): 1205–1234.

[72] M. Krusemeyer, Differential Equations, Macmillan College Publishing, New York, (1994).

[73] J. C. Lagarias, J. A. Reeds, M. H. Wright, and P. E. Wright , Convergence properties of the Nelder-Mead simplex method in low dimensions, SIAM Journal of Optimizationl, 9 (1998): 112–147

[74] T.I. Lakoba and J. Yang, A generalized Petviashvili iteration method for scalar and vector Hamiltonian equations with arbitrary form of nonlinearity, J. Comput. Phys. 226 (2007a): 1668–1692.

[75] J. D. Lawson, Generalized Runge-Kutta Processes for stable Systems with large Lipschitz Constants, SIAM J. Numer. Anal. 4 (1967): pp. 372–380.

[76] S.P. Levandosky and Y. Liu, Stability of solitary waves of a generalized Ostrovsky equation, SIAM J. Math. Anal. 38(3) (2006): 985–1011.

[77] F. Linares and A. Milanes, A note on solutions to a model for long internal waves in a rotating, Mat. Contemp. 27 (2004): 101–115.

[78] F. Linares and M. Scialom, On generalized Benjamin type equations, Discrete and Continuous Dynamical Systems. 12 (2005): 161–174.

[79] F. Linares, D. Pilod and J.-C. Saut, The Cauchy problem for the fractional Kadomtsev-Petviashvili equations, SIAM J. Math. Anal. 50 (3) (2018): 3172–3209.

[80] Y. Liu, M. Wang, and L. Meng, Spectral Collocation Method in the Large Deformation Analysis of Flexible Beam, IAENG International Journal of Applied Mathematics. vol. 48, no.4 (2018): 416-423.

[81] Y. Liu and V. Varlamov, Stability of solitary waves and weak rotation limit for the Ostrovsky equation, J. Diff. Eq. 203 (2004): 159–183.

[82] W. Malfliet, Solitary wave solutions of nonlinear wave equations, Am. J. Phys. 60 (7) (1992): 650–654.

[83] Y. Martel and D. Pilod, Construction of a minimal mass blow-up solution of the modified Benjamin-Ono equation

[84] R. I. McLachlan and P. Atela, The accuracy of symplectic integrators, Nonlinearity. 5 (1992): 541–562.

[85] P. A. Milewski and E. G. Tabak, A pseudospectral procedure for the solution of nonlinear wave equations with examples from free-surface flows, SIAM J. Sci. Comput. 21 (1999): 1102–1114.

[86] Z. Musslimani and J. Yang, Self-trapping of light in a two-dimensional periodic structure. J. Opt. Soc. Amer. B. Opt. Phys. 21 (2004): 973–981.

[87] L. Molinet and F. Ribaud, Wel l-posedness results for the generalized Benjamin-Ono equation with arbitrary large initial data, Int. Math. Res. Not. 70 (2004): 3757–3795.

[88] L. Molinet and F. Ribaud, Wel l-posedness results for the generalized Benjamin-Ono equation with small initial data, J. Math. Pures Appl. (2004): 277–311.

[89] A.C. Newell, Solitons in Mathematics and Physics, Society for Industrial and Applied Mathematics, Philadelphia (1985).

[90] F.Z Nouri, D. Sloan, A Comparison of Fourier Pseudospectral Methods for the Solution of the Korteweg-de Vries Equation,J. of Comp. Physics. Volume. 83, Issue 2 (1989): 324–344.

[91] S. Novikov, S.V. Manakov, L.P. Pitaevskii and V.E. Zakharov, Theory of Solitons: The Inverse Scattering Method, Plenum Publihing, New York, (1984).

[92] G. C. Nwachukwu, and N.E. Mokwunyei, Generalized Adams-Type Second Derivative Methods for Stiff Systems of ODEs, IAENG International Journal of Applied Mathematics, vol. 48, no.4 (2018): 455–465.

[93] H. Ono, Algebraic solitary waves in stratified fluids, J. Phys. Soc. Japan. 39 (1975): 1082–1091.

[94] D.E. Pelinovsky and Y.A. Stepanyants, Convergence of Petviashvilis iteration method for numerical approximation of stationary solutions of nonlinear wave equations, SIAM J. Numer. Anal. 42 (2004): 1110–1127.

[95] G. Preciado. López and F. H. Soriano Méndez, On the existence and analycity of solitary waves solutions to a two-dimesional Benjamin-Ono equation, preprint (2018)

[96] J. M. Sanz-Serna and M. P. Calvo, Numerical Hamiltonian Problems, Chapman and Hall, London, (1994).

[97] J. C. Saut, Benjamin-Ono and intermediate long wave equations: modeling, IST and PDE, Preprint (2018).

[98] M. Schatzman, Toward non-commutative numerical analysis: High order integration in time, J. Sci. Comput. 17 (2002): 99–116.

[99] C. Sulem, P.-L. Sulem, The nonlinear Schrodinger equation — Self-focusing and wave collapse, Applied Mathematical Sciences., Springer. 139 (1999).

[100] E. Tadmor, The exponential accuracy of Fourier and Chebyshev differerencing methods, SIAM J. Numer. Anal. 23 (1986),110.

[101] T. Tao, Multilinear weighted convolution of $L^2$ functions, and applications to nonlinear dispersive equations, Amer. J. Math. 123 (2001): 839–908.

[102] T. Tao, Global well-posedness of the Benjamin–Ono equation in H1(R), J. Hyperbolic Differ. Equ. 1 (2004): 27–49

[103] L. Trefethen, Spectral Methods in MATLAB, vol. 10 of Software, Environments, and Tools, Society for Industrial and Applied Mathematics (SIAM), Philadelphia, PA, (2000).

[104] K. Tsugawa, Well-posedness and weak rotation limit for the Ostrovsky equation, J. Differential Equationsi. 247 (2009): 3163–3180.

[105] H. Wang and S. Cui, Well-posedness of the Cauchy problem of Ostrovsky equation in anisotropic Sobolev spaces, J. Math. Anal. Appl. 327 (2007): 88–100.

[106] J. Wang and W. Yan, The Cauchy problem for quadratic and cubic Ostrovsky equation with negative dispersion, Nonlinear Anal. Real World Applications. 43 (2018): 283–307.

[107] W. Yan, Y.S. Li, J.H. Huang and J.Q. Duan, The Cauchy problem for the Ostrovsky equation with positive dispersion in $H^{-3/4}(R)$, Nonlinear Differ. Equ. Appl. 25 (2018): 1–37.

[108] J. Yang, Nonlinear Waves in Integrable and Nonintegrable Systems, SIAM, Philadelphia. (2010).

[109] J.Yang and T.I. Lakoba, Universally-convergent squared-operator iteration methods for solitary waves in general nonlinear wave equations, Stud. Appl. Math. 118 (2007): 153–197.

[110] J. Yang and T.I. Lakoba, Accelerated imaginary-time evolution methods for the computation of solitary waves, Stud. Appl. Math. 120 (2008): 265–292.

[111] H. Yoshida, Construction of higher order symplectic integrators, Phys. Lett. A. 150 (1990): 262–268.

[112] A.M. Wazwaz, Peakons and kinks, Compactons and solitary patterns solutions for a family of Camassa–Holm equations by using new hyperbolic schemes, Appl. Math. Comput., 182(1) (2006): 412–424.

[113] M. Willem, Minimax Theorems, Progress in Nonlinear Differential Equations and Their Applications, Birkhäuser Boston Inc. 24 (1996).

[114] Z. XU, Analysis and numerical analysis of the Benjamin-Ono equation, PhD thesis, University of Michigan, (2010).